Facultad de Ciencias

INTRACELLULAR CALCIUM MANAGEMENT, LED BY *sca-1* AND *mcu-1*, IS KEY IN DIAPAUSE-INDUCED AXONAL REGENERATION IN *CAENORHABDITIS ELEGANS*

Doctorado en Ciencias, Mención Neurociencias

TESIS

Scarlett Elizabeth Delgado Gallardo

2022

INTRACELLULAR CALCIUM MANAGEMENT, LED BY *sca-1* AND *mcu-1*, IS KEY IN DIAPAUSE-INDUCED AXONAL REGENERATION IN *CAENORHABDITIS ELEGANS*.

Tesis entregada a

LA UNIVERSIDAD DE VALPARAÍSO

en Cumplimiento Parcial de los requisitos para optar al grado de

Doctor en Ciencias con Mención en Neurociencias

Facultad De Ciencias

Por

Scarlett Elizabeth Delgado Gallardo

Noviembre, 2022

Dirigida por: Dra. Andrea Calixto

Co-Dirigida por: Dra. Chiayu Chiu

FACULTAD DE CIENCIAS

UNIVERSIDAD DE VALPARAÍSO

INFORME DE APROBACION TESIS DE DOCTORADO

Se informa a la Facultad de Ciencias que la Tesis de Doctorado presentada por:

SCARLETT ELIZABETH DELGADO GALLARDO

Ha sido aprobada por la comisión de Evaluación de la tesis como requisito para optar al grado de Doctor en Ciencias con mención en Neurociencia, en el examen de Defensa de Tesis rendido el día 12 del Mes de Octubre de 2022

Directora de Tesis:

Dra. Andrea Calixto

Co-Directora de Tesis:

Dra. Chiayu Chiu

Comisión de Evaluación de la Tesis

Dr. John Ewer .....

Dra. Karen Castillo .....

Dr. Leonardo Valdivia .....

Dedicado a todos quienes

han participado en mi vida

(Dedicated to everyone who

had participated in my life)

ACKNOWLEDGEMENTS

We appreciate the support from ANID Scholarship for Doctoral Studies (21181324/2018), ANID Operational expenses (2747/2019), FIB-UV Scholarship 2017, Millennium Scientific Initiative ICM-ANID (ICN09-022, CINV), the FONDEQUIP project ANID EQM160154, Universidad de Valparaíso, the Doctoral Program in Neuroscience from the University of Valparaíso, and the support the Caenorhabditis Genetics Center (CGC) (NIH P40 OD010440) gave during this project.

I thank the advice and guidance from members of the laboratories of Dr. Calixto and Dr. Chiu, especially Arles Urrutia (Ph.D) and Camila Morales (M.S.). Dr. Mpodozis, from the University of Chile, was always available to help with any last-minute requirement for my experiments.

This project would mean nothing without the help of the people that let me know the worm during my first year in the doctoral program at Dr. Latorre's Laboratory, especially Luisa Soto and Dr. Karen Castillo, who gave me the space and time to enchant myself with microbiology and molecular sciences.

On a special note, the support and counseling my husband and parents gave me were cherished during this whole process. An important role was played by my rescued dogs: Tayra, Morrigan "Morita", Melisa "Melly" del Tránsito, Anansi "Anny", and Margarita "Peggy" de las Mercedes, who mean the world to me.

LIST OF FIGURES

ABBREVIATIONS AND SYMBOLS

CNS	Central Nervous System
DRG	Dorsal Root Ganglia
WD	Wallerian Degeneration
TRN	Touch Receptor Neurons
DEG/ENaC	Degenerin/Epithelial Sodium (Na^+) Channel
TM	Transmembrane region
MEC-4	Mechanosensory ion channel subunit 4
MEC-4d	abnormal Mechanosensory subunit 4
ER	Endoplasmic Reticulum
SERCA	Sarcoendoplasmic Reticulum Calcium ATPase
MCU	Mitochondrial Calcium Uniporter
CICR	Calcium-Induced Calcium Release
RyRs	Ryanodine-Receptor channels
IP3R	Inositol 1,4,5-trisphosphate Receptor
VDAC	Voltage-Dependent Anion Channels
ROS	Reactive Oxygen Species
MAMs	Mitochondria-associated membranes
MIM	Mitochondrial Inner Membrane
MOM	Mitochondrial Outer Membrane
DAF-16	abnormal DAuer Formation gene 16, Forkhead box O1 Homolog
NMAT-2	Nicotinamide Nucleotide Adenylyl transferase 2
EGTA	Ethylene glycol-bis (β-aminoethyl ether)-N,N,N′,N′-tetraacetic acid
LB	Luria-Bertani broth
NGM	Nematode Growth Media
SDS	Sodium Dodecyl Sulfate
WT	wild type

L2	Larval stage 2
AVM	Anterior Ventral Microtubule cell
ALM	Anterior Lateral Microtubule cell
PLM	Posterior Lateral Microtubule cell
GFP	Green Fluorescent Protein
RNAi	Ribonucleic Acid interference (RNAi)
AxW	Axon WT-like
AxL	Axon Long
AxT	Axon Truncated
AxØ	Axon absent
AxØ-S	Axon absent and no soma
GECI	Genetically Encoded Calcium Indicators
MPM	Multi-Photon Microscopy
µm	micrometer
nm	Nanometer
µL	microliter
µg	microgram
µs	microsecond
mL	milliliter
mM	Millimolar
mW	milliwatt
MW	Molecular Weight
rpm	Revolutions per Minute

INDEX

RESUMEN

Se ha demostrado que la diapausa promueve la regeneración funcional de las neuronas en *Caenorhabditis elegans*, lo que ocurre predominantemente durante los primeros tres días de diapausa y alcanza su punto máximo en el séptimo día. La regeneración inducida por diapausa depende de DLK-1, una MAPK3 conservada en la evolución que depende del calcio para activarse, la que se ha mostrado necesaria para el nuevo crecimiento de axones después de otros tipos de lesiones neuronales. Nuestro modelo de estudio es un animal mutante que exhibe una ganancia de función dominante en una degenerina, MEC-4d, expresada en las neuronas mecanosensoriales de *C. elegans*. La expresión constitutiva de la degenerina mutante provoca la degeneración de estas neuronas, denominadas neuronas receptoras del tacto. MEC-4d es parte de una familia de canales, también llamados Canales de Sodio Epiteliales (ENaC), conservados a través de la filogenia.

En este trabajo, encontramos que el calcio es necesario para la degeneración, la regeneración inducida por diapausa y la neuroprotección inducida por dietas específicas. Consistentemente, encontramos que el uniporter de calcio mitocondrial y la bomba de calcio SERCA son importantes para la preservación de condiciones similares al estándar. También encontramos que la diapausa genera el alargamiento de las mitocondrias y un incremento en su número, lo que puede estar causado por el cambio metabólico inducido durante el arresto del desarrollo. Nuestros resultados sugieren que la regeneración inducida por diapausa se relaciona profundamente con las funciones intracelulares, lo que es consistente con otros trabajos en enfermedades degenerativas y otras manipulaciones que mejoran la función mitocondrial.

ABSTRACT

Diapause has been shown to promote the functional regeneration of neurons in *Caenorhabditis elegans*, which predominantly occurs during the first three days of diapause reaching a peak on the seventh day. Diapause-induced regeneration is dependent on DLK-1, a conserved MAPK3 dependent on calcium to activate, required for the regrowth of axons after other kinds of neuronal injuries. Our model of study is a mutant animal that exhibits a dominant gain-of-function mutation in a degenerin channel, MEC-4d, expressed in the mechanosensory neurons of *C. elegans*. Mutant degenerin constitutive expression causes the degeneration of these neurons, called Touch Receptor Neurons. MEC-4d is part of a family of channels called Epithelial Sodium Channel (ENaC)/degenerin (DEG), conserved through phylogeny.

In this work, we found that calcium is necessary for degeneration, diapause-induced regeneration, and neuroprotection induced by diet. We consistently found that mitochondrial calcium uniporter and SERCA pump are important for preserving WT-like conditions. We also found that diapause generates the elongation of mitochondria and an increment in their numbers, which may be supported by the metabolic shift induced during the developmental arrest. Our results suggest that diapause-induced regeneration relies deeply on intracellular functions, which is consistent with other works in degenerative diseases and other manipulations that improve mitochondrial function.

INTRODUCTION

General considerations about degeneration and regeneration

At the beginning of the last century, there was a widespread belief that inside the Nervous system "everything may die, nothing may be regenerated" (Colucci-D'Amato *et al*., 2006). This was considered a solid truth for the Central Nervous System of "most derived" animals, but as Cajal (1914) foretold, the expansion of knowledge has let us look into the discrete neurogenic areas in the Nervous System of different Metazoans, even humans, and elucidated some of the conditions to promote the recovery of a system affected by injury or illness (Temple and Alvarez-Buylla, 1999; Gritti *et al*., 2002; Schmitt *et al*., 2003; Al-Majed *et al*., 2004; Lie *et al*., 2004; McPhail *et al*., 2004; Colucci-D'Amato *et al*., 2006; Chen *et al*., 2015a; Zhou *et al*., 2015; Boldrini *et al*., 2018; Sorrels *et al*., 2018; Moreno-Jiménez *et al*., 2019; Flor-García *et al*., 2020; Han *et al*., 2020; Terreros-Roncal *et al*., 2021; Lu *et al*., 2022).

The Central and Peripheral Nervous Systems are susceptible to environmental injuries that could produce severe damage, inflammation, and the death of the cell (Stoll *et al*., 2002; Rock and Kono, 2008; Han *et al*., 2020; Zhang *et al*., 2020), but it is the Central Nervous System (CNS) of Mammals or Therians the one that does not recover spontaneously after the damage (Huebner and Strittmatter, 2009; Varadarajan *et al*., 2022).

There are two kinds of cellular recovery after a lesion or injury: regeneration, and regrowth. While regeneration restores the interrupted neuronal connectivity resulting in functional recovery (Namsolleck *et al*., 2015), regrowth involves repairing lost connectivity but not restoring function completely. An example of regeneration in vertebrates occurs in damaged limbs of salamanders where cells adjacent to the injury site de-differentiate to build bone, skin, and muscle in a process that recapitulates embryonic development (Morrison *et al*., 2006; Kragl *et al*., 2009; Khan and Crawford, 2021). Regrowth occurs in our liver where mature cells proliferate, a phenomenon called compensatory hyperplasia (Michalopoulos and DeFrance, 1997; Reuben, 2004; Michalopoulos, 2007; Zhang *et al*., 2008; Marongiu *et al*., 2017).

Mammalian CNS components such as the brain, and the Central component of the Dorsal Root Ganglia (DRG) exceptionally exhibit regrowth or regeneration (Cajal, 1914; Varadarajan *et al*., 2022), in general at early developmental stages (Kunkel-Bagden *et al*. 1992). The classic description of neuronal death is Wallerian Degeneration (WD), which occurs when the axon degenerates in a retrograde direction, from distal to proximal (Waller, 1950; 1981; 1985). This takes place in response to a crash or injury and throughout the distal nerve stump denervated by disconnection from the soma of the neuron, and the generation of an inflammatory response (Waller, 1850; Cajal, 1914; Kury *et al*., 2001; Stoll *et al*., 2002; Cámara-Lemarroy *et al*., 2010; Han *et al*., 2020). Wallerian-like degeneration occurs in many neurodegenerative diseases (Martini *et al*., 2008; Hilliard, 2009; Coleman and Freeman, 2010; Conforti *et al*., 2014), and there are several models described to study this phenomenon (Adalbert *et al*., 2005; Hilliard, 2009), one of them is the worm *Caenorhabditis elegans*.

Wallerian degeneration in *C. elegans*

C. elegans is well known for its many advantages as a behavioral and genetic model organism (Kaletta and Hengartner, 2006). The animal has 300 neurons, represented by 118 subtypes, ranging from motor to sensory neurons (Sulston and Horvitz, 1977; Sulston *et al*., 1983; White *et al*., 1986; Skuhersky *et al*., 2022). Examples of the latter are mechanosensory and chemosensory neurons.

Neurons known as Touch Receptor Neurons (TRNs) correspond to the mechanosensory type (Schafer, 2015), which are specialized in the gentle touch response (Chen and Chalfie, 2014). These neurons can be affected by WD when expressing a specific mutation of a degenerin (Driscoll and Chalfie, 1991; Brown *et al*., 2007), and under specific conditions, can regenerate from early and late degeneration (Calixto *et al*., 2012). One of the TRNs can undergo regeneration in most cases, the Anterior Ventral Microtubule cell or AVM (Wormbase ID: WBbt:0003832). The mutant who exhibits WD has a dominant mutation known as *e1611* (A713T) in the gene *mec-4* (known as *mec-4d*) (Driscoll and Chalfie, 1991; Huang and Chalfie, 1994; Bianchi *et al*., 2004; Park *et al*., 2008; Calixto *et al*., 2012; Chen *et al*., 2016).

Two subunits of MEC-4 and one of MEC-10 are the pore-forming units of the mechanosensory complex present in the TRN (Chen *et al*., 2015). This channel transduces mechanical energy to a sodium current (O'Hagan *et al*., 2005). The gain-of-function mutation *mec-4d* (e1611) is proposed to cause the channel to be constitutively open, which lead to increments of intracellular calcium concentration which in turn promotes the exposure of phosphatidyl serine residues, a death signal, and the degeneration of TRN (Bianchi *et al*., 2004; Furuta *et al*., 2021). MEC-4d is one of the DEGenerins of the worm and belongs to the Epithelial Sodium Channel/DEGenerin (DEG/ENaC) family of proteins that are conserved throughout evolution (Kellenberger and Schild, 2002; Jasti *et al*., 2007).

It has been described that changing a small amino acid for a bulkier one at the end of transmembrane segment 2 (TM2) of DEG/ENaC perturbs the gating (Jasti *et al*., 2007; Brown *et al*., 2008). Changes in TM2 alter other regions of the channel including the selectivity filter, solvent-accessible surface area, gating of the channel, and stability (Jasti *et al*., 2007; Brown *et al*., 2008). In the case of MEC-4d, this shift includes a supposed change in permeability which leads the channel to generate an intracellular increment of calcium, detected by the subsequent trigger of chlorine currents (Bianchi *et al*., 2004); it has been shown that this rise of the cation and the later mecrosis of the cells, is dependent on the activity of Ryanodine-Receptor channels (Furuta *et al*., 2021). This alteration disrupts the sensorial function of the channel, and it becomes a pro-degenerative stimulus for all TRN due to the increase of calcium concentration causes the activation of proteases, an increase of oxidative stress, and at later events, the energetic collapse of the cell (Xu *et al*., 2001; Calixto *et al*., 2012).

The AVM connects via chemical and electrical synapses with the AVD, PVC, and AVB interneurons, which intermediates the connection of the sensorial neuron with the motor neuron and finally muscles (Li *et al*., 2011a; Maguire *et al*., 2011; Piggott *et al*., 2011; Pirri and Alkema, 2012; Sakamoto *et al*., 2021). The functionality of the neuron can be tested by a gentle touch, using an

eyelash, in the anterior region of the worm (Chalfie and Sulston, 1981). If the AVM neuron is functional, the animal responds to touch by moving backward. If the AVM is not functional the animal is unresponsive (Faumont *et al*., 2012; Cohen and Sanders, 2014; Campbell *et al*., 2015). The AVM is one of the TRNs, which is born post-embryonically, at 12 hours after hatching (Chalfie, 1990). In *mec-4d* animals, the AVM begins to die immediately after the birth of the cell, in a stereotyped fashion (Calixto *et al*., 2012).

In *Xenopus laevis* oocytes, a heterologous expression system (Theodoulou and Miller, 1995; Marchant, 2018), it has been observed that worm proteins such as MEC-10 and MEC-19 reduce sodium currents of the MEC-4d channel (Chen *et al*., 2016b). Paraoxonase-like proteins, such as MEC-6 promote the accumulation of channels in the oocyte membrane (Chen *et al*., 2016a). At the same time, MEC-2 and MEC-6, proteins with high identity to mammal proteins, increase the currents of the MEC-4d channel (Brown *et al*., 2008; Chen *et al*., 2015b). This suggests that MEC proteins participate in different ways in degenerative signals associated with calcium influx.

The consequences of this process affect the dynamics of microtubule (MEC-7 and MEC-12 proteins) which can be rescued using overexpression of NMAT-2 (Calixto *et al*., 2012), a protein that generates the contraction of the axon in other models (Wang *et al*., 2012). In this condition, neither Sarcoendoplasmic Reticulum Calcium ATPase (SERCA) nor Mitochondrial Calcium Uniporter (MCU-1) pumps are enough to prevent ionic dyshomeostasis (Calvo-Rodriguez *et al*., 2020; Calvo Rodriguez and Bacskai, 2021). All these processes in parallel with the rise in osmotic pressure, leads to necrotic death.

Degeneration begins with the increase of cytoplasmic calcium and the process called "Calcium-induced calcium release" (CICR) mediated by calcium-permeable ion channels located at the Endoplasmic Reticulum, such as Ryanodine-receptor channels (RyRs), also known as *unc-68* in *C. elegans*, which is expressed in different isoforms in different tissues (Maryon, *et al*., 1996; Marques *et al*., 2020). Other Reticular mediators of *mec-4d* degeneration described are calreticulin (*crt-1*), a calcium-binding protein located in the lumen of the ER (Xu *et al*., 2001). In a nematode presenilin mutant (codified by mutation *ar131* and *ty11* of *sel-12*), a model for Alzheimer's disease, elevated calcium in ER, leads to mitochondrial oxidative stress due to increment of mitochondrial respiration (Sarasija *et al*., 2018), suggesting that calcium increments can trigger mitochondrial effects.

It has been shown by electron microscopy that there exists interorganellar connectivity between mitochondria and ER (Copperland and Dalton, 1959; Csordás *et al*., 2018), this information has been formulated as Mitochondria-associated membranes (MAMs) theory, which associates the presence of these contact regions with the accumulation of transmembrane proteins involved in senescence, aging, autophagia, and neuronal degeneration (Vance *et al*., 2014; Rodríguez-Arribas *et al*., 2017; Janikiewicz *et al*., 2018; Yang *et al*., 2020; Calvo-Rodriguez and Bacskai, 2021).

The connection between ER and mitochondria is stabilized by mitofusin present in both membranes, which favors the formation of a channel complex composed of inositol 1,4,5-trisphosphate receptor (IP3R) and Voltage-Dependent anion channels (VDAC), which connect with Mitochondria Calcium Uniporter (MCU) channels in mitochondria cristae (Fig. 1); this 3-channel

complex generates a by-pass for ions between the organelles (Decuypere *et al*., 2011; Rodríguez-Arribas *et al*., 2017). These reports suggest that blockade of calcium accumulation inside ER can indirectly reduce oxidative stress increase in mitochondria. Similar effects have been described for pharmacological reduction of ER stress by Loureirin B, which has shown improvement of neurodegenerative conditions in murine models of acute damage (Wang *et al*., 2019).

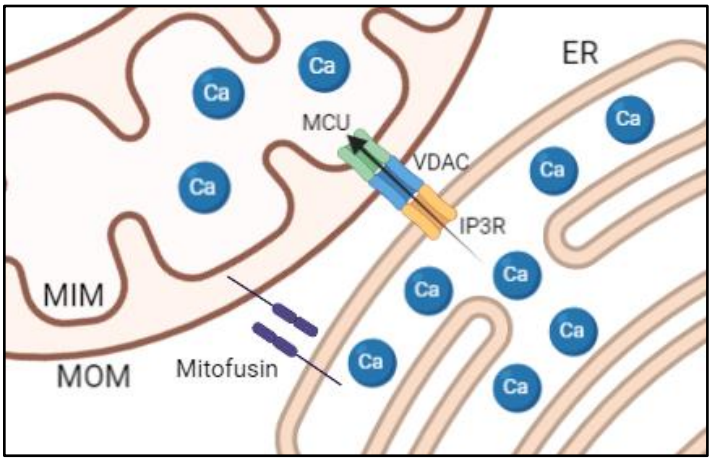

Figure 1: Schematic depicting the interoganelle connectivity between Endoplasmic Reticulum and Mitochondria. This type of interaction is known as Mitochondria-associated membranes (MAMs). ER: Endoplasmic Reticulum, MIM: Mitochondrial Inner Membrane, MOM: Mitochondrial Outer Membrane, MCU: Mitochondrial Calcium Uniporter, VDAC: Voltage-Dependent Anion Channel, IP3R: Inositol 1,4,5-triPhosphate Receptor (Created with BioRender.com).

When the worm stands still

The dauer stage of *C. elegans* is an arrest in development that occurs after the second molt in response to unfavorable environmental conditions, in which the worm can survive almost ten times its normal lifespan (Ewald *et al*., 2018). Diapausing animals have reduced metabolic rates, are resistant to oxidative stress due to elevated levels of superoxide-dismutase, have elevated levels of several heat shock proteins, and can protect and regenerate broken axons (Anderson, 1982; O'Riordan and Burnell, 1989, 1990; Dalley and Golomb, 1992; Hu, 2007; Calixto *et al*., 2012). It has been determined that when the worm is a dauer larva exhibits an extraordinary capacity to regenerate (Caneo *et al*., 2019; Park *et al*., 2021). Specifically damaged TRN, such as the AVM, can regenerate from a soma alone (Caneo *et al*., 2019).

The AVM of *C. elegans* is a complete and simple model to study WD and axon regeneration with an associated behavioral test (Calixto *et al*., 2010; Calixto *et al*., 2012; Caneo *et al*., 2019). A gentle touch is an important sensory input to facilitate escape from predacious fungi. Worms with touch response defects are more likely to be preyed on than wild type (Maguire *et al*., 2011; Pirri and Alkema, 2012). Protection and regrowth of TRNs expressing a degenerin is an energetically costly process. Despite this, dauers spend valuable energy to save them. It has been shown that *mec-4d*

dauers die significantly earlier than wild-type (Caneo *et al*., 2019), suggesting that the cost of maintaining a *mec-4d* expressing cell is at the expense of dauer lifespan.

In specific cases, like recovery after exposure to desiccation, mechanoreceptors might be crucial. It has been shown that under desiccation conditions *C. elegans* can activate molecular strategies, such as trehalose synthesis (Erkut *et al*., 2011, 2012, 2013) in order to resist water loss. These changes in osmolarity induce deformations of the cuticle, which in turn causes deformations on the hypodermis near the AVM of *C. elegans*; this change can be sensed by TRN (Goodman, 2006).

In dauers, elements that promote the regeneration and a healthy condition converge, like inhibition of mitochondrial permeability transition pore, overexpression of superoxide-dismutases and heat shock proteins, and Nicotinamide Nucleotide Adenylyltransferase (NMAT-2). Conditions that are involved in daf-16/FOXO signaling (Calixto *et al*., 2012); more importantly, it has been shown that DAF-16 can induce metabolic remodeling, along with the effects of dauer induction over (Artal-Sanz and Tavernarakis, 2009; Lourenço *et al*., 2015; Lourenço and Artal-Sanz, 2021), suggesting metabolic implications associated with neuronal regeneration (Zečić and Braeckman, 2020).

Energetic considerations in a regenerative context

Mitochondria have been known as the powerhouse of the cell (Siekevitz, 1957), but their involvement in different cellular and systemic processes is undeniable (Sims and Muyderman, 2010; Li *et al*., 2011b; Ahlqvist *et al*., 2015; Calaza *et al*., 2015; Luongo *et al*., 2017), as it has been shown that they even participate as "microlens" in photon transduction in the retina (Ball *et al*., 2022).

In the context of degeneration/regeneration balance, regrowth and maintenance of the axon require the preservation of calcium homeostasis and energy production, which is more crucial in chronic damage cases, this role has been appointed for mitochondria (Pathak *et al*., 2013; Calaza *et al*., 2015; Luongo *et al*., 2017; Sheng, 2017; Chamberlain and Sheng, 2019; Kiryu-Seo and Kiyama, 2019). Mitochondria not only provide energy and metabolites, but they also move to damaged regions (Han *et al*., 2016), which improves recovery (Zhou *et al*., 2015). Importantly, when mitochondrial function is impaired, mitochondria can not provide enough energy to sustain normal function, even less regeneration. Since regenerative processes also consume energy, generating more stress for the neuron (Chinopoulos and Adam-Vizi, 2010). Moreover, mitochondrial effects associated with neuronal degeneration manifestation include impairment of lipid synthesis and transport, Ca^{2+} transport, and consequences of the interruption of several metabolic pathways (Vance *et al*., 2014; Zhang *et al*., 2020), meaning that mitochondrial function in a degenerative context can be extensively affected.

Recently, it has been suggested that energetic stress is crucial for degeneration since cells that undergo this process are generally high energy-demanding cells, in which case, the first step involves mitochondrial damage (Pacelli *et al*., 2015; Muddapu *et al*., 2020).

A fistful of calcium indicators

The degeneration of the AVM depends on intracellular calcium concentration. While the pore domain of MEC-4, the wild-type form, is selective for sodium, when mutated to MEC-4d, the channel permeates both sodium and calcium. Since an increase of cytoplasmic calcium induces CICR, this shift in permeability of the channel results in higher concentrations than those physiologically admitted. To measure calcium increase, a calcium indicator is needed.

At present, there exist Fluo-4, Fura-2, the family of Cameleons, and GCaMP (Grynkiewicz *et al*., 1985; Miyawaki *et al*., 1999; Gee *et al*., 2000; Nakai *et al*., 2001; Yang *et al*., 2018). For *C. elegans* "Genetically Encoded Calcium Indicators" (GECI) such as GCaMP are commonly used (Kerr, 2006; Kerr and Schafer, 2006; Chung *et al*., 2013). GCaMP proteins are engineered from the fusion of green fluorescent protein (GFP), calmodulin (CaM), and a peptide sequence from myosin light chain kinase (M13) (Nakai *et al*., 2001). Each new generation of sensors increases the sensibility and specificity (Yang *et al*., 2018).

Currently, several GCaMP encoded strains of *C. elegans* are available from the *C. elegans* Genetic Center (CGC) at Minnesota University (NIH P40 OD010440). The observation of calcium dynamics, especially related to spontaneous activity, requires high temporal and spatial resolution, which can be increased using electrical devices directly in contact with the sample or Photomultiplier Modules (PMT). Those can increase the quantum efficiency and reduce noise for imaging (Svoboda and Yasuda, 2006). These conditions are found in multi-photon microscopy (MPM) (Zipfel *et al*., 2003; Waharte *et al*., 2006; Corbin *et al*., 2014; Mondal, 2014). As another bonus, Multi-Photon Microscopy allows thin optical cuts which can also reduce noise (König, 2000) coming from worm body autofluorescence. In short, the implementation of Two-photon microscopy for calcium imaging in worms increases the reliability and detection of the measurements.

HYPOTHESIS AND OBJECTIVE

Hypothesis:

- Intracellular arrangements of organelles and calcium transporters, *sca-1,* and *mcu-1*, induced by diapause are required for the regeneration of AVM neurons in *Caenorhabditis elegans*

General Objective:

- To determine the contribution of intracellular calcium transporters and organelles in axonal regeneration induced by diapause

Specific Objectives:

1. To reveal the effects of diapause on intracellular calcium concentration and channel expression in TRN *in vivo.*

1.1 To test the changes in cytoplasmic calcium concentration of the MEC-4d channel using calcium imaging:

Using the GCaMP transgenic *C. elegans* to reveal the effects of diapause in the activity of the channel.

1.2 To determine changes of MEC-4d channel expression induced by dauer entrance:

Using the reporter *mec-4p::mec-4::gfp* to reveal changes in channel puncta in different larval stages.

2. To elucidate the dependence of calcium management in the regeneration of AVM

2.1 To uncover the dependence of axonal regeneration on intracellular calcium in diapause:

Culture of *mec-4d* animals in absence of calcium in the media and follow degeneration/regeneration process.

2.2.1. To reveal effects induced by diapause in organelle related to degeneration/regeneration balance:

Silencing of intracellular calcium transporters during development and diapause using *C. elegans* RNA interference library.

2.2.2. To find out the dependence of regeneration induced by the developmental arrest in intracellular dynamics:

To test the role of organelle related to intracellular calcium management, specifically the Mitochondria, to understand the changes associated with diapause-induced regeneration.

MATERIALS AND METHODS

C. elegans growth and maintenance

Wild type, transgenic and mutant *C. elegans* were maintained at 20°C as reported previously (Brenner, 1974; Stiernagle, 2006). Nematode strains used are the following: wild type (N2), TU3755 (*uIs58 [Pmec-4mec-4::yfp]*) (Árnadóttir *et al.*, 2011; Petzold *et al*., 2013), WCH41 (*uIs58 [Pmec-4mec-4::yfp]; mec-4d[e1611]*) (Urrutia *et al*., 2020), TU2773 *[uIs31(Pmec-17mec-17::gfp);mec-4d(e1611)X*], WCH 6 [*uIs71[Pmec-18sid-1; Pmyo-2mcherry*], *uIs31[Pmec-17mec-17::gfp], sid-1[pk3321], mec-4d[e1611]*] (Calixto *et al*., 2010), AQ3236 [*ljSi2 [mec-7::GCaMP6m::SL2::TagRFP + unc-119(+)] II*] (Cho *et al*., 2017), WCH37 [*ljSi2 [mec-7::GCaMP6m::SL2::TagRFP + unc-119(+)] II; e1611 [mec-4d] X*], js609 [*jsIs609:Is[Pmec-4::MLS::gfp]*] (Fatouros *et al*., 2012*)*, WCH42 [*jsIs609:Is[Pmec-4::MLS::gfp]; mec-4d [e1611]*]. All animals were maintained in *E. coli* OP50 before using or feeding other bacteria.

Bacterial growth

E. coli OP50 and HT115 bacteria were grown overnight on Luria-Bertani (LB) agar plates at 37°C from glycerol stocks. The next morning, a large amount of the bacterial lawn was inoculated in LB broth and grown for 6 hours on agitation at 200-220 rpm at 37°C. 300 µL of bacterial culture was seeded onto 60 mm Nematode Growth Media (NGM) plates and allowed to dry overnight. Over-day growth is general for all bacterial strains used, including dsRNA bacteria.

Count of MEC-4 puncta

Between 30-60 newly hatched animals were placed in either *E. coli* OP50 or HT115, and images were taken after 24 hours. Dauers were obtained one week later from the same plate by Sodium Dodecyl Sulfate (SDS) 1% treatment, lay on an NGM plate without bacteria, and were taken after crawling outside. Living animals were mounted on 2% agarose pads and photographs were taken at different focal points, each set was associated with an animal, and counted separately using ImageJ. To measure the length of the axons, the scale was set on ImageJ using a Neubauer chamber. The process was repeated in 21 to 37 individuals for each replicate.

Feeding RNAi

Bacterial clones from Ahringer Library were taken from glycerol stocks and grown overnight on LB-agar plates containing carbenicillin (PhytoTechnology Laboratories) (50 µg/mL) and tetracycline (PhytoTechnology Laboratories) (25 µg/mL) (Timmons and Fire, 1998; Timmons *et al*., 2001; Daegelen *et al*., 2009). Isolated bacteria are grown subsequently at least 2 times in LB media with antibiotics for selection. The next morning, a chunk of bacterial lawn was grown on liquid LB containing carbenicillin (Santa Cruz Biotechnology) (50 µg/mL) for 6 hours at 200-220 rpm. NGM plates were prepared including 1mM of IPTG and 400 µL of bacterial growth was seeded, covering all plate surfaces. Plates were used before 6 days to ensure silencing conditions.

RNAi in animals in development

Over dry plates, between 30 – 60 newly hatched animals were placed on RNAi plates. Silencing was tested on two strains, *mec-17::GFP; mec-4d*, which conduces to systemic knockdown in the *mec-4d* context, and *mec-18::sid-1; mec-17p::GFP; mec-4d; sid-1*, which enhances silencing exclusively on TRNs (Calixto *et al*., 2010). AVM morphology was scored after 72 hours. This experiment is replicated 3 or 4 times for each gene, and values correspond to the percent of animals that have the indicated morphology from each replicate.

Multiphoton imaging

Multi-photon microscopy gives high temporal and spatial resolution to image living worms. We use levamisole hydrochloride (MW=240.73 g/mole) to paralyze animals, either at 1mM or 20mM concentration, depending on the stage. We use a 12 mm round coverslip to cover a chunk of 2% agarose in which animals are laid on a drop of paralyzing solution (Fig. 2). The two-photon microscope is set up to excite the GECIs in the infrared at 980nm wavelength. Laser power was set between 15 to 40mW at the objective, and we collected the emitted red and green signals using photomultiplier tubes at top of the sample. Resolution for recordings was set at 128x128 pixels, and a dwelling time of 8 µs. Each recording was set for 20 seconds, and three trials were performed.

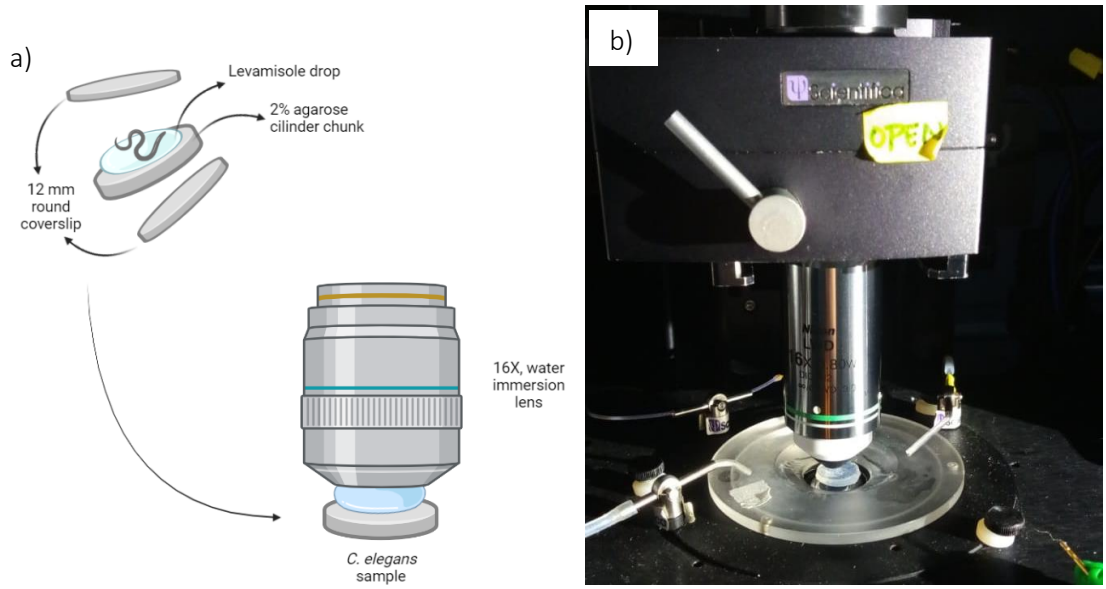

Figure 2: Montage of *C. elegans* for Two-Photon imaging. a) Schematics that show the procedure to mount *C. elegans* to observe under Two-Photon conditions (Created with BioRender.com), b) Photograph of actual montage.

Dauer synchronization

As it was described previously (Caneo *et al*., 2019), after the detection of a few dauers by direct observation, plates were washed using SDS 1% and centrifuged for 2 minutes at 4000 - 6000 rpm. The supernatant was removed, and the worms were washed for 15 minutes with a solution of SDS 1% with 2,5 µg/mL of Carbenicillin (Santa Cruz Biotechnology) and 2,5 µg/mL of Amphotericin B (Fungizone, Gibco/Thermofisher). Animals were washed 3 times with sterile distilled water and antibiotics. The pellet was placed on NGM media plates and after one hour the portion of agar where the pellet was put is cut using a stainless-steel spatula, and then washed with the same mixture of sterile distilled water with antibiotics. Microbe-free worms were centrifuged for 2 minutes at 4500 rpm and placed in Cell Culture Plates (TrueLine®) with the same mixture. The media was replaced every 2 weeks (Fig. 3).

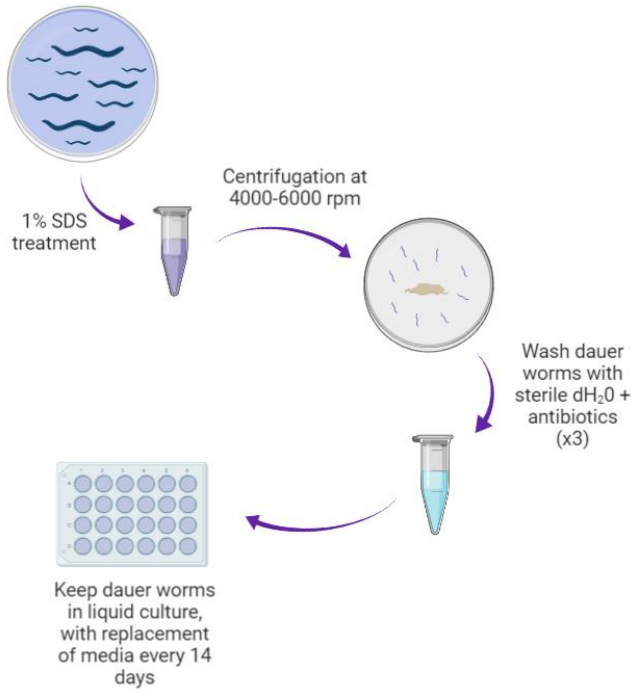

Figure 3: Schematics showing the protocol for dauer synchronization (Created with BioRender.com).

Feeding RNAi to dauers

The same base from the RNAi feeding applies to feed dauers with dsRNA bacteria to observe their effects during diapause; due to dauer restricted conditions, it may be difficult to recover translation levels during diapause, and the accumulation of RNAi in the egg should be enough to produce effects on protein synthesis (Grishok *et al*., 2000; Grishok, 2005). We use a two-

generation treatment without replenishment of food, to generate starvation in the population (Caneo *et al*., 2019). For this protocol only, we started with bleaching to ensure sterile conditions. By observing plates, we detected the first day of dauers on the plate; animals were synchronized on day 2 or 3 depending on the number of dauers required for observation. The protocol was followed as it was described in Dauer synchronization. After some animals crawled out of the drop, 25 animals were picked to observe on the microscope. Remanent animals were maintained in liquid cultured as described previously. The experiment was replicated 3 to 4 times for each condition and values correspond to the percent of animals that have the indicated morphology in each replicate.

Culture in absence of calcium

To eliminate calcium from the culture media, calcium chloride ($CaCl_2$) was not included in the NGM media preparation. Ethylene glycol-bis (β-aminoethyl ether)-N, N,N′,N′-tetraacetic acid (EGTA) (Winkler) is added in LB broth, at 500 mM concentration, to the bacteria used to feed animals, which was grown over-day (Calixto *et al*., 2012).

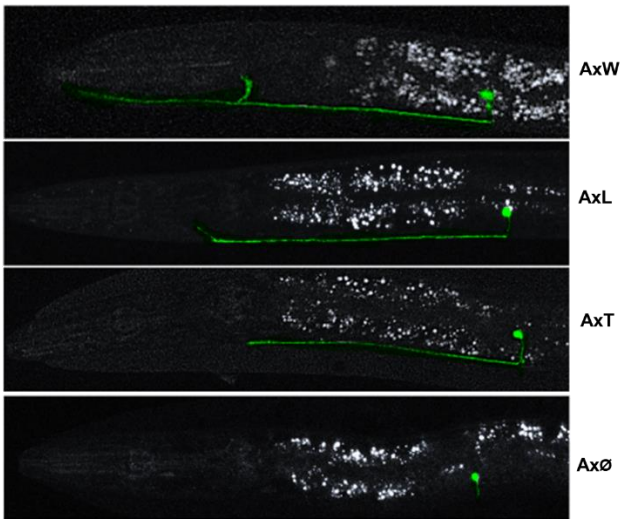

Figure 4: Progression of degeneration in a *mec-4d* mutant strain (Urrutia *et al*., 2020).

Scoring of neuronal integrity

For morphological evaluation, worms were mounted on 2% agarose pads, paralyzed with 20 mM levamisole for dauers and 1 mM for other developmental stages. Morphological categories were assigned using the same criteria as in Urrutia *et al*. (2020) (Fig. 4). Neurons with full-length axons, as well as those with anterior processes that passed the point of bifurcation to the nerve ring, were classified as AxW. Axons with only a process connected to the nerve ring were classified as AxL, and those that did not reach the bifurcation to the nerve ring were classified as AxT. Lack of axon and soma only were classified as AxØ, and the total absence was indicated as AxØ-S. Due to

requirements from parametric statistical tests, for the statistical analysis other categories than AxW are considered damaged axons (AxD).

Quantitative measurements of mitochondrial morphology

Between 30 - 60 newly hatched animals were placed in either *E. coli* OP50 or HT115, and images were taken after 24 hours. Dauers were obtained one week later from the same plate by SDS 1% treatment, lay on an NGM plate without bacteria, and were taken after crawling outside. Living animals were mounted on 2% agarose pads and photographs were taken at different focal points, each set was associated with an animal, and measured separately using ImageJ as shown (Fig. 5), and each mitochondrion length in µm was registered independently (like α, β, γ, δ, and ε). The process was repeated for 10 animals for each replicate. The scale was set on ImageJ using a Neubauer chamber.

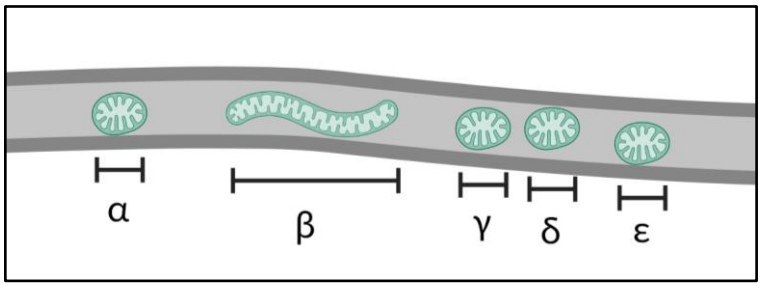

Figure 5: Schematics showing the methodology for measurement of mitochondrial length. Each value, depicted as α, β, γ, δ, and ε, was registered individually (Created with BioRender.com).

Microscopy and photography

Images were taken using DSLR Remote Pro (Breeze Systems Ltd., UK), a Canon Rebel T3i camera, and a fluorescence microscope (Nikon Eclipse Ni-U). Configuration was set up at 1/10 exposure time and ISO correction at 200 for fluorescence images. FigureJ plugin was used for multifigure arrangements and scale bar addition.

Statistical analysis

All experiments included in this work consider at least three different biological replicates. Statistical evaluation was performed using parametric statistical tests, like Welch's t-test, one or two-way ANOVA, followed by Tukey's Honestly Significant Difference, Dunnett-Tukey-Kramer Pairwise Multiple Comparison, or Dunn–Šidák correction. A parametric test requires the analysis of a set of data that has a normal distribution, which can be achieved for percentage data under dichotomous classifications, like AxW/AxD (Lunney, 1970).

RESULTS

1. To reveal the effects of diapause on intracellular calcium concentration and channel expression in TRN *in vivo*.

1.1 To test the changes in cytoplasmic calcium concentration of the MEC-4d channel using calcium imaging:

It was shown by Bianchi *et al*. (2004) that *mec-4d* has higher calcium signals than WT animals, which along with other experiments that show calcium signaling-associated proteins, like calreticulin, are absent *mec-4d* degeneration does not happen (Xu *et al*., 2001). These facts lead us to guess that axonal regeneration in dauers may require a reduction in the permeability of the channel, and by extension a reduction of cytoplasmic concentration. This idea that reducing calcium may lead to regeneration is widely spread, and the blockade of that increment can maintain cells alive (Calvo-Rodriguez *et al*., 2020).

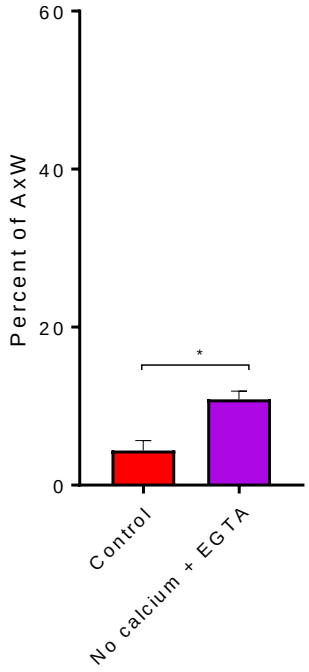

Figure 6: Culture without calcium conditions increases WT-like axons on mec-4d TRNs. Percent of AxW morphology found in the environmental absence of calcium at 24 hours post-hatching. No calcium considers not adding $CaCl_2$ to the media for nematodes (N=3 plates; t-test with Welch correction; * p= 0.0173)

We approach this problem using GECIs, specifically GCaMP6m, to qualitatively estimate calcium concentration in AVMs from wild-type and mutant strains. To standardize the signal and remove artifacts from the analysis we use tagRFP, as a fluorophore that is not affected by calcium concentration. The recording was done for 20 seconds in a 6.74 frames-per-second configuration. We record animals at dauer and L2 as control. The reasons behind this are due to the fact that at L2 AVM extend their axons in a similar pattern as axonal regeneration (Xu *et al*., 2011; Caneo *et al*., 2019), along with developmental similarities (Karp and Ambros, 2012).

Another point to assess is the calcium role in the *mec-4d* context. Previously it was described that the addition of EGTA can counter the effects of *mec-4d* degeneration at 72 hours post-hatching (Calixto *et al*., 2012), which corresponds to a different developmental stage. To standardize the treatment, we observed the effects at L2 by not adding $CaCl_2$ in the preparation of the media or adding EGTA to the food given to animals, and combination. We found that calcium removal is more effective than EGTA addition (Fig.6). The absence of $CaCl_2$ in the media in combination with EGTA addition to the bacteria will be referred to as calcium removal from here.

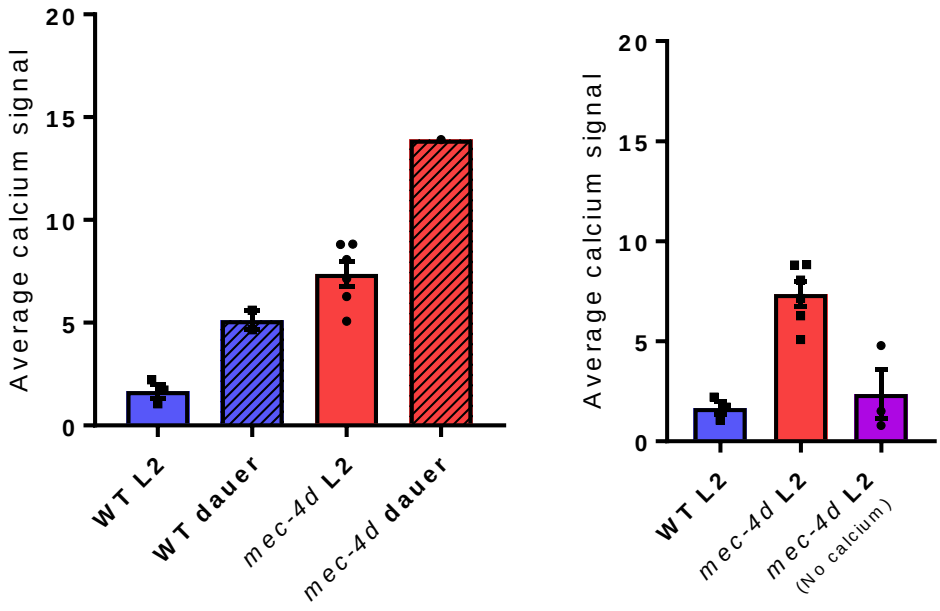

Figure 7: Calcium is increased by *mec-4d* mutation and diapause, and removal of environmental calcium restores GCaMP signals. A) Average calcium signal from the AVM soma in different strains and developmental stages. B) Comparison of average calcium signals found in L2 larval stage in WT, mutant, and mutant without calcium. (Each dot represents the average of the trials for each different individual).

The normalized signal and average of each animal are depicted in Figure 7. Our results corroborate previous observations that *mec-4d* animals tend to show higher calcium signals than WT (Bianchi *et al*., 2004). Surprisingly, we also found that diapause tends to increase calcium signals in AVM soma, both in WT and *mec-4d* strains (Fig. 7A), which can suggest that calcium increment is common and is possibly related to the metabolic changes involved (Lourenço and Artal-Sanz, 2021). Calcium removal can reduce calcium signals in *mec-4d* mutants (Fig. 7B), which, under that condition, exhibit a tendency to change into a similar signal as WT L2.

The effects of calcium removal corroborate that morphology is directly related to calcium signal during development and that the signal detected corresponds to calcium. As an increment of calcium during the regenerative stage was a surprise, it led to other interesting questions.

1.2 To determine changes of MEC-4d channel expression induced by dauer entrance:

To understand the factors that influence the presence of higher calcium concentrations in diapausing animals, we estimate the expression of the MEC-4 channel under the different developmental stages using a fusion protein of the channel and YFP, observed in a punctuated pattern in the axon of TRNs. These strains correspond to TU3755 (*uIs58 [mec-4p::mec-4::yfp]*), and WCH41 (Urrutia *et al*., 2020) (Fig. 8A). We found no differences in puncta from the axon under *E. coli* OP50 diet that may be physiologically relevant for the neuron between L2 and dauer stages, in WT and mutant animals (Fig. 8B). While the presence of MEC-4 is present in the soma, identify and measure the clusters of channels require different approach.

Can other neuroprotective or regenerative conditions induce changes in MEC-4 expression and transport to the axon membrane? We propose to repeat the measurement of puncta under a different diet, one that can elicit neuroprotection and regeneration, the *E. coli* K12-derived strain *E. coli* HT115 (Daegelen *et al*., 2009). Similar to what was reported by Urrutia *et al*., (2020), there were no major changes in MEC-4 puncta between L2 and dauer in mutants (Fig. 8C).

These results suggest neuroprotective or regenerative effects are not consequences of the reduction in the presence of the channel in the neuron membrane, which correspond to a chronic damage signal. The mechanism involves other physiological factors.

a

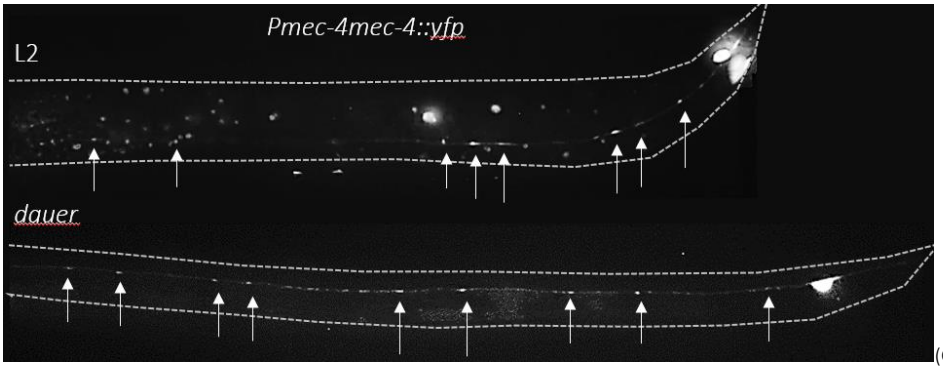

(Continues)

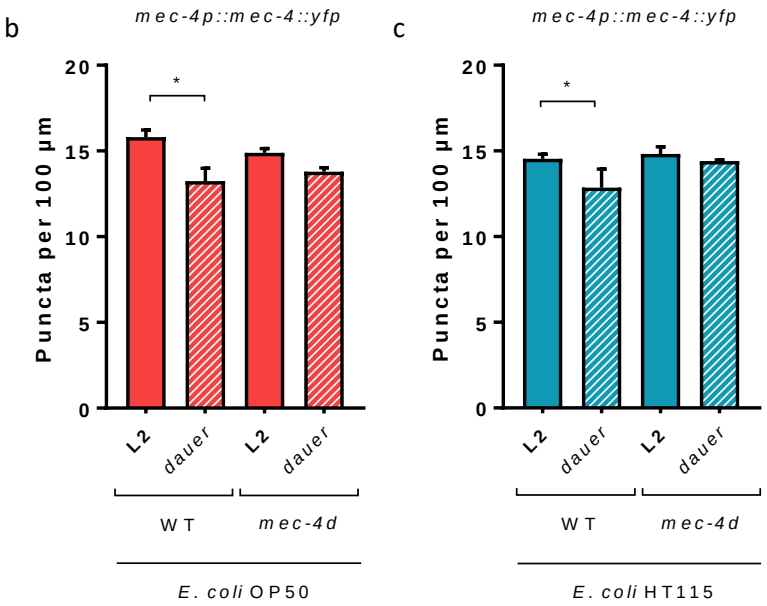

Figure 8: MEC-4 channel expression does not change in different larval stages in mutant animals. A) Representative image of WT animals (*uIs58 [mec-4p::mec-4::yfp]*), depicting the measurement method in L2 and dauer animals. B) Number of puncta standardized by axon length of L2 and dauer in *E. coli* OP50 diet. C) Number of puncta standardized by axon length of L2 and dauer in *E. coli* HT115 diet.(N=3 plates; one-way ANOVA *p<0.05).

2. To elucidate the dependence of calcium management in the regeneration of AVM

2.1 To uncover the dependence of axonal regeneration on intracellular calcium in diapause:

As previous results show, even when calcium is increased it does not lead only to necrotic death, and these calcium levels are independent of channel expression (Objectives 1.1 and 1.2). To understand the role of calcium in regeneration and degeneration we compared the effect of calcium limitation in media prepared without calcium in addition to EGTA (50 mM), as shown previously, and follow the degeneration rate at 24-, 48- and 72 hours post-hatching. We scored every worm's axon shape and classified them (Fig.4, Urrutia *et al.*, 2020). A similar experiment was performed during diapause, but this time we follow regeneration at 2, 7, and 14 days in diapause.

In our experiment for mutant animals, specifically TU2773 (*mec-17p::GFP*; *mec-4d*), similar to previous reports (Calixto *et al.*, 2012), the removal of calcium significantly slows the degeneration rate at 24- and 48 hours post-hatching while eating *E. coli* OP50 (Fig. 9A). New insight comes from the effects of the absence of calcium in the regenerative phase. We found that, from the very beginning of the dauer stage, animals previously cultured in plates without calcium exhibit a lower

percentage of AxW morphology in the OP50 diet (Fig.9B), compared to control and previous reports (Caneo *et al.*, 2019).

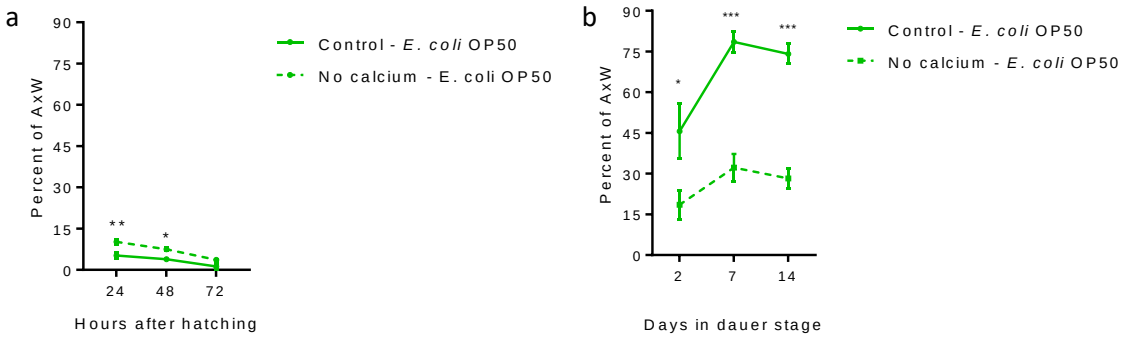

Figure 9: Calcium is necessary for degeneration and regeneration in AVM neurons in the *E. coli* OP50 diet. A) Percentage of Axon-W morphology in *mec-17p::GFP*; *mec-4d* animals at 24-, 48- and 72-hours post-hatching in E. coli OP50 culture with and without environmental calcium; **p = 0.0034, *p = 0.0284. B) Percentage of Axon-W morphology in *mec-17p::GFP; mec-4d* animals at days 2, 7, and 14 days in dauer stage, cultured before synchronization in *E. coli* OP50 with or without environmental calcium; (N=3 plates; two-way ANOVA *p=0.0185, ***p=0.0003).

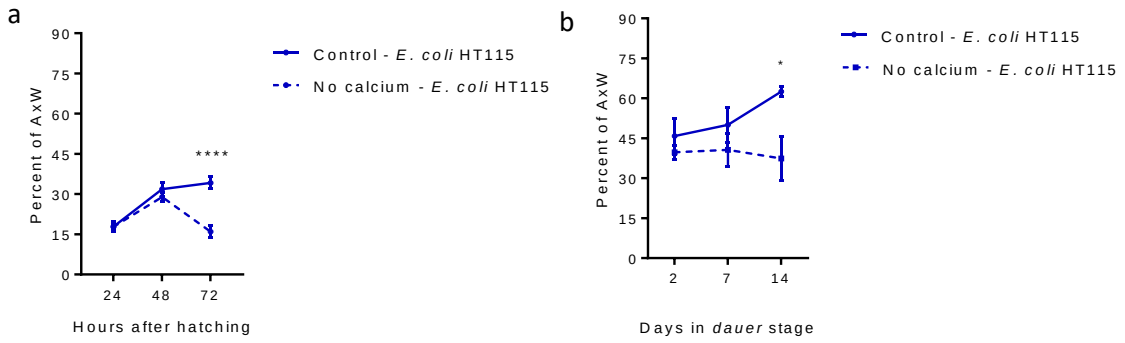

Figure 10: Calcium is necessary for neuronal protection of AVM neurons in the *E. coli* HT115 diet. A) Percentage of Axon-W morphology in *mec-17p::GFP; mec-4d* animals at 24-, 48- and 72 hours post-hatching in E. coli HT115 culture with and without environmental calcium; ****p < 0.0001. B) Percentage of Axon-W morphology in *mec-17p::GFP; mec-4d* animals at days 2, 7, and 14 days in dauer stage, cultured before synchronization in E. coli HT115 with or without environmental calcium; (N=3 plates for A), and N=3-4 plates for B); two-way ANOVA * p=0.0263)

Data from degeneration and regeneration experiments in absence of calcium led us to think that calcium may be implicated in the regenerative process and diapause's tendency to show higher calcium concentrations may be not harmful to the cell, but maybe it is a requirement to induce

repair of damaged axons. To elucidate this idea, we use another manipulation that has shown neuroprotective properties, the *E. coli* HT115 diet. For animals under this diet, we found that treatment does not slow degeneration in development, but it does affect neuroprotection at 72 hours post-hatching (Fig. 10A). In contrast to the OP50 diet, dauers do not exhibit effects of the calcium removal until day 14 of diapause (Fig. 10B).

On another point, not only is the percentage of animals exhibiting WT-like morphology reduced, but we also observed abnormalities in pathfinding after calcium removal (Fig.11A, B, and C), which may be related to calcium's role in regeneration. It has been shown that DLK-1 signaling is important for the regeneration and maintenance of regenerated axons (Yan *et al*., 2009; Nadeau *et al*., 2007; Caneo *et al*., 2019). DLK-1 is a MAPK3 that requires calcium to activate, downstream this pathway is CEBP-1. We found that systemic (Fig. 11D), nor cell autonomous (Fig. 11E), blockade of *cebp-1* significantly reduces AxW morphology, which can suggest that calcium deficiency effects are related to DLK-1/CEBP-1 signaling.

To summarize, the contrasting effects of calcium removal in different diets and different stages may suggest that the role of calcium is more dependent on neuronal context than just its cytoplasmic presence, as has been questioned previously (Kachaturian, 1989).

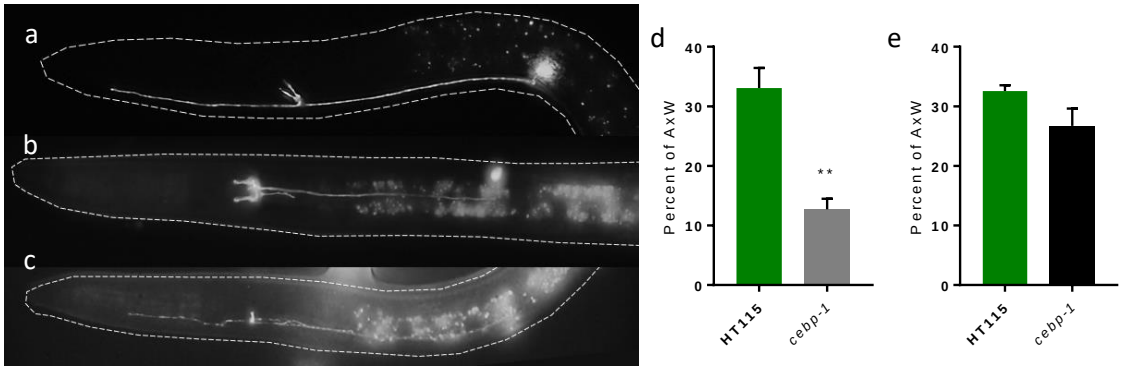

Figure 11: Abnormalities found after calcium removal treatment during diapause. A) Representative image of AVM regenerated axon in diapause. B-C) Examples of abnormalities found in dauers after growth in absence of calcium. D-E) Systemic (D) and TRNs specific (E) silencing of *cebp-1* (N=4 plates for D) and E); t-test with Welch correction **p-value= 0.0041).

2.2.1. To reveal effects induced by diapause in organelle related to degeneration/regeneration balance:

Intracellular calcium transporters have the function to recapture calcium from the cytoplasm in organelles like mitochondria and Endoplasmic Reticulum, which is important after a propagated and transient increase of calcium concentration triggered by CICR (Berridge, 1998). If these transporters are involved in AVM neuron regeneration, then a reduction in the translation of these proteins by RNAi may reveal it. We choose silencing to analyze the effect of the genes involved

due to the lethality of complete mutants of intracellular calcium transporters (Cho *et al*., 2000; Zwaal *et al*., 2001).

Mitochondria have a protein called Mitochondrial Calcium Uniporter or MCU-1, that corresponds to a pentameric structure (Oxenoid *et al*., 2016; Fan *et al*., 2018; Yoo *et al*., 2018), encoded in *C. elegans* by homonymous gene (*mcu-1*). It has been shown that mutations of this gene in *C. elegans* do not interfere in the development of different systems, but it is required for muscular regeneration after ablation (Xu and Chisholm, 2014); in contrast, *mcu-1* is not essential for neuronal regeneration after nerve axotomy (Han *et al*., 2016), but it has an important role in chronic damage models, like Alzheimer's Disease (Sarasija *et al*., 2018).

Sarco/endoplasmic reticulum Ca^{2+}-ATPase, also known as SERCA is codified in *C. elegans* by the *sca-1* gene and corresponds to an important pump that removes calcium from the cytoplasm and concentrates it in the ER which is expressed as two different isoforms (Cho *et al*., 2000; Wray, 2010; Nogami *et al*., 2021; Xu and Van Remmen, 2021). While its role in regeneration is still unclear, the mutation, silencing, and pharmacological blockade dramatically produce the death of worms, developmental arrest, and sick animals (Cho *et al*., 2000; Zwaal *et al*., 2001), while in contrast, the pharmacological treatment in adults increases their lifespan in *C. elegans* (García-Casas *et al*., 2018).

We are interested in the effects of silencing both genes in Touch Receptor Neurons (TRN) regeneration. We propose to use two different worm strains, a systemic case, TU2773 [*mec-17::GFP; mec-4d*], and a TRN-specific, WCH-6 [*uIs71(Pmec-18sid-1;Pmyo-2mcherry), uIs31(Pmec-17mec17::gfp), sid-1(pk3321), mec-4d(e1611)*], in which only neurons are affected by the silencing (Calixto *et al*., 2010).

mcu-1 and *sca-1* dsRNA bacteria are present in Ahringer Library for *C. elegans* (Fraser *et al*., 2000; Kamath *et al*., 2003; Qu *et al*., 2011). Since the Ahringer library uses *E. coli* HT115 to feed animals, we will be analyzing the effects of these proteins in a neuroprotective condition.

Our results show that the RNAi treatment of both *sca-1* and *mcu-1*, TRN-specifically, affects the protection given by HT115, in a *mec-4d* context. We found that under this type of silencing intermediate axons, such as long and truncated, are reduced, and AxW percentage is significantly reduced (Fig. 12A). In comparison, no treatment shows any significant difference in systemic silencing of selected intracellular calcium transporters (Fig. 12B). When calcium is absent, these effects are nullified (Fig. 13A and B). These results suggest that the Endoplasmic reticulum and the mitochondria balance the increase of calcium caused by MEC-4d.

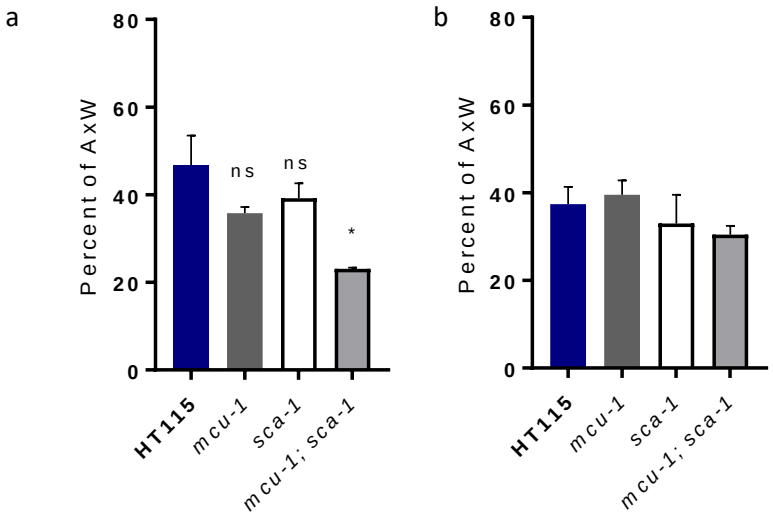

Figure 12: The absence of *mcu-1* and *sca-1* increases the degeneration rate in a *mec-4d* context in development. Percentage of Axon-W morphology in animals feeding on ds-RNA-expressing bacteria of different intracellular calcium transporters after 72 hours post-hatching in (A) TRNs specific affected strain, and (B) a systemically affected strain. (N=3-6 plates; one-way ANOVA *p< 0.05)

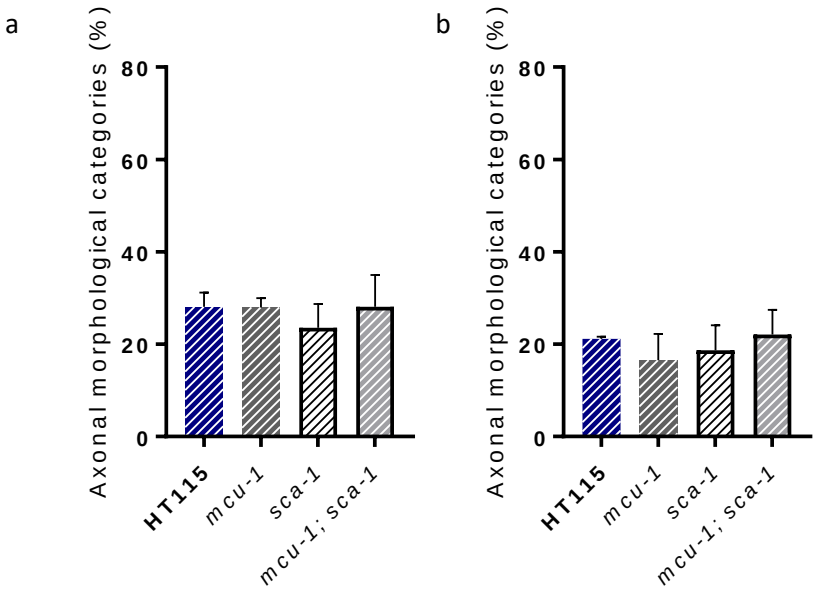

Figure 13: Absence of calcium nullifies the effect of silencing intracellular calcium transporters in a *mec-4d* context in development. Percentage of Axon-W morphology in animals feeding on ds-RNA-expressing bacteria of different intracellular calcium transporters in absence of calcium after 72 hours post-hatching in (A) TRNs specific affected strain, and (B) a systemically affected strain. (N=4 plates)

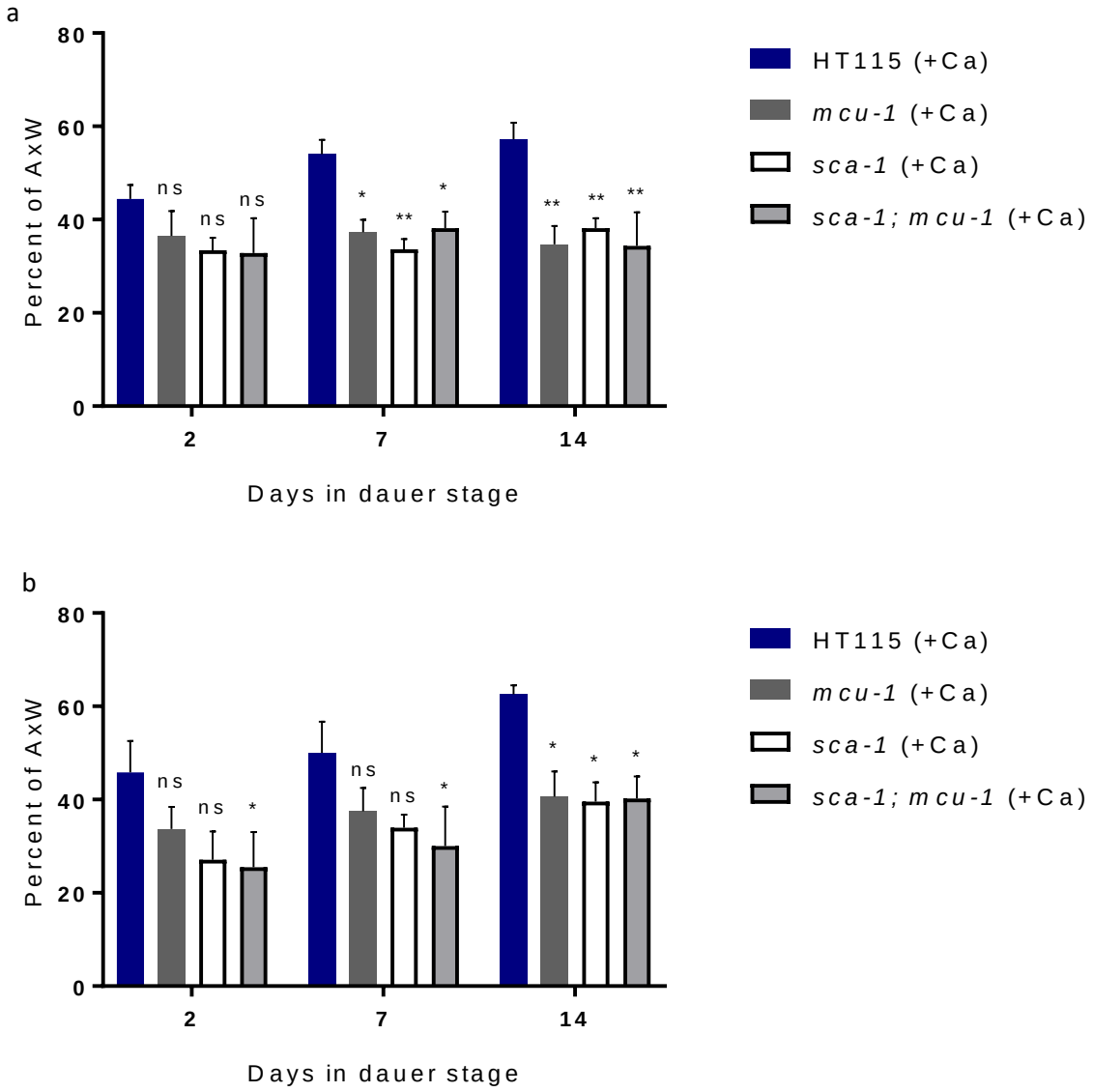

Figure 14: Mitochondrial and Reticular calcium transporters are required TRN-autonomously for regeneration promoted by developmental arrest. A-B) Percentage of Axon-W morphology in animals feeding on ds-RNA-expressing bacteria of different intracellular calcium transporters at days 2, 7, and 14 in the dauer stage in a TRNs-specific affected strain (A), and in a systemically affected strain (B).(N=4 plates; two-way ANOVA **p< 0.005, *p< 0.05).

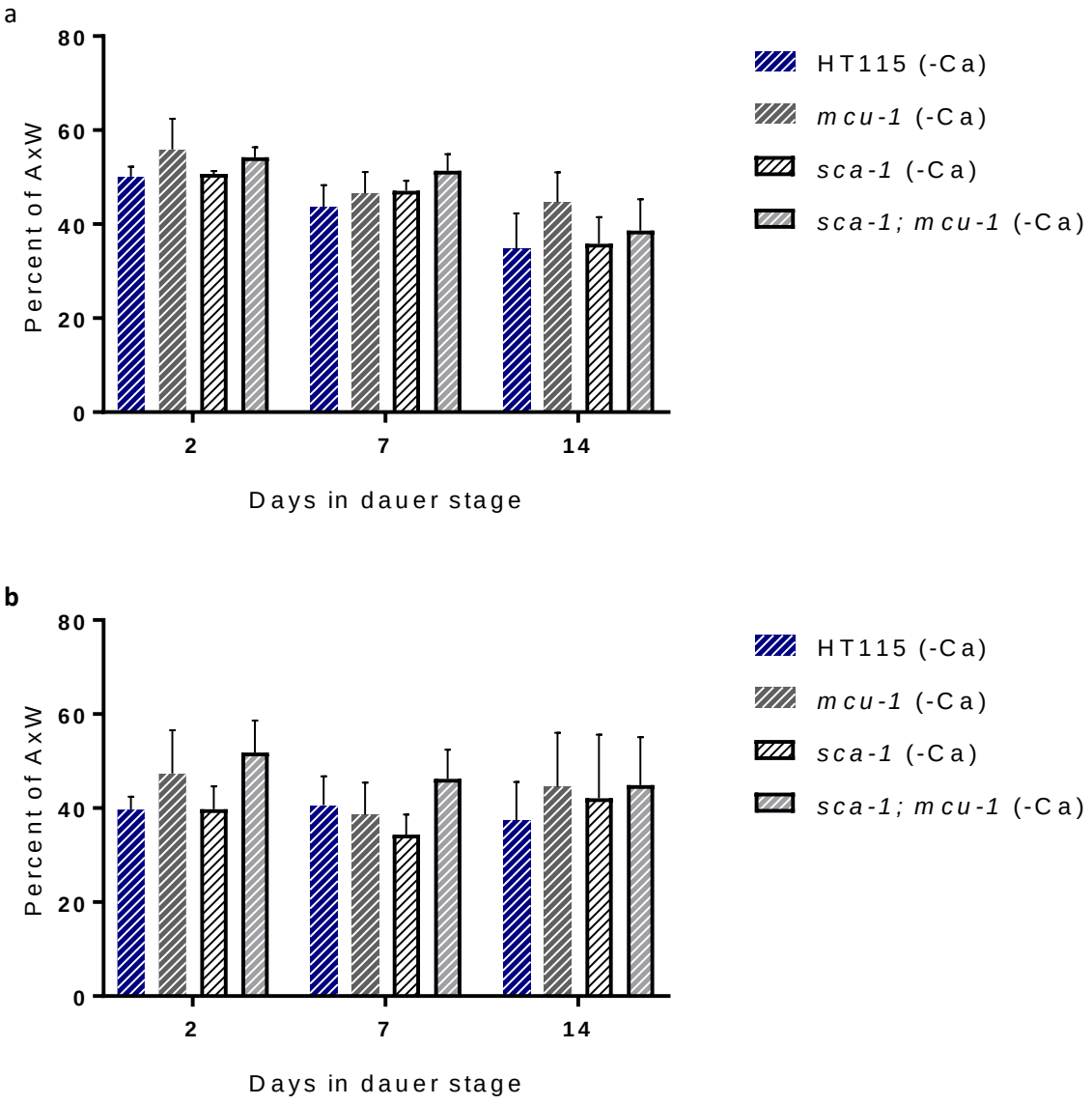

Figure 15: Effects of silencing of intracellular calcium reporters require calcium in diapause. A-B) Morphological categories found in animals feeding on ds-RNA-expressing bacteria of different intracellular calcium transporters in absence of environmental calcium, at days 2, 7, and 14 in the dauer stage in (A) TRN-specific strain and B) a systemically affected strain. (N=3 plates).

Previously there was no described protocol to induce silencing in dauers through food, since dauers do not eat in that stage; we propose a two-generation treatment without replenishment of food, to generate starvation and silencing over the population. Because diapause restricted conditions for synthesis, it is possible that the silencing affecting the parental line may still affect the offspring, until four generations (Grishok, 2005), L2 can reach the stage of pre-dauer larvae

(L2d) with a reduction of protein synthesis; since the recovery of translation levels in diapause may be difficult, those levels should maintain the effects of silencing.

Using this approach, we found that the silencing of *sca-1* and *mcu-1* during diapause impairs regeneration for TRN-specific, from day 7, and systemic silencing, from day 2 in combined treatment (Fig.14A and B), suggesting that the capture of the calcium by intracellular calcium transporters is required for the regenerative process. We support that the effect of silencing intracellular calcium transporters is due to a calcium effect because the absence of the ion neutralizes significant differences between treatments (Fig. 15A and B).

Based on the presented data, mitochondria, and the ER are important organelles for regeneration and degeneration signaling, and the effects of silencing differ according to the developmental stage observed. We investigate transcriptomic data available in GExplore for the expression of these two intracellular calcium transporters and, both are upregulated at dauer entry (Fig. 16) (Hutter *et al*., 2009; Hutter and Suh, 2016). *mcu-1* is found upregulated only at dauer entry compared with L2, L4, or young adults; in comparison, *sca-1* is upregulated during all dauer-related stages. This data shows that it is possible that intracellular calcium plays an important role in calcium signals observed in this work.

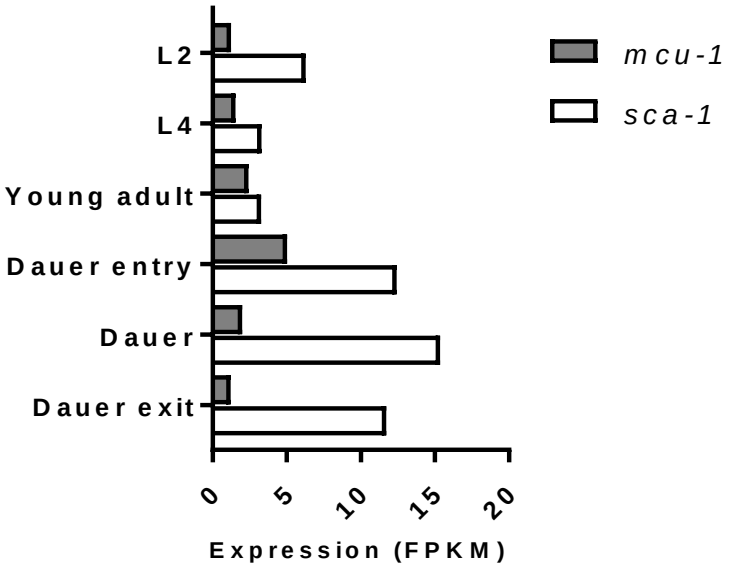

Figure 16: *mcu-1* and *sca-1* are upregulated in the dauer stage: Expression of intracellular calcium transporters in different stages of *Caenorhabditis elegans* obtained from *GExplore*. FPKM= Fragments Per Kilobase of transcript per Million.

2.2.2. To find out the dependence of regeneration induced by the developmental arrest in intracellular dynamics:

Since *mcu-1* and *sca-1* are required for *mec-4d*-induced degeneration, it is possible that this mutation or axonal regeneration generates morphological effects in the respective organelles. It is technically possible to analyze and follow mitochondrial morphology to answer this question.

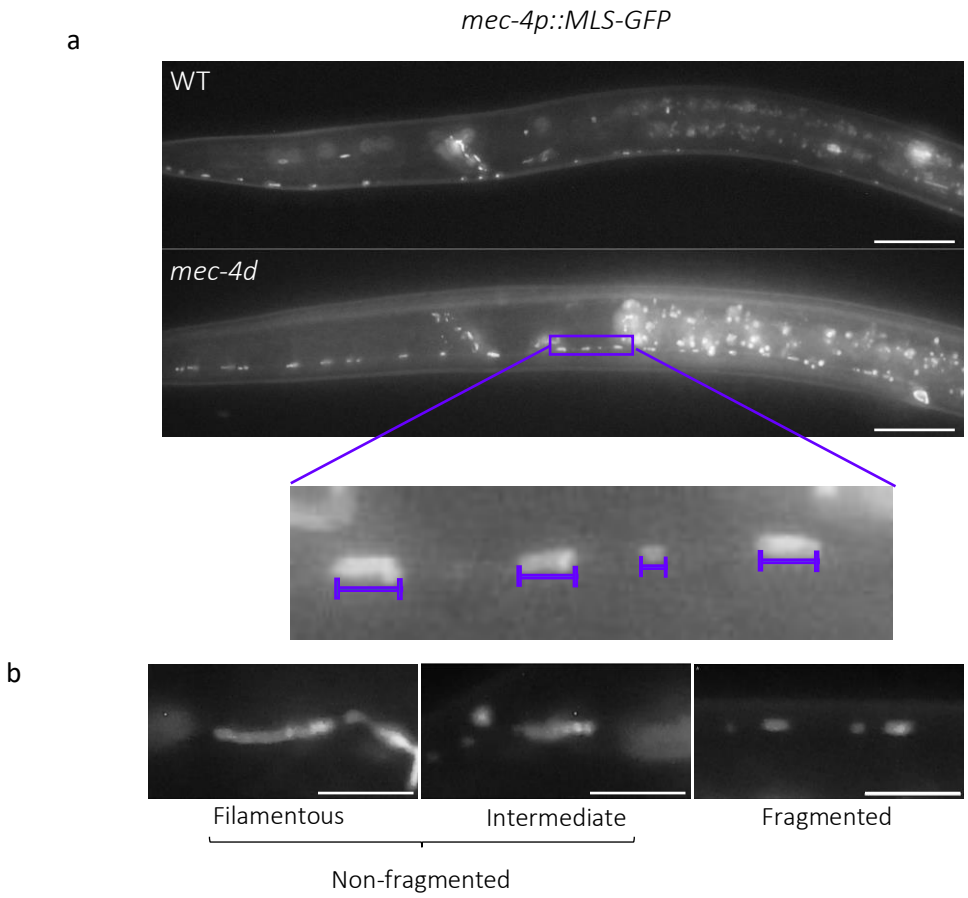

Figure 17: Measurement and classification of mitochondrial morphology. A) Representative image of *mec-4p::MLS-GFP* and *mec-4p::MLS-GFP; mec-4d*, depicting the measurement method. Scale bar= 20 µm. B) Representative images of filamentous, intermediate, and fragmented mitochondria found in TRNs from *mec-4p::MLS-GFP* and *mec-4p::MLS-GFP; mec-4d*. Scale bar= 5µm. Filamentous and intermediate mitochondria are mentioned in Fig. 20 and 22 as non-fragmented.

We used a *C. elegans* strain that drives the expression of GFP in TRN fused with an MLS (mitochondrial localization signal) (*jsIs609:Is[Pmec-4::MLS::gfp]*) (Fatouros *et al*., 2012) (Fig. 17). After photomicrographs were taken, mitochondria were counted, measured, and classified (Fig. 18A). Mitochondria shorter than 2µm were classified as fragmented, between 2 and 4 µm are intermediate, and longer than 4µm mitochondria correspond to filamentous (Neve *et al*., 2020). Following this classification, we considered filamentous and intermediated mitochondria as non-fragmented (Fig. 18B).

The number and length of mitochondria found were compared between the different TRNs. We found that different TRNs, such as ALM (Anterior Lateral Microtubule cell), PLM (Posterior Lateral Microtubule cells), and AVM, has a significantly different number of mitochondria, and in diapause, different mitochondrial length in *E. coli* OP50 (Figure 19A and B). In L2, both ALM and PLM have fewer mitochondria than AVM, and their length is very similar. In contrast, diapause induces different numbers in the TRNs and a reduction in mitochondrial length in AVM. This data suggest that comparison should be done using just AVM data to compare between stages and diet. From here, the data shown will only correspond to AVM neurons

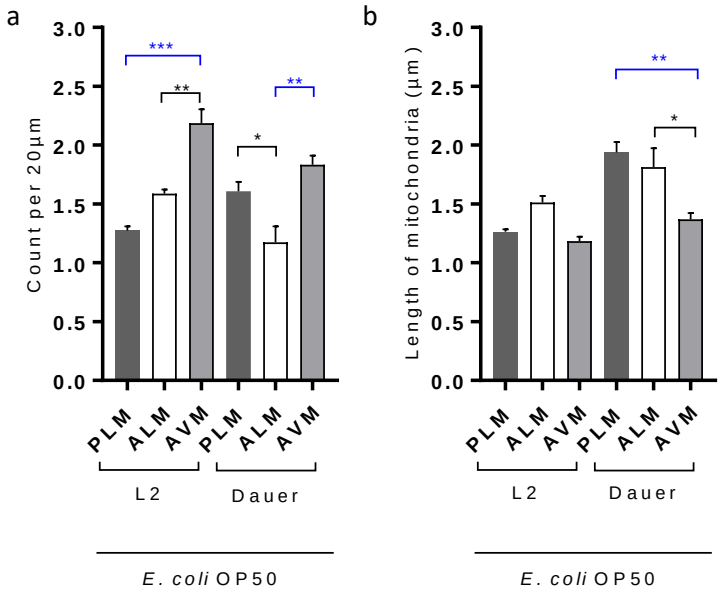

Figure 18: TRNs have significant differences in mitochondrial number and average length. A-B) Morphological measurements of, A) number, B) length of mitochondria from different Touch Receptor Neurons in *E. coli* OP50 diet (N=3 plates; one-way ANOVA ***p<0.001, **p< 0.005, *p<0.05).

We found significant differences in the *E. coli* OP50 diet, that were induced by *mec-4d* in L2, fewer and shorter mitochondria were found compared to wild-type animals. It is possible to also note

that, the number and length of mitochondria are recovered in diapause under chronic stress signals (Fig. 19A, and B); it is clearer that diapause induces changes in mitochondrial morphology considering that mutants L2 exhibits a fraction of the population with non-fragmented mitochondria (>2.0 µm) compared to wild type L2 (Fig. 19C). This condition dramatically changes in diapause, improving mitochondrial physiology and by extension, function. These findings suggest that *mec-4d* mutants have injured mitochondria which are rescued in diapause.

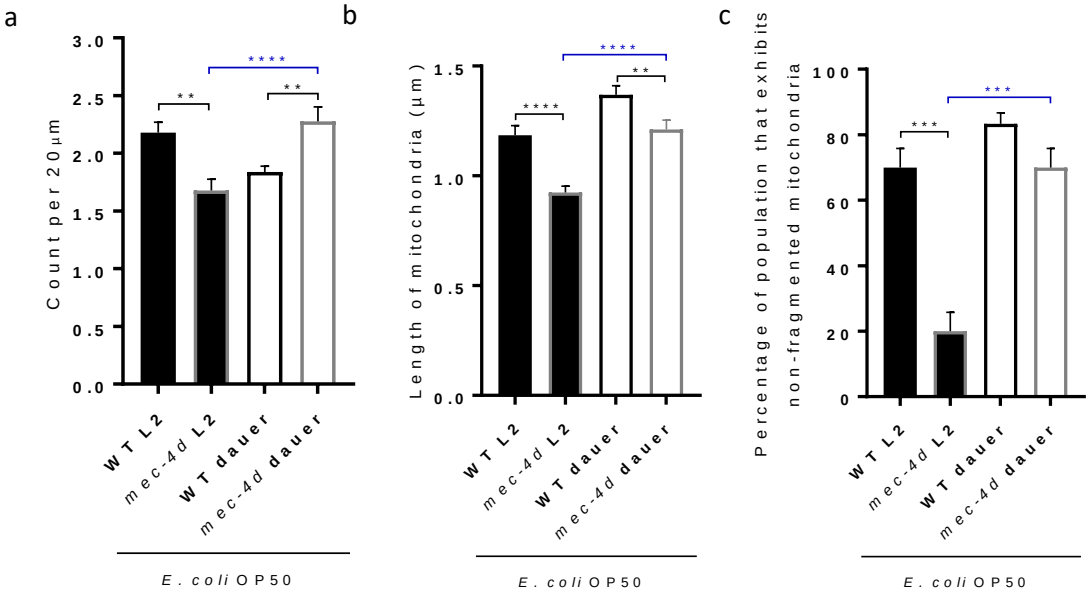

Figure 19: Diapause induces improvement of mitochondrial morphology in a non-protective diet in a *mec-4d* context. A-B) Morphological measurements of, A) number, B) length of mitochondria in *E. coli* OP50 diet. C) Percentage of the population of wild-type and *mec-4d* animals that exhibits non-fragmented mitochondria in the *E. coli* OP50 diet. (N=3 plates; one-way ANOVA ****p<0.0001, ***p<0.001, **p< 0.005).

These differences are maintained in absence of environmental calcium, due to the dependence of muscular mitochondrial biogenesis on calcium signaling, specifically calcium/calmodulin-dependent protein kinase, or CaMK (Wu *et al*., 2002; Wright, 2007) and MCU-1 (Liu *et al*., 2020). While similar differences can be found between stages (Fig. 20A and B), the improvement in mitochondrial length in diapause is absent when calcium is removed (Fig 20B). Specifically, a difference in number during diapause between mutants and wild types is no longer found, and neither are significant increments in length after dauer entry.

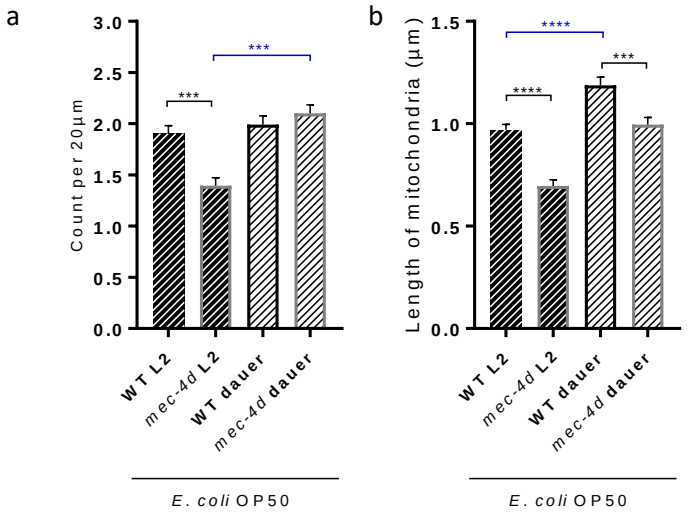

Figure 20: The absence of calcium changes mitochondrial effects in WT dauers eating a non-protective diet. A-B) Morphological measurements of, A) number, B) length of mitochondria in *E. coli* OP50 diet in absence of environmental calcium. (N=3 plates; one-way ANOVA ****p<0.0001, ***p<0.001).

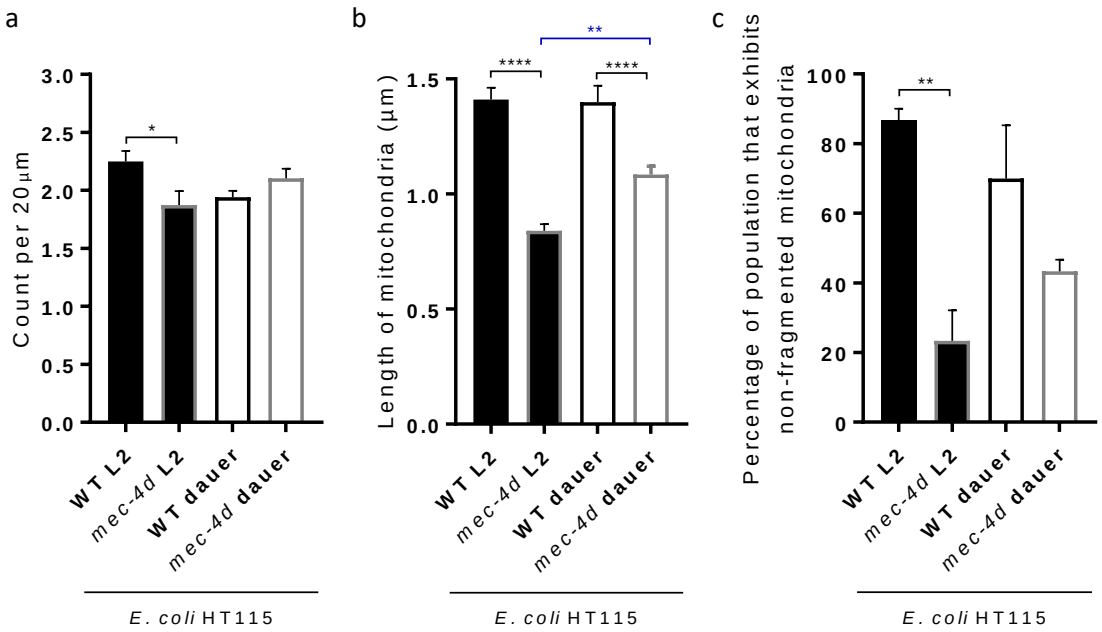

Figure 21: Neuroprotective diet neutralizes improvements of mitochondrial morphology induced by diapause in the *mec-4d* context. A-B) Morphological measurements of, A) number and B) length of mitochondria in *E. coli* HT115 diet. C) Percentage of the population of wild-type and *mec-4d* animals that exhibits non-fragmented mitochondria in the *E. coli* HT115 diet. (N=3 plates; one-way ANOVA ****p<0.0001, **p< 0.005, *p< 0.05).

We took the same measurements for animals eating *E. coli* HT115 to control those similar conditions were ensured for RNAi experiments. HT115 diet does not rescue mitochondrial size or number compared to wild-type animals. Furthermore, HT115-fed *mec-4d* dauers exhibited an increase in mitochondrial length but not in number compared to the L2 mutants (Fig.21A, and B). In another point, the portion of mutants that exhibits non-fragmented mitochondria is reduced compared to wild type, and in this case, diapause does not improve the fraction (Fig. 21 C).

Although previous observations have shown that HT115 improves wild-type-like morphology in a *mec-4d* background (Urrutia *et al*., 2020), it does not significantly induce improvements in mitochondrial morphology in comparison with the OP50 diet. We report a significant difference in length between diets in WT strain (p-value=0.0002). With this information, we may argue that the RNAi experiment may not differ if done for the OP50 diet.

After these measurements in triplicates of 10 animals, the average of each replicate was associated with the percentage of AxW observed under development or diapause and the correlation between mitochondrial morphology characteristics and AxW was calculated. We found significant correlations between mitochondrial length and number standardized by axonal length for *E. coli* OP50 diet (Mitochondrial length r=0.9744, p=0.0010; Mitochondrial count r=0.98, p=0.0013) (Fig. 22A), but for HT115 diet, it was only found an association to AxW with mitochondrial length (Mitochondrial length r=0.8194; p=0.0460; Mitochondrial count r=0.1564; p=0.7673) (Fig. 22B). These results reveal a relationship between neuronal protection and mitochondrial morphology.

We tested the influence of mitochondrial dynamics, fusion, and fission on neuronal protection. We used a similar intervention in Objective 2.2.1. We selected *drp-1*, which corresponds to a membrane protein located in the external mitochondrial membrane linked to fission. We also knocked down proteins that participate in mitochondrial fusion genes like *eat-3*, which corresponds to a protein located on the mitochondrial cristae, and *fzo-1*, located in the external membrane (Kanazawa *et al*., 2008; Lu *et al*., 2011; Byrne *et al*., 2019) (Fig. 23A).

The principal function described for mitochondria is energy production, along with other functions like lipid metabolism, calcium chelation, or stress neutralization. Energy is highly required for the effects observed previously because both SERCA and MCU-1 require ATP to work, so we also tested the involvement of the *cts-1* and *icl-1* genes which correspond to citrate synthase and isocitrate lyase enzymes. Both correspond to rate-limiting enzymes of the Tricarboxylic Acid Cycle, and when affected impair energy production and metabolic alternatives (Fig. 23B).

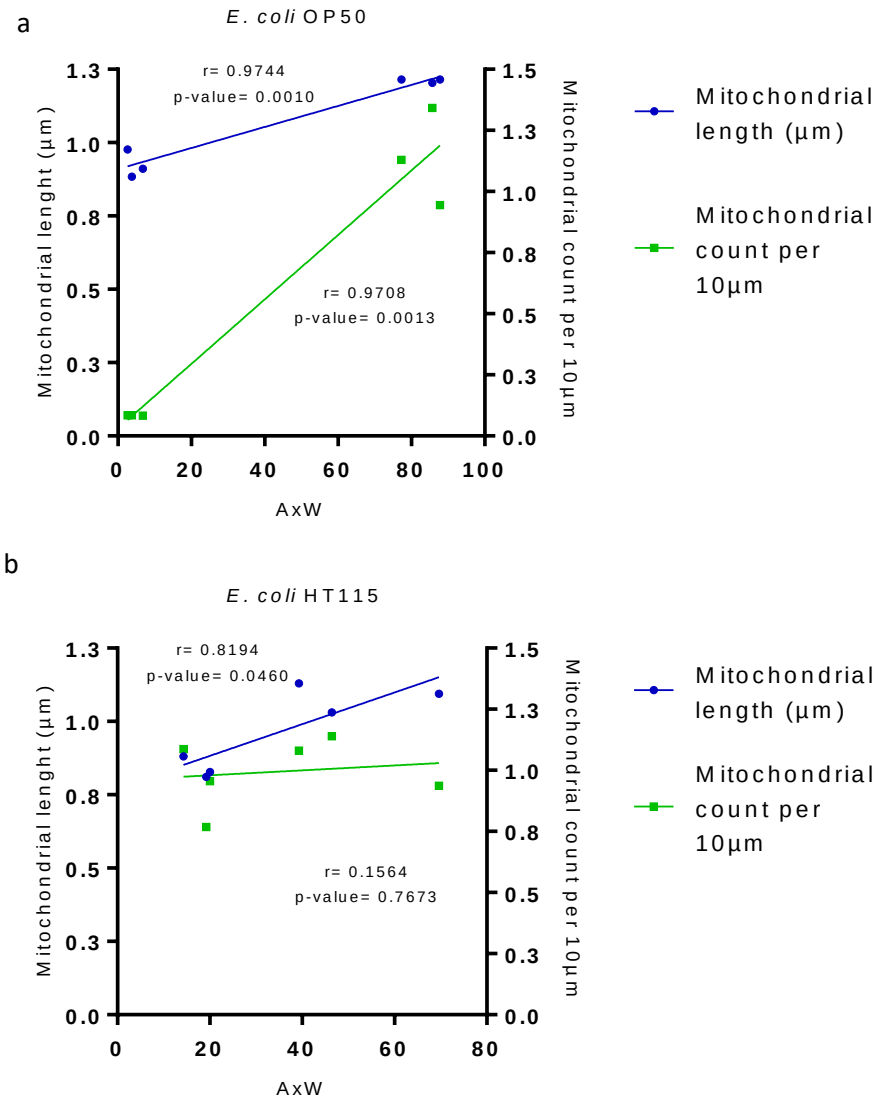

Figure 22: Axon wild-type-like presence is proportional to mitochondrial length observed, in two different diets. A-B) Pearson Correlation Coefficient between mitochondrial length and the number of mitochondria normalized by the axonal length in *mec-4d* animals growing in A) *E. coli* OP50 and B) *E. coli* HT115 in L2 and early dauer stages (N=3 plates).

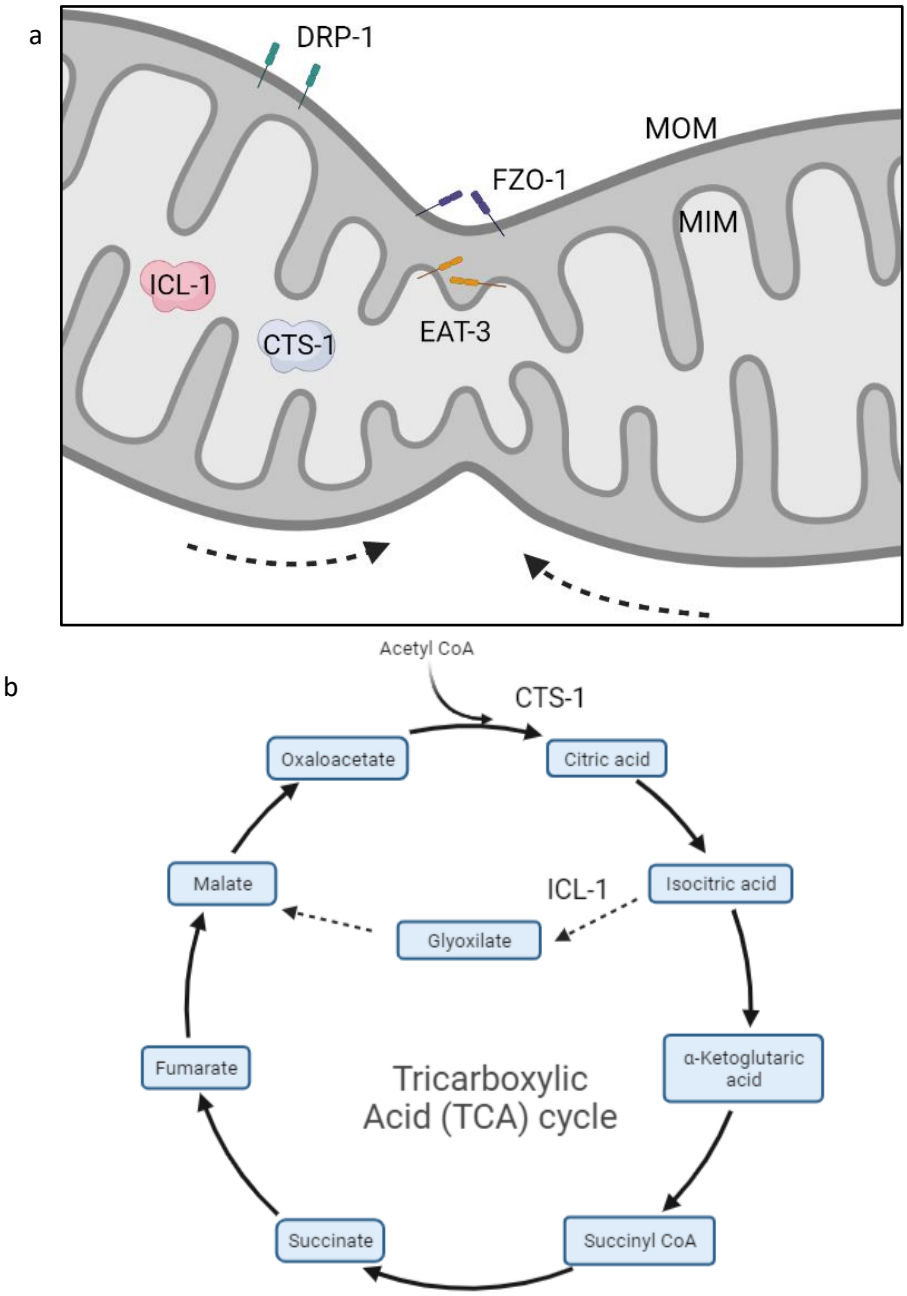

Figure 23: Selection of genes associated with fusion and fission dynamics and energy production in *Caenorhabditis elegans*: A-B) Schematics that shows the association of different regulators of A) mitochondrial dynamics and B) specific steps affected of the Tricarboxylic Acid Cycle (Created with BioRender.com)

Because energy production-related genes also perturb mitochondrial biogenesis we had proposed previously the silencing of *mtcu-2* and *mttu-1*, which reduce energy production without affecting mitochondrial biogenesis (Navarro-Gonzalez *et al*., 2017), but the problem with that proposal is that both, *mtcu-2* and *mttu-1*, correspond to mitochondrial tRNA, non-coding genes, then the silencing could not be as effective and it has only been described effects on mutants strains.

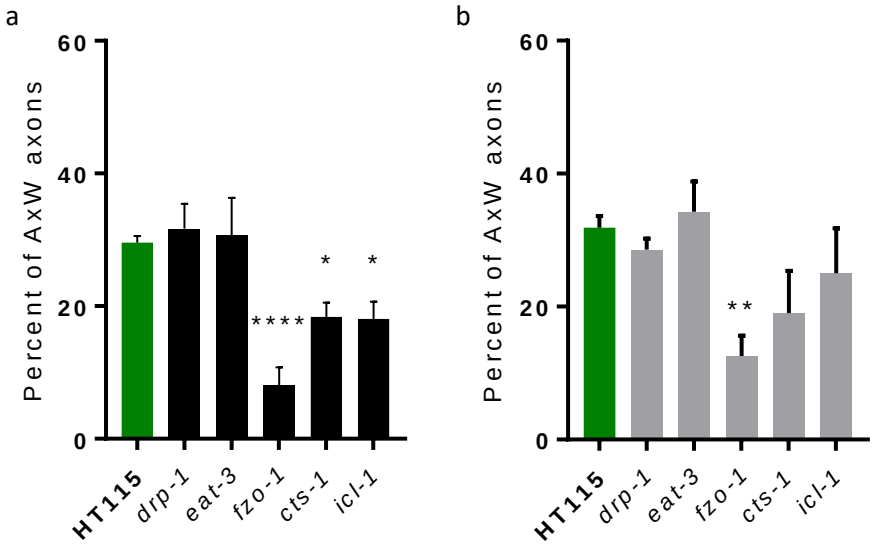

Figure 24: Neuronal protection depends cell-autonomously on mitochondrial fusion and energy production. A-B) Percentage of Axon-W morphology in animals feeding on ds-RNA-expressing bacteria of mitochondrial genes A) in a TRNs specific affected strain, *mec-18::sid-1; mec-17p::GFP; mec-4d; sid-1*, and B) in a systemically affected strain, *mec-17p::GFP; mec-4d*, after 72 hours post-hatching. (N=3-4 plates; one-way ANOVA, ****p<0.0001, **p< 0.005, *p< 0.05).

Our results (Fig.24A, and B) show that neither *drp-1* nor *eat-3* silencing reduces neuronal protection in *mec-4d* mutants in cell-autonomous and systemic silencing. *fzo-1* silencing does affect neuronal protection, which means that while fission may not be required, the fusion of external membrane is necessary for protection. Knockdown of *eat-3* is an interesting case to analyze because cristae fusion requires first the link generated by *fzo-1*, which could mean that the limiting point of the processes is directed by the external membrane of each mitochondrion. The effects observed by energy production-related genes knockdown, *cts-1,* and *icl-1*, reveal that cell-autonomous energy production is required for protection.

Our results highlight the physiological effects lead by diapause that promotes neuronal recovery, along with intracellular calcium transporters, energetic profile of the cell is important to support the functions we found as important. This improvement has other consequences, changing the

morphology of organelles like mitochondria, closely related to ER, that under other circumstances can be assessed to provide more information about regenerative environments.

ANNEX 1: Modeling MEC-4 channel

The mechanosensory complex is composed principally of MEC-4, MEC-10, MEC-2, and MEC-6 (Chen *et al*., 2015; Shi *et al*., 2018). Total Internal Reflection Fluorescence (TIRF) microscopy has shown that MEC-4 spontaneously forms trimers, but the normal stoichiometry of the mechanosensory pore is 2:1 of MEC-4: MEC-10, revealed by bleaching steps (Chen *et al*., 2015b). MEC-6 and MEC-2 can be found sporadically in the mechanosensory complex.

Many structures can be found in the Protein Data Bank (PDB), but models with similar protein sequences are few. We find the structure of the Acid-sensing channel of *Gallus domesticus* (3S3W in PBD) (Dawson *et al*., 2012), which has a 27.94% identity with the MEC-4 channel. That level of identity makes it difficult to predict the structure and it is called the Twilight Zone (Khor *et al*., 2015). To date, there is no sequence with an available model in PDB with more than 32% identity with MEC-4.

Using Modeller (Eswar *et al*., 2006; Webb and Sali, 2016) the first step corresponds to comparing the sequences of MEC-4 with another protein, like 3S3W. "align2d.py" script is used to compare both sequences, this algorithm includes gaps in the template sequence where there is no coincidence with the protein to model in the ".txt" document obtained.

```
from modeller import *

env = environ()
aln = alignment(env)
mdl = model(env, file='3s3w', model_segment=('FIRST:A','LAST:A'))
aln.append_model(mdl, align_codes='3s3wA', atom_files='3s3w.pdb')
aln.append(file='mec4.ali', align_codes='mec4')
aln.align2d()
aln.write(file='mec4-3s3wA.ali', alignment_format='PIR')
aln.write(file='mec4-3s3wA.pap', alignment_format='PAP')
```

The document obtained are the following:

```
>P1;3s3wA
structure: 3s3w.pdb
-------------------------AL----------------------CF------------MGSLALLALVCTNRIQYYF------- ----------
--------------LY-PHVTKLD-----------EVAATRLTFPAVTFCNLNEFRFSRVTK NDLYH------AGELLALLNN----
--R---YEIP----------------D----------------TQ-------TADEKQ LEILQDKAN--FR--------------------NFKPK---
PFNMLE---------FYDRAGHDIR---------EMLL SCFFRG----EQCSP--E------DFKVVFT-R-------
YGKCYTFNAG----------QDGKP----RLITM KG--G--------TGNGLEIMLDIQ----QD-------------------------
EYL----PVWG---------ETDETS F----------------------EA-
```

```
GIKVQIHSQDEPPLIDQLGFGVAPGFQTFVSCQEQRLIYLPPPW GDCKA---TYD------
TYSITACRIDCETRYLVENCNCRMVHMP--GDAPYC—TPEQYKE CADPALDFLVEKDNEY-
CVCEMPCNVTRYGKELSMVKIPSKASAKYLAKKYNKSE----
QYIGENILVLDIFFEALNYETIEQKKAYEVAGLLGDIGGQMGLFIGASILT----V----------
*
```

```
>P1;mec4
sequence: MEC-4
MSWMQNLKNYQHLRDPSEYMSQVYGDPLAYLQETTKFVTEREYYEDFGYGECFNSTESEVQCELITGEFD
PKLLPYDKRLAWHFKEFCYKTSAHGIPMIGEAPNVYYRAVWVVLFLGCMIMLYLNAQSVLDKYNRNEKIVD
IQLKFDTAPFPAITLCNLNPYKASLATSVDLVKRTLSAFDGAMGKAGGNKDHEEEREVVTEPPTTPAPTTKP
ARRRGKRDLSGAFFEPGFARCLCGSQGSSEQEDKDEEKEEELLETTTKKVFNINDADEEWDGMEEYDNEH
YENYDVEATTGMNMMEECQSERTKFDEPTGFDDRCICAFDRSTHDAWPCFLNGTWETTECDTCNEHAF
CTKDNKTAKGHRSPCICAPSRFCVAYNGKTPPIEIWTYLQGGTPTEDPNFLEAMGFQGMTDEVAIVTKAKE
NIMFAMATLSMQDRERLSTTKRELVHKCSFNGKACDIEADFLTHIDPAFGSCFTFNHNRTVNLTSIRAGPM
YGLRMLVYVNASDYMPTTEATGVRLTIHDKEDFPFPDTFGYSAPTGYVSSFGLRLRKMSRLPAPYGDCVPD
GKTSDYIYSNYEYSVEGCYRSCFQQLVLKECRCGDPRFPVPENARHCDAADPIARKCLDARMNDLGGLHGS
FRCRCQQPCRQSIYSVTYSPAKWPS-LSLQIQLGSCNGTAVECNKHYKENGAMVEVFYEQLNFEML
TESEAYGFVNLLTDFGGQLGLWCGISFLTCCEFVFLFLETAYMSAEHNYSLYKKKKAEKAKKIASGSF*
```

“model-single.py” creates different models for the new model from (a.starting_model = 1 a.ending_model = 5), which are restricted by the align (mec4-3s3w.ali) with the template 3W3S (knowns=’3s3wA’). This script generates 5 different models to evaluate later, which are named “mec4.V9999000X”, X signaling the respective model.

```
from modeller import *
from modeller.automodel import *

env = environ()
a = automodel(env, alnfile='mec4-3s3wA.ali',
          knowns='3s3wA', sequence='mec4',
               assess_methods=(assess.DOPE, assess.DOPEHR, assess.GA341))
a.starting_model = 1
a.ending_model = 5
a.make()
```

“evaluate_model.py” calculates the energetic profile the model selected, which passes from the name “mec4.V9999000X” to “mec4.pdb”. This script uses parameters of the topology of the protein and calculates the Discrete Optimized Protein Energy, or DOPE, of the whole structure. Similar to other energetic estimations, a lower value is related to more stable structure.

```
from modeller import *
from modeller.scripts import complete_pdb

log.verbose()    # request verbose output
env = environ()
env.libs.topology.read(file='$(LIB)/top_heav.lib') # read topology
env.libs.parameters.read(file='$(LIB)/par.lib') # read parameters

# read model file
mdl = complete_pdb(env, 'mec4.pdb')

# Assess with DOPE:
s = selection(mdl)   # all atom selection
s.assess_dope(output='ENERGY_PROFILE NO_REPORT', file='mec4.profile',
                    normalize_profile=True, smoothing_window=15)
```

To compare the DOPE for each residue is used the script “plot_profiles.py” compares the structure for each amino acid. The resultant plot is shown in Fig. 25.

```
import pylab
import modeller

def r_enumerate(seq):
   """Enumerate a sequence in reverse order"""
   # Note that we don't use reversed() since Python 2.3 doesn't have it
   num = len(seq) - 1
   while num >= 0:
      yield num, seq[num]
      num -= 1

def get_profile(profile_file, seq):
   """Read `profile_file` into a Python array, and add gaps corresponding to
      the alignment sequence `seq`."""
   # Read all non-comment and non-blank lines from the file:
   f = open(profile_file)
   vals = []
   for line in f:
      if not line.startswith('#') and len(line) > 10:
         spl = line.split()
         vals.append(float(spl[-1]))
   # Insert gaps into the profile corresponding to those in seq:
   for n, res in r_enumerate(seq.residues):
      for gap in range(res.get_leading_gaps()):
         vals.insert(n, None)
```

```
    # Add a gap at position '0', so that we effectively count from 1:
    vals.insert(0, None)
    return vals

e = modeller.environ()
a = modeller.alignment(e, file='TvLDH-1bdmA.ali')

template = get_profile('1bdmA.profile', a['1bdmA'])
model = get_profile('TvLDH.profile', a['TvLDH'])

# Plot the template and model profiles in the same plot for comparison:
pylab.figure(1, figsize=(10,6))
pylab.xlabel('Alignment position')
pylab.ylabel('DOPE per-residue score')
pylab.plot(model, color='red', linewidth=2, label='Model')
pylab.plot(template, color='green', linewidth=2, label='Template')
pylab.legend()
pylab.savefig('dope_profile.png', dpi=65)
```

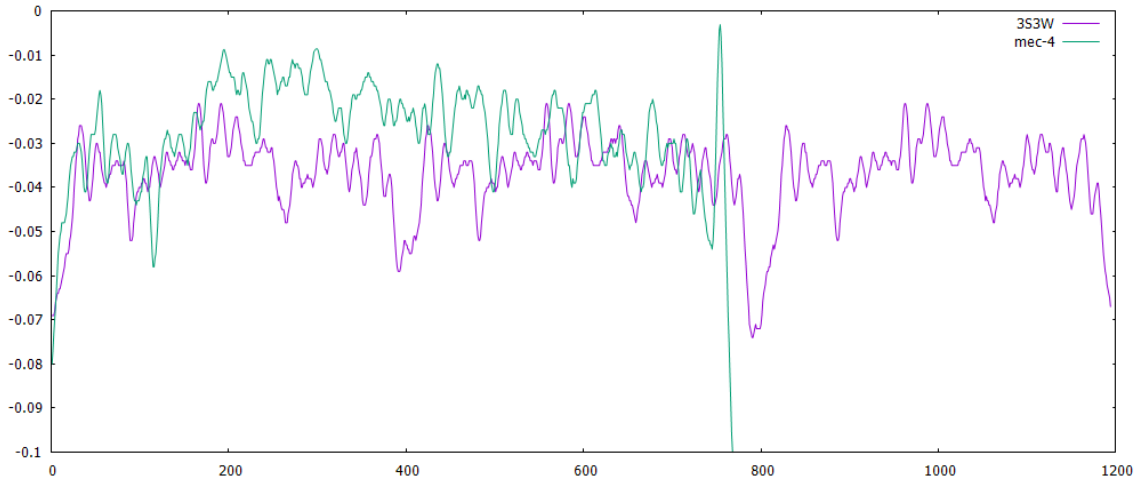

Figure 25: Energetic profile of MEC-4 models compared with ASIC1 profile. Discrete Optimized Protein Energy (DOPE) of MEC-4 channel compared with ASIC1 of *Gallus domesticus*.

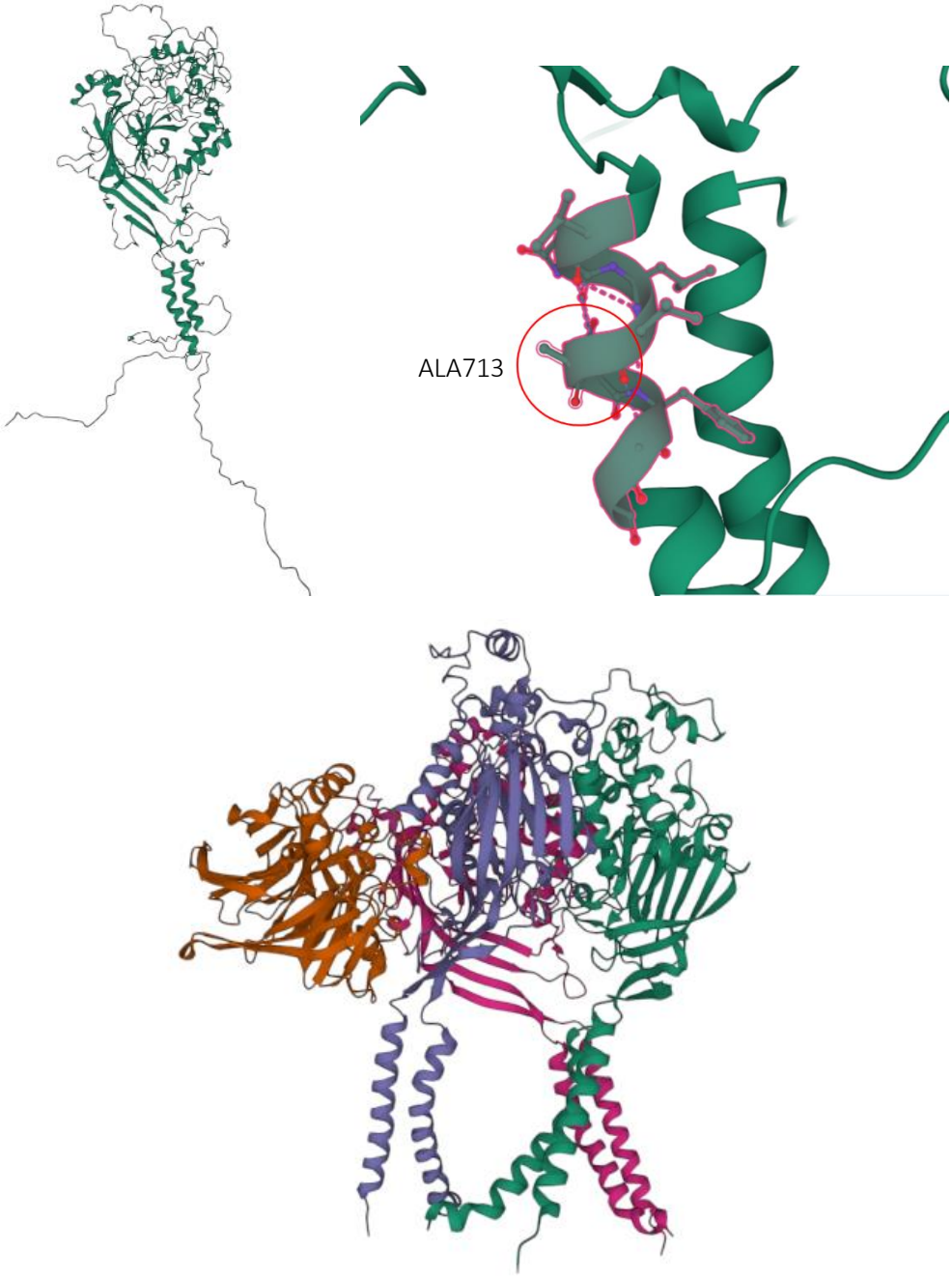

Figure 26: Structural findings of MEC-4 channel. A) 3D representation of MEC-4 subunits based on the structure of chicken acid-sensing ion channel with unedited carboxy and amino-terminal regions. B) Detail of the transmembrane region, which details the position of Ala713 in the model at the second loop from the TM2. C) Result of modeling and docking of MEC-4, MEC-10, and MEC-6 proteins in a structural model of the mechanosensory complex.

The final model is shown in Figure 26A. In the resultant model, the mutated residue that generates the degenerative condition, A713T, is in the second loop of the second transmembrane region (TM2) (Fig. 26B). This position has been described for other mutations that change the gating properties of other ENaC channels (Jasti *et al*., 2007).

The described process was repeated for MEC-10 and MEC-6, other subunits of the mechanosensory complex, each subunit was added using docking from the PatchDock server (Schneidman-Duhovny *et al*., 2005) (https://bioinfo3d.cs.tau.ac.il/PatchDock/php.php), and a model of the worm mechanosensory channel is shown in Figure 26C.

DISCUSSION

Regeneration is a process that in the Central Nervous System (CNS) of most derived animals is disturbed by an unregulated response, called reactive gliosis (Pekny and Nilsson, 2005; Fitch and Silver, 2008; Tran *et al*., 2021). This response that generates the glial scarring makes it difficult to continue with the regenerative conditions observed in other branches of Urbilaterians along the evolution.

Extrinsic conditions that are difficult for the regenerative process correspond to inflammatory response, Extracellular Matrix components of the glial scar, and progressive senescence. In parallel, it has been described that the availability of growth factors, mitochondrial function, high levels of cAMP, and improvements in the cytoskeleton are cell-autonomous requirements for nerve regeneration (Bradbury and Burnside, 2019; Han and Xu 2020; Assinck *et al*., 2020; Tran *et al*., 2021; Wang *et al*., 2021).

In short, it is indispensable a balance between cell-autonomous repair and systemic damage response after injury (Yang *et al*., 2021). How this balance is managed by the cell is something we are still trying to understand.

Calcium's role in the degeneration and regeneration process

Historically, it has been indicated that high levels of intraxonal calcium are, both, necessary and sufficient for neurodegeneration to occur (Wang *et al*., 2012), same as the activation of proteases, principally intramembrane and metalloproteases (Saftig and Bovolenta, 2015), which in turn are activated by the ion.

The notion that MEC-4d heterologous expression generates compensatory Cl^- currents and *in vivo* increases in cytoplasmic calcium signals (Kuruma and Hartzell, 1999; Bianchi *et al*., 2004) leads to the idea that MEC-4d channel changes in gating directly increase calcium permeability for the cell (Brown *et al*., 2007; Shi *et al*., 2018). These facts, along with the proposed role of calcium toxicity in neurodegenerative diseases (Marambaud *et al*., 2009; Calvo-Rodriguez *et al*., 2020; Singh *et al*., 2022) direct the idea that this increment of calcium is the cause of MEC-4d induced death.

Nevertheless, when calreticulin or aspartyl and calpain proteases expression is reduced, MEC-4d death is diminished (Xu *et al*., 2001; Syntichaki *et al*., 2002), meaning that even when calcium is present and calcium may be higher than normal, calcium by itself is not enough to induce necrosis. These results are in line with our findings that *mec-4d* dauers tend to have higher calcium signals when regeneration of the TRNs is happening, but also that calcium is necessary for diapause-induced regeneration to occur in the *E. coli* OP50 diet (Fig. 7 and 9).

In the case of the *E. coli* HT115 diet (Fig. 10), the timings in which neuroprotection is lost coincide with the timings proposed for the maintenance of regenerated axons, which are 72 hours post-hatching in development, and 2 weeks in diapause (Caneo *et al*., 2020; Urrutia *et al*., 2020). This result suggests that after regeneration is induced by neuroprotective microbiota, the main role of calcium in this condition is the maintenance of the axons. In contrast, in the *E. coli* OP50 diet, animals actively require calcium for diapause-induced regeneration, which could suggest that the mechanism in which HT115 induces protection, is independent of calcium, which differs from the non-protective diet.

Our results suggest that during diapause-induced regeneration the proteins like proteases that participate in signaling degeneration may have a reduced expression or reduced function, along with enhanced regenerative elements, like the DLK-1 pathway (Nakata *et al*., 2005; Yan *et al*., 2009; Caneo *et al*., 2019), may be favored in neuroprotective and regenerative conditions. This is also in line with the fact that MEC-4 expression does not change between degenerative and protective conditions (Fig. 8), and the tendency exhibited by diapause to increase intracellular calcium concentration (Fig. 7), because that means that even the chronic damage signal may be present when the axons regenerate.

Axons affected by the absence of calcium are similar to those found in mutants of DLK-1 (Fig. 11; Caneo *et al*., 2019), then it is possible that this treatment is affecting that pathway. Downstream of DLK-1 is CEBP-1, a conserved transcription factor in metazoans that participates in memory, plasticity, neuroinflammation, and axonal regeneration (Li *et al*., 2015; Yan *et al*., 2009; Malinow *et al*., 2019). CEBP-1 then is dependent on calcium due to DLK-1, which is also dependent on cAMP signaling (Li *et al*., 2015). Neuroprotective conditions while eating *E. coli* HT115, compared to the *cebp-1* dsRNA bacteria for silencing, are reduced when the blockade affects systemically, which is interesting, and suggests that the participation of CEBP-1 may depend on other cells surrounding the AVM. It is possible that the induction of CEBP-1 depends on somatic cells instead of neurons.

Calcium by itself is not damaging, that is what our results show, which is in the same line as other authors that have shown that increases in intracellular calcium by themselves cause no harm to cells (Kachaturian, 1989; Harman and Maxwell, 1995, Gitler and Spira, 1998; Chierzi *et al*., 2004; Ghosh-Roy *et al*., 2010); instead, the uncaging of calcium in the cytoplasm and even calcium released during electrical activity may be enough to induce regeneration in neurons under specific conditions (Nakata *et al*., 2005; Sun *et al*., 2014). This data indicates we need to focus on the effectors of the degeneration.

Role of intracellular components

Intracellular calcium transporters' transfer calcium from the cytosol into a specific organelle to stop the signal and restore previous conditions (Periasamy and Kalyanasundaram, 2007; Wray, 2010; Nogami *et al*., 2021; Xu and Van Remmen, 2021). Neuronal calcium homeostasis depends on mitochondria-Endoplasmic Reticulum transfer (Csordás *et al*., 2018; Calvo-Rodriguez and Bacskai, 2021).

We focused on two, the MCU and the SERCA; while the role of SERCA under neuronal degeneration is still unclear, it is one of the important calcium regulatory mechanisms of the cell (Pottorf *et al*., 2001), and MCU has been identified as a target for a possible therapy for Alzheimer's Disease (Calvo-Rodriguez *et al*., 2020); even more, a regulator of MCU activity, called Mitochondrial Calcium Uptake 1 or MICU1, has been identified as a common loss-of-function mutation in patients of neurodegenerative diseases (Singh *et al*., 2022).

Most of the neurons of *C. elegans* do not express SID-1, required for the uptake of dsRNA (Jose and Hunter, 2007; Calixto *et al*., 2010), and for the induction of specific neuronal phenotypes using RNAi giving dsRNA through the food, it is necessary to induce the expression of it. TRN-specific strain corresponds to a mutant of *sid-1* and rescue of the gene guided by *mec-18* promoter, specific for TRNs (Calixto *et al*., 2010).

We found that under neuroprotective conditions, like the *E. coli* HT115 diet, it is required to silence both SERCA and MCU, TRN-specifically to affect the percentage of AxW in the population observed. This is interesting since shows that when one is blocked the other can compensate for the effect (Fig.12), suggesting that the function of these genes is redundant for neuroprotection. Systemic and silencing in absence of calcium generates no significant effects.

A different effect is observed under diapause, on day two of the systemic blockade, there is a significant reduction of AxW percent, only when both proteins are affected, like the effect in development. But on day 7 all the treatments show significant effects in the TRN-specific case, and only in the combination of the treatments in systemic conditions (Fig.14). This result may imply that there is a systemic component that requires both proteins to be affected early in diapause, and a neuronal component that may be observed on day 7 and may be more fragile since the compensatory effects, previously found in development, were not observed. We argue that these effects are due to the movement of calcium by these transporters since when calcium is absent none of these significant effects can be detected (Fig.13 and 15).

It is important to note, that under diapause, a regenerative condition for TRN, the percentage of AxW may be significantly reduced compared to the control, but in all the cases is near ~30% of AxW, or even higher, which is similar to what is found in development under protective conditions, which could imply that even in diapause regeneration may be impaired but neuronal death cannot be increased. It is possible that these effects are related to the levels of expression of RNA of *mcu-1* and *sca-1* early in diapause (Fig. 16), and it is possible that those levels may be partially affected by the two-generation treatment proposed.

Mitochondrial effects of a chronic damage signal

It has been shown using electron microscopy that there exists interorganellar connectivity between mitochondria and ER (Copperland and Dalton, 1959; Csordás *et al*., 2018), these contact regions and the accumulation of proteins in those, have been reported related to different cellular alteration like senescence, aging, autophagia, and degeneration (Vance *et al*., 2014; Janikiewicz *et al*., 2018; Yang *et al*., 2020; Calvo-Rodriguez and Bacskai, 2021), and even, pharmacological

reduction of ER stress has shown improvement of neurodegenerative conditions in mammals (Wang *et al*., 2019), suggesting that either ER or mitochondria can trigger the degenerative signal. Mitochondrial effects associated with Alzheimer's Disease manifestation include impairment of lipid synthesis and transport, Ca^{2+} transport, and consequences of the interruption of several metabolic pathways (Vance *et al*., 2014). Mitochondrial function and neuronal regeneration have been linked in several reports previously (Chen *et al*., 2007; Knott *et al*., 2008; Chen and Chan, 2010; Chang *et al*., 2019; Wang *et al*., 2019).

Mitochondrial involvement in different neuronal processes even concerns the Immune System in neuroinflammation. Macrophages, that accumulate in the Dorsal Root Ganglion, can donate their mitochondria to sensory neurons, which improves the energetic profile of the neurons and favors the resolution of inflammatory pain (van der Vlist *et al*., 2022). This report and others (Banks *et al*., 1995; Muszyński *et al*., 2017; Mapunda *et al*., 2022; Palominos *et al*., 2022), challenge our understanding of the relationship between the Immune and the Nervous Systems in health and sickness, and how mitochondria participate in the communication between different types of cells (Picard and Shirihai, 2022).

We used a reporter of mitochondria specific for the TRNs, and due to the tight functional relation between ER and mitochondrial, it is possible that similar morphological changes can be detected in both organelles. Our first quantitative result (Fig. 18) corresponds to the measurements of mitochondrial number and length in 3 different TRNs, which are different. This result is relatively surprising because these neurons have been considered homogeneous, and in some single-cell transcriptional experiments, they have been grouped together (Cao *et al*., 2017). In general, measurement of channels has been done in PLM (Caneo *et al*., 2019; Urrutia *et al*., 2020; Fig. 8), nevertheless, in light of our results for mitochondrial number and length (Fig. 18), it is possible that those measurements differ for the AVM.

We found significant effects induced by diapause in mitochondrial length in *mec-4d* mutants, similar effects were found in two diets tested, and even more, the differences between *E. coli* OP50 diet and HT115 were only found when WT L2 were compared (p-value=0.0002). Then, diapause induction is more important than a neuroprotective diet to induce mitochondrial morphological changes, and with this in mind, the silencing experiments may not differ if those were done in OP50 RNAi bacteria. Continuing with this idea, prohibitin, also called PHB, has been shown that mediates mitochondrial effects induced by diapause entry (Artal-Sanz and Tavernarakis, 2009; Lourenço *et al*., 2015; Lourenço and Artal-Sanz, 2021), then it is feasible that regeneration observed in diapause is a consequence of higher calcium buffering (Fig. 16), by intracellular calcium transporters, and an improved condition in energy management and production.

In a worm model of Alzheimer's Disease, it has been shown that impaired fission does not improve mitochondrial function (Sarasija *et al*., 2018), which is similar to our findings about *drp-1* silencing, which has no significant effect on neuronal protection. Another gene that is not required for neuroprotection is *eat-3*, which was unexpected, since it has been shown that *mec-4d* mutation induces oxidative damage (Calixto *et al*., 2012), and *eat-3* participates in ROS neutralization in the

mitochondria (Kanazawa *et al*., 2008), but the silencing causes no detectable effect. It is possible that in this case, it is due to a stage-specific outcome since it has been described that *drp-1* and *eat-3* have more impact on mitochondrial physiology after the adult stage, and we are observing these effects earlier than that (Byrne *et al*., 2019).

In contrast, the same authors showed that fusion is necessary through all developmental stages (Byrne *et al*., 2019) and in this case, the silencing of *fzo-1* induced a significant reduction in the AxW percentage. In conclusion, the fusion of the Mitochondrial Outer Membrane is more important for protection than the fusion of mitochondria cristae induced by *eat-3* (Fig. 23A).

There is a tight relationship between mitochondrial fusion and energy production (Skulachev, 2001), which can be improved when MCU-1 activity increases calcium concentration inside mitochondria cristae (Glancy *et al*., 2013; Díaz-Vegas *et al*., 2018) even under degenerative conditions if they are maintained below the bursting threshold (Calvo-Rodriguez *et al*., 2020; Zampese *et al*., 2022).

For genes like *cts-1* and *icl-1*, which have significant effects on cell-autonomous silencing, show that TCA and Glyoxylate cycles (Fig. 23B), are required for the induction of neuroprotection, and both may generate a reduction in ATP production or mitochondrial biogenesis (Plancke *et al*., 2014; Navarro-Gonzalez *et al*., 2017). It is possible that this result is related to their function in energy production, and it is interesting that this coincides with the enhanced activity of the Glyoxylate Cycle during the duration of the diapause arrest (O'Riordan and Burnell, 1990). In a parallel effect, related to the reduced metabolic rates and increment of heat shock proteins in diapause, it has been shown that intermittent fasting, which causes similar effects in mammals, has also generated an improvement in cognitive traits, mitochondrial function, and reduction of toxicity of damaging compounds (Fariss *et al*., 2005; Labbadia *et al*., 2017; Liu *et al*., 2020).

These results of ATP production reduction are in line with other reports that conclude that neurons and cells that require more energy are more susceptible to suffering neurodegeneration due to the energetic collapse of the cells previous (Pacelli *et al*., 2015; Muddapu *et al*., 2020). It is clearly possible that not all neuroprotection cases require a mitochondrial effect to protect the cells, this is more related to protection caused by diet, *E. coli* HT115 specifically, which may depend on other metabolic effects. We focused on mitochondrial morphology because of the availability of the transgenic strain, but it is certainly possible that ER may show similar dynamics due to diapause induction.

Comments on structural data

During this work, we modeled the structure of MEC-4 using Modeller in Python (Eswar *et al*., 2006; Webb and Sali, 2016) to reveal important structural information about the MEC-4 channel that is suggested by comparison with similar channels, since there is no known structure. Other mechanosensory channels that respond to changes of pressure of the membrane has specific subunits that interact with fatty acids surrounding them, these residues can be identify if a validated model of the MEC-4/MEC-10 channel is available (Jeong *et al*., 2022).

We found that the same position proposed for other channels, the second loop of the second transmembrane domain, is the region affected by a bulkier residue, like threonine, compared to the original alanine (Snyder *et al*., 2000; Kellenberger and Schild, 2002; Brown *et al*., 2007). We proposed the modeling of the structure (Fig.26), but the main problem of this proposal is due to the low identity of sequence that MEC-4 has with other proteins that have their structure described in PDB (<30%) (Dawson *et al*., 2012), which makes it difficult to validate.

In recent years, there are other tools developed based on protein sequence, like AlphaFold which since the publication of the web service in 2021 has modeled the structure of around 200 million different proteins (Jumper *et al*., 2021; Callaway, 2022). The implementation of this method for structural understanding of phenotypic effects of MEC-4d mutation is an option, much more feasible than modeling the structure by homology.

A validated structure for this channel could help the understanding of temperature effects over axonal degeneration (Royal *et al*., 2005; Caneo *et al*., 2019), the role of specific proteins like MEC-6 or POML-1 that affect the functional expression of the mechanosensory complex (Chen *et al*., 2016a), other domains or subunits associated with bilipid layer interaction (Jeong *et al*., 2022), and the mechanism directly involved in the increment of cytoplasmic calcium concentration (Bianchi *et al*., 2016).

Evolutionary and developmental points of view

The vast majority of genes in bilateral animals, such as *C. elegans* and humans, are proposed to be shared from Urbilateria, their common ancestor (Hall, 2003; De Robertis, 2008; Miller and Ball, 2009). What differs between the "endless forms most beautiful and most wonderful" are, in general, the regulators of their gene expression (Darwin, 1859; Britten and Davidson, 1969; Trizzino *et al*., 2017). Under the light of the fifth synthesis of Darwin's Theory of Evolution, also known as Evolutionary Development Biology or Evo-Devo (Ureta, 2011), the processes of development, such as proliferation, differentiation, and regeneration are part of related processes which elicit the expression of similar or even the same genetic programs in different moments.

One of the main observations of Evo-Devo is the mosaic pleiotropy (Carroll, 2008; Kiefer, 2010), which refers to the fact that genetic programs that build an organ, tissue, or cell, can be called upon in different stages of development and, most surprisingly, when they regrow or regenerate (Akimenko *et al*., 1995; Wu *et al*., 1996; Trusolino *et al*., 2010; Levin, 2014; Hill *et al*., 2017). This happens for example in the case of the limbs of the axolotl (Khan and Crawford, 2021). It is possible that some of the intracellular calcium transporters and mitochondrial genes analyzed in this work may be classified as genes required for development and regeneration. We know that most of them are necessary until the young adult stage is reached, but due to technical restrictions, we could not know if these genes are required specifically at L2 when the AVM neuron is born.

In addition, the fact that loss of regenerative abilities has occurred in different branches of Teleostei during evolution (Tran *et al*., 2021; Blackshaw, 2022), like medaka fish, which cannot

regenerate their nerves after injury (Lust and Wittbrodt, 2018; Shimizu and Kawasaki, 2021), is important because it shows that is less probable that a common ancestor of chordates has lost the capacity to regenerate in evolutionary history, suggested by Occam's razor. It is more probable that difficulties to regenerate nerves in Metazoans correspond to a case of convergent evolution.

There is a role of development in the prevalence of regenerative capacity, since some of the animals that lost the capability, lost it after a developmental transition. In the case of anuran amphibians, they lost regeneration after their immune system matures, which coincides with their metamorphosis (Fukazawa *et al*., 2009; Bertolotti *et al*. 2013, Edwards-Faret *et al*. 2021). Mammals or therians lost this capacity early in their development, with metatherians, like the opossum losing it at P17, and eutherians, like the mice at P2 (Gearhart *et al*. 1979; Kunkel-Bagden *et al*. 1992; Mladinic and Wintzer 2002).

Development and evolution have a significant role in a plethora of biological processes and considering these factors may be of help to understanding the circumstances that influence nerve regeneration. As Theodosius Dobzhansky told many years ago, *nothing in biology makes sense except in the light of evolution* (1973), and regeneration may be a place where this light is needed for its understanding.

CONCLUSIONS

- *mec-4d* mutation tends to increase cytoplasmic calcium signals in development and calcium removal can neutralize the effects
- Damage induced by *mec-4d* requires calcium, but calcium is also necessary for axonal repair in dauer stage
- Intracellular calcium transporters are key to determining the output of *mec-4d* gain-of-function mutation, and their expression is dependent on the developmental stage
- Diapause induces an increase in the number and length of the mitochondrion. Improvement in mitochondrial energetic function can compensate for the effects of *mec-4d* mutation
- Mitochondrial fusion of MOM is crucial for neuronal protection, and its fusion is more important than the fusion of MIM or mitochondrial fission
- Improvement in ATP production may be important for diapause-induced regeneration since the glyoxylate cycle is essential for the presence of AxW morphology

ANNEX 2: COMPLETE DATA

Percent of AxW found in different treatments of environmental calcium reduction (Fig. 6). Each value considers the percentage found in one plate.

	Percent of AxW		
Control	2.6	6.8	3.8
Control + EGTA	4.1	5.4	2.7
No calcium	6.7	11.5	11.6
No calcium + EGTA	9.3	10.5	12.8

Average of calcium signal from each trial and animal analyzed (Fig. 7).

	Animal ID	Average Calcium Signal per trial			Average
WT L2	20200614_L2_2	2.53	2.38	1.74	**2.22**
	20200614_L2_3	1.02	1.11	1.05	**1.06**
	20200614_L2_5	1.73	1.72	1.72	**1.72**
WT Dauer	20191017_16_06_25	4.42	6.52	5.86	**5.60**
	20191128_12_44_46	5.41	3.91	-	**4.66**
mec-4d L2	20191017_12_46_24	8.38	7.98	7.86	**8.07**
	20191017_12_56_53	8.95	8.74	8.80	**8.83**
	20191017_15_21_49	5.53	8.74	-	**7.14**
	20200123_19_50_50	6.12	7.04	5.65	**6.27**
	20200123_14_54_52	4.43	5.73	-	**5.08**
	20191107_13_29_45	9.30	10.27	6.87	**8.81**
mec-4d Dauer	20191107_11_44_36	15.37	12.62	13.71	**13.90**
mec-4d L2 EGTA	20200124_10_55_53	0.86	0.77	0.74	**0.79**
	20200124_10_50_17	1.49	1.59	1.50	**1.52**
	20200124_14_17_57	4.65	4.92	-	**4.79**

MEC-4 channel puncta observed in different condition normalized by 100 µm (Fig. 8)

			Puncta per 100 µm		
E. coli OP50	WT	L2	16.62	15.48	15.34
		dauer	11.75	13.93	14.06
	mec-4d	L2	14.37	15.22	15.07
		dauer	13.6	13.5	14.27
E. coli HT115	WT	L2	14.85	14.35	14.4
		dauer	11.75	12.88	13.92
	mec-4d	L2	15.17	14.37	14.93
		dauer	14.38	14.48	14.34

Percent of AxW observed in each replicate through AVM degeneration in two diets (Fig. 9-10)

	Hours post-hatching	Percent of AxW		
Control - *E. coli* OP50	24	7.4	3.9	4.4
	48	3.9	3.5	4.4
	72	0.0	0.0	3.7
No calcium - *E. coli* OP50	24	11.5	8.3	10.7
	48	8.7	6.9	6.9
	72	3.5	4.0	3.6
Control - *E. coli* HT115	24	14.3	20.0	19.2
	48	34.4	26.7	34.5
	72	30.8	38.5	33.3
No calcium - *E. coli* HT115	24	16.0	17.4	20.0
	48	26.9	31.8	28.0
	72	16.0	12.0	20.0

Percent of AxW observed in each replicate in diapause in two diets (Fig. 9-10)

	Days in diapause	Percent of AxW			
Control - *E. coli* OP50	2	43.4	64.1	29.2	
	7	72.6	77.3	85.7	
	14	78.5	77.2	66.7	
No calcium - *E. coli* OP50	2	11.5	14.8	29.2	
	7	38.7	22.2	35.7	
	14	24.1	25.0	35.7	
Control - *E. coli* HT115	2	65.4	34.6	42.3	40.9
	7	69.6	39.3	46.4	44.8
	14	60	67.9	59.3	63
No calcium - *E. coli* HT115	2	40.7	43.8	34.6	
	7	48.5	44.8	28.6	
	14	53.6	31	27.6	

Percent of AxW observed for *cebp-1* RNAi treatment (Fig. 11)

		Percent of AxW			
Systemic	*E. coli* HT115	31.8	42.9	28.0	29.6
	cebp-1	7.7	13.6	16.0	13.6
TRN-specific	*E. coli* HT115	33.3	32.3	34.6	30.0
	cebp-1	35.0	24.1	26.1	21.7

Percent of AxW observed in different RNAi treatments targeting intracellular calcium transporters at 72 hours post-hatching. Each value corresponds to one replicate.

			Percent of AxW					
Control	TRN specific	HT115	33.3	30.0	71.0	63.6	38.7	43.3
		mcu-1	30.4	37.0	35.7	36.7	34.5	40.6
		sca-1	39.1	53.6	35.7	32.3	43.3	31.0
		mcu-1; sca-1	23.5	23.1	22.6			
	Systemic	HT115	46.2	47.8	29.6	31.3	32.1	
		mcu-1	41.7	44.0	41.7	26.3	43.8	
		sca-1	55.6	36.7	18.8	32.1	21.7	
		mcu-1; sca-1	29.0	34.4	28.0			
No calcium	TRN specific	HT115	20.7	35.7	28.6	27.3		
		mcu-1	10.7	28.0	34.8	20.7		
		sca-1	26.7	28.0	33.3	24.0		
		mcu-1; sca-1	11.5	36.0	42.3	22.7		
	Systemic	HT115	20.0	20.7	21.7	22.2		
		mcu-1	7.4	17.4	33.3	16.7		
		sca-1	4.5	11.5	31.0	19.2		
		mcu-1; sca-1	6.9	29.2	29.6	22.7		

Percent of AxW observed in different RNAi treatments targeting intracellular calcium transporters in diapause (Fig. 14)

		Days in diapause	Percent of AxW			
TRN specific	HT115	2	50.0	36.7	48.1	42.9
		7	62.5	48.1	51.9	53.6
		14	66.7	51.9	51.7	58.6
	mcu-1	2	33.3	23.1	41.9	47.6
		7	43.5	39.3	35.5	30.8
		14	29.6	33.3	29.6	46.2
	sca-1	2	37.9	28.0	29.6	38.1
		7	29.2	38.7	35.7	31.0
		14	38.5	34.5	35.7	44.0
	mcu-1; sca-1	2	32.1	12.0	44.4	42.9
		7	28.0	42.3	43.3	39.1
		14	20.0	25.9	39.3	52.2
Systemic	HT115	2	65.4	34.6	42.3	40.9
		7	69.6	39.3	46.4	44.8
		14	60.0	67.9	59.3	63.0
	mcu-1	2	39.3	20.0	40.7	34.8
		7	48.1	38.5	39.4	24.1
		14	48.0	41.4	48.1	25.0
	sca-1	2	10.7	25.0	35.7	37.0
		7	37.5	34.5	37.9	25.9
		14	35.7	50.0	41.7	30.8
	mcu-1; sca-1	2	8.3	21.4	44.4	28.0
		7	5.6	38.5	44.0	32.0
		14	30.8	37.9	53.6	38.5

Percent of AxW observed in absence of calcium for different RNAi treatments targeting intracellular calcium transporters in diapause (Fig. 15).

			Days in diapause	Percent of AxW		
No calcium	TRN specific	HT115	2	46.4	53.8	50.0
			7	50.0	46.4	34.6
			14	34.3	48.1	21.7
		mcu-1	2	45.5	54.2	68.0
			7	53.6	48.1	37.9
			14	50.0	52.0	32.1
		sca-1	2	50.0	50.0	52.0
			7	48.3	50.0	42.9
			14	38.5	44.0	25.0
		mcu-1; sca-1	2	50.0	57.1	55.6
			7	53.6	56.0	44.4
			14	29.6	51.7	34.6
	Systemic	HT115	2	40.7	43.8	34.6
			7	48.5	44.8	28.6
			14	53.6	31.0	27.6
		mcu-1	2	35.3	65.4	41.4
			7	34.4	51.9	29.6
			14	65.5	42.3	25.9
		sca-1	2	40.6	47.8	30.8
			7	38.7	38.5	25.9
			14	65.4	42.3	18.5
		mcu-1; sca-1	2	56.3	60.7	38.5
			7	48.0	56.0	34.6
			14	60.7	48.1	25.9

Mitochondrial number and length from different TRNs in a wild-type background (Fig. 18)

	Stage	TRN	Count per 20 µm			Length (µm)		
E. coli OP50	L2	PLM	1.3	1.3	1.2	1.23	1.30	1.26
		ALM	1.7	1.6	1.5	1.43	1.49	1.62
		AVM	2.0	2.4	2.1	1.25	1.13	1.17
	dauer	PLM	1.8	1.6	1.5	1.76	2.03	2.02
		ALM	1.1	1.4	1.0	1.59	1.73	2.12
		AVM	1.7	1.8	2.0	1.28	1.46	1.37

Mitochondrial number from wild-type and mec-4d strains in two different diets (Fig. 19, 21). Each row corresponds to the number of mitochondria in each animal measured. Each replicate considers 10 animals.

	E. coli OP50					*E. coli* HT115			
	WT L2	WT dauer	*mec-4d* L2	*mec-4d* dauer		WT L2	WT dauer	*mec-4d* L2	*mec-4d* dauer
Count per 20 µm	2.6	2.0	0.6	2.3		2.8	2.1	1.2	1.8
	1.3	1.8	0.8	2.3		1.7	1.9	2.1	1.9
	2.7	1.4	1.7	3.4		1.8	2.5	1.6	1.5
	2.1	1.7	3.2	2.3		2.6	1.8	2.3	2.5
	1.7	1.4	2.5	1.4		1.8	1.6	2.5	1.6
	1.7	1.2	1.3	1.9		1.8	2.1	2.5	1.2
	1.3	1.8	1.8	2.4		2.0	1.6	3.1	2.4
	2.4	1.8	1.6	2.1		2.1	1.9	2.0	2.4
	2.5	2.1	1.9	2.1		2.4	2.0	1.7	1.4
	2.0	2.0	1.4	2.4		2.2	1.9	2.8	2.0
	2.3	1.7	1.6	1.9		2.1	1.7	1.5	2.0
	1.5	1.6	1.3	1.8		2.9	1.7	1.7	2.2
	1.7	1.9	1.8	2.2		2.3	2.0	2.1	2.0
	3.5	1.2	2.2	1.9		1.8	2.0	3.0	2.6
	3.1	2.0	1.6	2.1		2.1	2.4	1.8	1.8
	2.4	1.9	2.4	1.7		1.8	2.5	1.3	2.0
	2.5	1.8	1.2	1.7		1.8	1.7	0.8	2.0
	2.2	1.7	1.4	1.7		2.1	2.9	1.6	2.5
	2.7	2.2	1.5	2.0		2.4	2.1	3.2	2.9
	2.3	1.9	1.6	1.9		1.5	2.0	2.0	1.7
	2.6	1.8	2.3	1.9		2.8	1.7	0.6	1.9
	1.9	2.4	1.3	3.4		2.4	1.5	1.6	2.1
	1.9	2.1	2.3	2.3		1.9	1.6	1.2	2.1
	2.2	1.9	1.2	2.0		3.9	2.1	1.3	3.0
	1.8	2.1	1.6	2.9		2.8	1.8	1.8	2.2
	2.3	1.8	1.1	1.9		2.2	2.0	1.5	2.5
	2.4	2.3	2.3	2.2		2.3	1.9	1.1	2.1
	1.7	2.0	1.4	3.1		1.9	1.9	2.6	1.8
	2.3	1.8	1.6	4.8		2.9	1.5	1.6	2.0
	1.8	1.6	1.8	2.3		2.4	2.0	2.0	3.1

Mitochondrial length from wild-type and mec-4d strains in two different diets (Fig. 19, 21). Each row corresponds to the average length of mitochondria in each animal measured. Each replicate considers 10 animals

	E. coli OP50					*E. coli* HT115			
	WT L2	WT dauer	*mec-4d* L2	*mec-4d* dauer		WT L2	WT dauer	*mec-4d* L2	*mec-4d* dauer
Length (um)	1.0	1.2	1.4	1.2		1.2	1.0	0.8	1.0
	1.6	1.3	1.2	0.8		1.7	1.2	0.8	1.0
	1.0	1.7	0.9	0.9		1.2	1.1	0.9	1.4
	1.8	1.2	1.0	1.5		1.3	0.9	1.3	1.1
	1.3	1.1	1.1	1.8		1.2	1.2	0.8	0.8
	1.6	1.3	0.9	1.1		1.5	1.1	0.7	1.2
	0.9	1.4	0.8	1.2		0.9	1.0	1.1	1.1
	1.3	1.1	0.8	1.3		1.6	1.4	1.0	1.2
	1.4	1.3	0.8	1.2		1.5	1.1	0.7	1.2
	0.8	1.3	1.1	1.1		0.9	1.2	0.8	1.0
	1.2	1.2	0.7	1.0		1.2	2.3	0.9	1.0
	1.6	1.3	0.9	1.1		1.4	2.3	0.9	0.9
	1.4	1.1	0.8	1.2		1.4	1.9	1.0	0.7
	1.1	2.0	1.1	1.0		1.7	1.9	0.9	1.2
	1.0	1.5	0.9	1.2		2.0	1.7	1.0	1.6
	0.9	1.4	1.1	1.2		1.5	1.5	1.0	1.2
	0.9	1.1	0.9	1.2		2.2	2.1	0.7	1.2
	0.8	1.9	1.0	1.7		1.2	1.2	0.7	1.0
	1.2	1.6	0.8	1.3		1.5	1.6	0.6	1.2
	1.1	1.6	0.9	1.2		1.4	1.3	0.6	1.1
	1.2	1.4	0.8	1.6		1.3	0.9	0.8	1.1
	1.1	1.2	0.8	0.9		1.6	1.2	0.8	1.0
	1.3	1.2	1.0	1.6		1.3	1.3	0.8	0.7
	1.3	1.6	0.6	1.3		1.3	1.2	1.0	1.2
	1.1	1.5	0.9	1.0		1.2	1.2	0.7	1.2
	1.3	1.5	1.0	1.1		2.0	1.3	0.7	1.1
	1.0	1.1	1.0	1.1		1.4	1.1	1.1	0.9
	1.2	1.4	1.0	1.1		1.1	1.7	0.7	1.2
	1.1	1.4	0.7	1.4		1.3	1.8	0.8	0.9
	1.1	1.3	1.0	1.1		1.4	1.4	0.8	1.1

Mitochondrial number and length from wild-type and *mec-4d* strains in absence of environmental calcium (Fig. 20). Each row corresponds to the number of mitochondria and the average of them in each animal measured. Each replicate considers 10 animals.

E. coli OP50							
Count per 20 µm				Length (µm)			
WT L2	WT dauer	*mec-4d* L2	*mec-4d* dauer	WT L2	WT dauer	*mec-4d* L2	*mec-4d* dauer
2.8	2.3	0.9	1.3	0.9	1.0	0.6	0.9
2.2	1.9	0.6	2.0	0.9	1.2	0.6	0.9
2.0	1.2	1.3	1.9	0.9	1.4	0.8	0.9
1.6	1.9	1.5	2.2	1.1	1.2	0.6	0.9
2.0	2.1	1.5	1.2	1.1	1.2	0.8	0.9
1.7	1.9	1.2	3.0	1.1	1.3	0.7	0.7
1.8	1.8	0.7	1.3	1.0	1.4	0.4	1.4
1.4	1.7	1.7	1.4	1.1	1.6	0.6	1.1
2.6	1.6	1.2	1.8	0.8	1.2	0.7	1.1
2.2	1.2	2.5	2.3	1.2	1.7	0.6	1.1
1.3	1.7	0.9	2.0	0.7	0.9	0.7	0.6
2.0	1.6	1.6	2.1	0.9	1.3	0.7	0.9
1.6	3.7	2.0	2.2	0.8	1.2	0.5	1.1
2.0	2.1	1.6	2.0	0.8	1.3	0.6	1.0
1.6	1.9	1.3	1.5	0.9	1.2	0.8	1.1
1.2	2.1	1.5	1.9	0.9	1.4	0.6	1.1
2.4	1.8	1.6	2.5	0.8	1.1	0.6	1.2
1.4	1.4	1.6	2.7	1.2	1.4	0.6	0.8
1.5	2.3	1.8	2.5	1.0	0.8	1.0	0.9
1.9	1.9	1.0	2.2	0.9	0.8	0.9	1.5
1.6	2.9	1.9	1.9	1.1	0.9	0.5	1.4
1.6	2.1	1.0	2.2	1.0	0.9	0.7	0.9
2.0	2.0	1.2	2.9	1.1	1.0	0.8	0.8
1.6	2.5	1.3	2.1	1.2	1.1	0.6	0.9
2.0	2.0	1.3	2.4	1.2	1.3	0.6	1.0
2.1	1.7	1.1	1.8	1.0	1.2	0.8	0.9
2.8	2.1	1.6	2.6	1.0	1.1	0.8	1.1
1.9	2.1	1.3	2.2	0.9	1.3	0.6	1.0
1.6	1.9	2.3	2.6	0.8	1.2	0.7	0.9
2.6	2.2	0.9	2.3	0.7	1.1	1.3	1.0

Percentage of the population of wild-type and *mec-4d* animals that exhibits non-fragmented mitochondria in two different diets (Fig. 19, 21)

		Percentage of the population exhibiting non-fragmented mitochondria		
E. coli OP50	WT L2	60	70	80
	mec-4d L2	10	20	30
	WT dauer	80	80	90
	mec-4d dauer	70	60	80
E. coli HT115	WT L2	80	90	90
	mec-4d L2	20	40	10
	WT dauer	40	90	80
	mec-4d dauer	40	50	40

Axon WT-like correlated with different mitochondrial attributes in two different diets (Fig. 22)

		AxW	Mitochondrial length (µm)	Mitochondrial count	Mitochondrial count per 10µm
E. coli OP50	Dauer	77.3	1.215	19	1.130
		87.8	1.215	16	0.944
		85.7	1.204	20	1.342
	L2	2.6	0.977	13	0.084
		6.8	0.911	12	0.083
		3.8	0.884	15	0.084
E. coli HT115	Dauer	69.6	1.094	14	0.937
		39.3	1.130	18	1.080
		46.4	1.031	18	1.139
	L2	14.29	0.881	17	1.087
		20.0	0.828	13	0.956
		19.23	0.811	11	0.768

Percent of AxW observed in different RNAi treatments targeting mitochondrial genes related to fusion-fission dynamics and energy production at 72 hours post-hatching (Fig. 24). Cells in the same column were done in parallel experiments.

		Percent of AxW										
TRN specific	HT115	33.3	32.3	34.6	30.0	24.0	27.3	26.1	31.0	29.6	30.0	27.3
	drp-1	27.6	23.1	37.5	38.5							
	eat-3	19.0	23.1	40.0	40.7							
	fzo-1					3.7	12.9	7.7				
	cts-1	23.1	20.7	13.6	16.0							
	icl-1								14.3	25.9	16.0	16.0
Systemic	HT115	31.8	42.9	28.0	29.6	28.0	40.7	36.0	29.6	28.0	32.0	24.1
	drp-1	29.6	28.6	24.1	32.0							
	eat-3	45.5	37.5	29.2	25.0							
	fzo-1					7.4	12.5	17.9				
	cts-1	32.0	26.9	4.2	13.0							
	icl-1								44.0	12.0	21.4	22.6

ANNEX 3: STATISTICAL RESULTS

One-way ANOVA of culture under no calcium conditions (Fig. 6)

Column B	No calcium + EGTA
vs.	vs.
Column A	Control
Unpaired t test with Welch's correction	
P value	0.0173
P value summary	*
Significantly different (P < 0.05)?	Yes
One- or two-tailed P value?	Two-tailed
Welch-corrected t, df	t=3.999 df=3.856

One-way ANOVA of Puncta Number in L2 and dauer while eating *E. coli* OP50 (Fig 8B)

Number of families	1				
Number of comparisons per family	6				
Alpha	0.05				
Tukey's multiple comparisons test	Mean Diff.	95.00% CI of diff.	Significant?	Summary	Adjusted P Value
L2 WT OP vs. *dauer* WT OP	2.567	0.4756 to 4.658	Yes	*	0.0183
L2 WT OP vs. L2 mec-4d OP	0.9267	-1.164 to 3.018	No	ns	0.5226
L2 WT OP vs. *dauer* mec-4d OP	2.023	-0.06774 to 4.114	No	ns	0.0579
dauer WT OP vs. L2 mec-4d OP	-1.64	-3.731 to 0.4511	No	ns	0.1323
dauer WT OP vs. *dauer* mec-4d OP	-0.5433	-2.634 to 1.548	No	ns	0.838
L2 mec-4d OP vs. *dauer* mec-4d OP	1.097	-0.9944 to 3.188	No	ns	0.3924

One-way ANOVA of Puncta Number in L2 and dauer while eating *E. coli* HT115 (Fig 8C)

Number of families	1				
Number of comparisons per family	6				
Alpha	0.05				
Tukey's multiple comparisons test	Mean Diff.	95.00% CI of diff.	Significant?	Summary	Adjusted P Value
L2 WT HT vs. *dauer* WT HT	1.683	0.1213 to 3.245	Yes	*	0.0353
L2 WT HT vs. L2 *mec-4d* HT	-0.29	-1.852 to 1.272	No	ns	0.9309
L2 WT HT vs. *dauer mec-4d* HT	0.1333	-1.429 to 1.695	No	ns	0.9923
dauer WT HT vs. L2 *mec-4d* HT	-1.973	-3.535 to -0.4113	Yes	*	0.0157
dauer WT HT vs. *dauer mec-4d* HT	-1.55	-3.112 to 0.01198	No	ns	0.0518
L2 *mec-4d* HT vs. *dauer mec-4d* HT	0.4233	-1.139 to 1.985	No	ns	0.8211

Two-way ANOVA comparing the progression of degeneration in *E. coli* OP50 diet during development (Fig. 10A)

Number of families	1				
Number of comparisons per family	3				
Alpha	0.05				
Sidak's multiple comparisons test	Mean Diff.	95.00% CI of diff.	Significant?	Summary	Adjusted P Value
Control - *E. coli* OP50 - No calcium - E. coli OP50					
24	-4.99	-8.245 to -1.735	Yes	**	0.0034
48	-3.617	-6.871 to -0.3622	Yes	*	0.0284
72	-2.44	-5.695 to 0.8145	No	ns	0.1693

Two-way ANOVA comparing the progression of regeneration in diapause after exposure to *E. coli* OP50 (Fig. 10B)

Number of families	1				
Number of comparisons per family	3				
Alpha	0.05				
Sidak's multiple comparisons test	Mean Diff.	95.00% CI of diff.	Significant?	Summary	Adjusted P Value
Control - *E. coli* OP50 - No calcium - *E. coli* OP50					
2	27.07	4.421 to 49.71	Yes	*	0.0185
7	46.33	23.69 to 68.98	Yes	***	0.0003
14	45.87	23.22 to 68.51	Yes	***	0.0003

Two-way ANOVA comparing the progression of degeneration in *E. coli* HT115 diet during development (Fig. 11A)

Number of families	1				
Number of comparisons per family	3				
Alpha	0.05				
Sidak's multiple comparisons test	Mean Diff.	95.00% CI of diff.	Significant?	Summary	Adjusted P Value
Control - *E. coli* HT115 - No calcium - *E. coli* HT115					
24	0.04333	-7.779 to 7.866	No	ns	>0.9999
48	2.93	-4.893 to 10.75	No	ns	0.6854
72	18.19	10.36 to 26.01	Yes	****	<0.0001

Two-way ANOVA comparing the progression of regeneration in diapause after exposure to *E. coli* HT115 (Fig. 11B)

Number of families	1				
Number of comparisons per family	3				
Alpha	0.05				
Sidak's multiple comparisons test	Mean Diff.	95.00% CI of diff.	Significant?	Summary	Adjusted P Value
Control - *E. coli* HT115 - No calcium - *E. coli* HT115					
2	6.1	-16.35 to 28.55	No	ns	0.8569
7	9.392	-13.06 to 31.84	No	ns	0.6252
14	25.15	2.698 to 47.6	Yes	*	0.0263

t-test of AxW percentage observed for *cebp-1* silencing (Fig. 12D)

Column B	*cebp-1*
vs.	vs.
Column A	HT115
Unpaired t test with Welch's correction	
P value	0.0041
P value summary	**
Significantly different (P < 0.05)?	Yes
One- or two-tailed P value?	Two-tailed
Welch-corrected t, df	t=5.352 df=4.538

One-way ANOVA comparing the presence of AxW under different silencing (Fig. 13A).

Number of families	1				
Number of comparisons per family	3				
Alpha	0.05				
Dunnett's multiple comparisons test	Mean Diff.	95.00% CI of diff.	Significant?	Summary	Adjusted P Value
HT115 vs. *sca-1*	7.483	-7.903 to 22.87	No	ns	0.4708
HT115 vs. *mcu-1*	10.83	-4.553 to 26.22	No	ns	0.2036
HT115 vs. *mcu-1; sca-1*	23.58	4.739 to 42.43	Yes	*	0.0133

Two-way ANOVA comparing the percentage of AxW observed in TRN-specific silencing in dauer stage (Fig. 15A).

Number of families	3				
Number of comparisons per family	3				
Alpha	0.05				
Dunnett's multiple comparisons test	Mean Diff.	95.00% CI of diff.	Significant?	Summary	Adjusted P Value
2					
HT115 (+Ca) vs. *mcu-1* (+Ca)	7.95	-6.84 to 22.74	No	ns	0.4208
HT115 (+Ca) vs. *sca-1* (+Ca)	11.03	-3.765 to 25.82	No	ns	0.1817
HT115 (+Ca) vs. *sca-1; mcu-1* (+Ca)	11.58	-3.215 to 26.37	No	ns	0.153
7					
HT115 (+Ca) vs. *mcu-1* (+Ca)	16.75	1.96 to 31.54	Yes	*	0.0233
HT115 (+Ca) vs. *sca-1* (+Ca)	20.38	5.585 to 35.17	Yes	**	0.0049
HT115 (+Ca) vs. *sca-1; mcu-1* (+Ca)	15.85	1.06 to 30.64	Yes	*	0.0333
14					
HT115 (+Ca) vs. *mcu-1* (+Ca)	22.55	7.76 to 37.34	Yes	**	0.0018
HT115 (+Ca) vs. *sca-1* (+Ca)	19.05	4.26 to 33.84	Yes	**	0.0089
HT115 (+Ca) vs. *sca-1; mcu-1* (+Ca)	22.88	8.085 to 37.67	Yes	**	0.0016

Two-way ANOVA comparing the percentage of AxW observed in systemic silencing in the dauer stage (Fig. 15B).

Number of families	3				
Number of comparisons per family	3				
Alpha	0.05				
Dunnett's multiple comparisons test	Mean Diff.	95.00% CI of diff.	Significant?	Summary	Adjusted P Value
2					
HT115 (+Ca) vs. *mcu-1* (+Ca)	12.1	-7.533 to 31.73	No	ns	0.314
HT115 (+Ca) vs. *sca-1* (+Ca)	18.7	-0.9331 to 38.33	No	ns	0.0648
HT115 (+Ca) vs. *sca-1; mcu-1* (+Ca)	20.28	0.6419 to 39.91	Yes	*	0.0416
7					
HT115 (+Ca) vs. *mcu-1* (+Ca)	12.5	-7.133 to 32.13	No	ns	0.2896
HT115 (+Ca) vs. *sca-1* (+Ca)	16.08	-3.558 to 35.71	No	ns	0.1287
HT115 (+Ca) vs. *sca-1; mcu-1* (+Ca)	20	0.3669 to 39.63	Yes	*	0.045
14					
HT115 (+Ca) vs. *mcu-1* (+Ca)	21.93	2.292 to 41.56	Yes	*	0.0255
HT115 (+Ca) vs. *sca-1* (+Ca)	23	3.367 to 42.63	Yes	*	0.0184
HT115 (+Ca) vs. *sca-1; mcu-1* (+Ca)	22.35	2.717 to 41.98	Yes	*	0.0224

One-way ANOVA for mitochondrial number in different TRN (Fig-19A).

Number of families	1				
Number of comparisons per family	15				
Alpha	0.05				
Tukey's multiple comparisons test	Mean Diff.	95.00% CI of diff.	Significant?	Summary	Adjusted P Value
L2 PLM vs. L2 ALM	-0.3133	-0.7364 to 0.1098	No	ns	0.2022
L2 PLM vs. L2 AVM	-0.9133	-1.336 to -0.4902	Yes	***	0.0001
L2 PLM vs. Dauer PLM	-0.3333	-0.7564 to 0.08977	No	ns	0.1589
L2 PLM vs. Dauer ALM	0.1	-0.3231 to 0.5231	No	ns	0.9633
L2 PLM vs. Dauer AVM	-0.56	-0.9831 to -0.1369	Yes	**	0.008
L2 ALM vs. L2 AVM	-0.6	-1.023 to -0.1769	Yes	**	0.0048
L2 ALM vs. Dauer PLM	-0.02	-0.4431 to 0.4031	No	ns	>0.9999
L2 ALM vs. Dauer ALM	0.4133	-0.009766 to 0.8364	No	ns	0.0569
L2 ALM vs. Dauer AVM	-0.2467	-0.6698 to 0.1764	No	ns	0.4163
L2 AVM vs. Dauer PLM	0.58	0.1569 to 1.003	Yes	**	0.0062
L2 AVM vs. Dauer ALM	1.013	0.5902 to 1.436	Yes	****	<0.0001
L2 AVM vs. Dauer AVM	0.3533	-0.06977 to 0.7764	No	ns	0.1239
Dauer PLM vs. Dauer ALM	0.4333	0.01023 to 0.8564	Yes	*	0.0436
Dauer PLM vs. Dauer AVM	-0.2267	-0.6498 to 0.1964	No	ns	0.5004
Dauer ALM vs. Dauer AVM	-0.66	-1.083 to -0.2369	Yes	**	0.0022

One-way ANOVA for Mitochondrial Length in different TRN (Fig. 19B).

Number of families	1				
Number of comparisons per family	15				
Alpha	0.05				
Tukey's multiple comparisons test	Mean Diff.	95.00% CI of diff.	Significant?	Summary	Adjusted P Value
L2 PLM vs. L2 ALM	-0.2477	-0.6382 to 0.1429	No	ns	0.3348
L2 PLM vs. L2 AVM	0.07867	-0.3119 to 0.4692	No	ns	0.9814
L2 PLM vs. Dauer PLM	-0.6743	-1.065 to -0.2838	Yes	***	0.0009
L2 PLM vs. Dauer ALM	-0.5507	-0.9412 to -0.1601	Yes	**	0.005
L2 PLM vs. Dauer AVM	-0.1057	-0.4962 to 0.2849	No	ns	0.9369
L2 ALM vs. L2 AVM	0.3263	-0.06425 to 0.7169	No	ns	0.1237
L2 ALM vs. Dauer PLM	-0.4267	-0.8172 to -0.03608	Yes	*	0.0297
L2 ALM vs. Dauer ALM	-0.303	-0.6936 to 0.08758	No	ns	0.1691
L2 ALM vs. Dauer AVM	0.142	-0.2486 to 0.5326	No	ns	0.8189
L2 AVM vs. Dauer PLM	-0.753	-1.144 to -0.3624	Yes	***	0.0003
L2 AVM vs. Dauer ALM	-0.6293	-1.02 to -0.2388	Yes	**	0.0017
L2 AVM vs. Dauer AVM	-0.1843	-0.5749 to 0.2062	No	ns	0.6219
Dauer PLM vs. Dauer ALM	0.1237	-0.2669 to 0.5142	No	ns	0.8866
Dauer PLM vs. Dauer AVM	0.5687	0.1781 to 0.9592	Yes	**	0.0039
Dauer ALM vs. Dauer AVM	0.445	0.05442 to 0.8356	Yes	*	0.0227

One-way ANOVA of mitochondrial number in *E. coli* OP50 diet (20A).

Number of families	1				
Number of comparisons per family	4				
Alpha	0.05				
Sidak's multiple comparisons test	Mean Diff.	95.00% CI of diff.	Significant?	Summary	Adjusted P Value
WT L2 vs. WT dauer	0.342	0.003555 to 0.6804	Yes	*	0.0466
WT L2 vs. *mec-4d* L2	0.5021	0.1636 to 0.8405	Yes	**	0.0011
mec-4d L2 vs. *mec-4d* dauer	-0.6001	-0.9386 to -0.2617	Yes	****	<0.0001
WT dauer vs. *mec-4d* dauer	-0.4401	-0.7785 to -0.1016	Yes	**	0.0053

One-way ANOVA of mitochondrial length in *E. coli* OP50 diet (20B).

Number of families	1				
Number of comparisons per family	4				
Alpha	0.05				
Sidak's multiple comparisons test	Mean Diff.	95.00% CI of diff.	Significant?	Summary	Adjusted P Value
WT L2 vs. WT dauer	-0.1846	-0.327 to -0.04213	Yes	**	0.0055
WT L2 vs. *mec-4d* L2	0.261	0.1186 to 0.4035	Yes	****	<0.0001
mec-4d L2 vs. *mec-4d* dauer	-0.2872	-0.4297 to -0.1448	Yes	****	<0.0001
WT dauer vs. *mec-4d* dauer	0.1584	0.01593 to 0.3008	Yes	*	0.0228

One-way ANOVA of the percentage of the population that exhibits non-fragmented mitochondria in *E. coli* OP50 diet (20C).

Number of families	1				
Number of comparisons per family	4				
Alpha	0.05				
Sidak's multiple comparisons test	Mean Diff.	95.00% CI of diff.	Significant?	Summary	Adjusted P Value
WT L2 vs. *mec-4d* L2	50	26.2 to 73.8	Yes	***	0.0006
mec-4d L2 vs. *mec-4d* dauer	-50	-73.8 to -26.2	Yes	***	0.0006
WT dauer vs. *mec-4d* dauer	13.33	-10.47 to 37.13	No	ns	0.3766
WT L2 vs. WT dauer	-13.33	-37.13 to 10.47	No	ns	0.3766

One-way ANOVA of mitochondrial number under no calcium conditions in *E. coli* OP50 diet (Fig.21A)

Number of families	1				
Number of comparisons per family	6				
Alpha	0.05				
Tukey's multiple comparisons test	Mean Diff.	95.00% CI of diff.	Significant?	Summary	Adjusted P Value
WT L2 vs. WT dauer	-0.08622	-0.3868 to 0.2144	No	ns	0.8775
WT L2 vs. *mec-4d* L2	0.5106	0.21 to 0.8112	Yes	***	0.0001
WT L2 vs. *mec-4d* dauer	-0.1977	-0.4983 to 0.1028	No	ns	0.3206
WT dauer vs. *mec-4d* L2	0.5968	0.2962 to 0.8974	Yes	****	<0.0001
WT dauer vs. *mec-4d* dauer	-0.1115	-0.4121 to 0.189	No	ns	0.7683
mec-4d L2 vs. *mec-4d* dauer	-0.7083	-1.009 to -0.4078	Yes	****	<0.0001

One-way ANOVA of mitochondrial length under no calcium conditions in *E. coli* OP50 diet (Fig.21B)

Number of families	1				
Number of comparisons per family	6				
Alpha	0.05				
Tukey's multiple comparisons test	Mean Diff.	95.00% CI of diff.	Significant?	Summary	Adjusted P Value
WT L2 vs. WT dauer	-0.2173	-0.3398 to -0.09485	Yes	****	<0.0001
WT L2 vs. *mec-4d* L2	0.2746	0.1521 to 0.3971	Yes	****	<0.0001
WT L2 vs. *mec-4d* dauer	-0.02467	-0.1472 to 0.09782	No	ns	0.9529
WT dauer vs. *mec-4d* L2	0.4919	0.3695 to 0.6144	Yes	****	<0.0001
WT dauer vs. *mec-4d* dauer	0.1927	0.07018 to 0.3152	Yes	***	0.0004
mec-4d L2 *vs. mec-4d dauer*	-0.2993	-0.4218 to -0.1768	Yes	****	<0.0001

One-way ANOVA of mitochondrial number in *E. coli* HT115 diet (22A).

Number of families	1				
Number of comparisons per family	4				
Alpha	0.05				
Sidak's multiple comparisons test	Mean Diff.	95.00% CI of diff.	Significant?	Summary	Adjusted P Value
WT L2 vs. WT dauer	0.31	-0.01289 to 0.6329	No	ns	0.065
WT L2 vs. *mec-4d* L2	0.3756	0.05268 to 0.6985	Yes	*	0.0156
mec-4d L2 vs. *mec-4d* dauer	-0.23	-0.5529 to 0.09292	No	ns	0.2652
WT dauer vs. *mec-4d* dauer	-0.1644	-0.4873 to 0.1585	No	ns	0.5909

One-way ANOVA of mitochondrial number in *E. coli* HT115 diet (22B)

Number of families	1				
Number of comparisons per family	4				
Alpha	0.05				
Sidak's multiple comparisons test	Mean Diff.	95.00% CI of diff.	Significant?	Summary	Adjusted P Value
WT L2 vs. WT dauer	0.0116	-0.1669 to 0.1901	No	ns	0.9997
WT L2 vs. *mec-4d* L2	0.5705	0.392 to 0.7491	Yes	****	<0.0001
mec-4d L2 vs. *mec-4d* dauer	-0.2449	-0.4235 to -0.06642	Yes	**	0.0029
WT dauer vs. *mec-4d* dauer	0.314	0.1355 to 0.4925	Yes	****	<0.0001

One-way ANOVA of the percentage of the population that exhibits non-fragmented mitochondria in *E. coli* HT115 diet (22C)

Number of families	1				
Number of comparisons per family	4				
Alpha	0.05				
Sidak's multiple comparisons test	Mean Diff.	95.00% CI of diff.	Significant?	Summary	Adjusted P Value
WT L2 vs. *mec-4d* L2	63.33	22.11 to 104.6	Yes	**	0.0047
WT L2 vs. WT dauer	16.67	-24.56 to 57.89	No	ns	0.6535
mec-4d L2 vs. *mec-4d* dauer	-20	-61.22 to 21.22	No	ns	0.502
WT dauer vs. *mec-4d* dauer	26.67	-14.56 to 67.89	No	ns	0.2607

Coefficient of Pearson Correlation for AxW observed in *E. coli* OP50 diet (23A)

Correlation			
	AxW vs. Mitochondrial length (μm)	AxW vs. Mitochondrial count	AxW vs. Mitochondrial count per 10μm
Pearson r			
r	0.9744	0.8354	0.9708
95% confidence interval	0.7785 to 0.9973	0.07389 to 0.9815	0.7504 to 0.9969
R squared	0.9495	0.6978	0.9424
P value			
P (two-tailed)	0.001	0.0384	0.0013
P value summary	***	*	**
Significant? (alpha = 0.05)	Yes	Yes	Yes
Number of XY Pairs	6	6	6

Coefficient of Pearson Correlation for AxW observed in *E. coli* HT115 diet (23B)

Correlation			
	AxW vs. Mitochondrial length (μm)	AxW vs. Mitochondrial count	AxW vs. Mitochondrial count per 10μm
Pearson r			
r	0.8194	0.2074	0.1564
95% confidence interval	0.02353 to 0.9796	-0.7264 to 0.8722	-0.7504 to 0.8589
R squared	0.6715	0.04301	0.02446
P value			
P (two-tailed)	0.046	0.6934	0.7673
P value summary	*	ns	ns
Significant? (alpha = 0.05)	Yes	No	No
Number of XY Pairs	6	6	6

One-way ANOVA comparing the effect of different mitochondrial genes knockdown TRN-specific in development (24A)

Number of families	1				
Number of comparisons per family	5				
Alpha	0.05				
Dunnett's multiple comparisons test	Mean Diff.	95.00% CI of diff.	Significant?	Summary	Adjusted P Value
HT115 vs. *drp-1*	-2.088	-11.38 to 7.208	No	ns	0.9599
HT115 vs. *eat-3*	-1.113	-10.41 to 8.183	No	ns	0.9971
HT115 vs. *fzo-1*	21.49	11.12 to 31.86	Yes	****	<0.0001
HT115 vs. *cts-1*	11.24	1.942 to 20.53	Yes	*	0.0141
HT115 vs. *icl-1*	11.54	2.242 to 20.83	Yes	*	0.0115

One-way ANOVA comparing the effect of different mitochondrial genes of systemic knockdown in development (24B).

Number of families	1				
Number of comparisons per family	5				
Alpha	0.05				
Dunnett's multiple comparisons test	Mean Diff.	95.00% CI of diff.	Significant?	Summary	Adjusted P Value
HT115 vs. *drp-1*	3.311	-9.952 to 16.57	No	ns	0.9396
HT115 vs. *eat-3*	-2.414	-15.68 to 10.85	No	ns	0.9831
HT115 vs. *fzo-1*	19.29	4.491 to 34.08	Yes	**	0.0077
HT115 vs. *cts-1*	12.86	-0.4018 to 26.12	No	ns	0.0595
HT115 vs. *icl-1*	6.886	-6.377 to 20.15	No	ns	0.5045

REFERENCES:

- Adalbert, R., Gillingwater, T.H., Haley, J.E., Bridge, K., Beirowski, B., Berek, L., Wagner, D., Grumme, D., Thomson, D., Celik, A., Addicks, K. (2005). A rat model of slow Wallerian degeneration (WldS) with improved preservation of neuromuscular synapses. European Journal of Neuroscience, 21(1), pp.271-277.

- Ahlqvist, K.J., Suomalainen, A., Hämäläinen, R.H. (2015). Stem cells, mitochondria and aging. *Biochimica et Biophysica Acta (BBA)-Bioenergetics*, 1847(11), pp.1380-1386.

- Akimenko, M.A., Johnson, S.L., Westerfield, M., Ekker, M. (1995). Differential induction of four msx homeobox genes during fin development and regeneration in zebrafish. *Development*, 121(2), pp.347-357.

- Al-Majed, A. A., Siu, L. T., Gordon, T. (2004). Electrical stimulation accelerates and enhances expression of regeneration-associated genes in regenerating rat femoral motoneurons. *Cellular and Molecular Neurobiology*, 24(3), pp. 379–402.

- Anderson, G. L. (1982). Superoxide dismutase activity in dauer larvae of *Caenorhabditis elegans* (Nematoda: Rhabditidae). *Canadian Journal of Zoology*, 60(3), 288-291.

- Árnadóttir, J., O'Hagan, R., Chen, Y., Goodman, M.B., Chalfie, M. (2011). The DEG/ENaC protein MEC-10 regulates the transduction channel complex in *Caenorhabditis elegans* touch receptor neurons. *Journal of Neuroscience*, 31(35), pp.12695-12704.

- Artal-Sanz, M., Tavernarakis, N. (2009). Prohibitin couples diapause signalling to mitochondrial metabolism during ageing in *C. elegans. Nature*, 461(7265), pp.793-797.

- Assinck, P., Sparling, J.S., Dworski, S., Duncan, G.J., Wu, D.L., Liu, J., Kwon, B.K., Biernaskie, J., Miller, F.D., Tetzlaff, W. (2020). Transplantation of skin precursor-derived Schwann cells yields better locomotor outcomes and reduces bladder pathology in rats with chronic spinal cord injury. *Stem Cell Reports*, 15(1), pp.140-155.

- Ball, J.M., Chen, S., Li, W. (2022). Mitochondria in cone photoreceptors act as microlenses to enhance photon delivery and confer directional sensitivity to light. *Science advances*, 8(9), p.eabn2070.

- Banks, W.A., Kastin, A.J., Broadwell, R.D. (1995). Passage of cytokines across the blood-brain barrier. *Neuroimmunomodulation*, 2(4), pp.241-248.

- Berridge, M.J. (1998). Neuronal calcium signaling. *Neuron*, 21(1), pp.13-26.

- Bertolotti, E., Malagoli, D., Franchini, A. (2013). Skin wound healing in different aged *Xenopus laevis. Journal of morphology*, 274(8), pp.956-964.

- Bianchi, L., Gerstbrein, B., Frøkjær-Jensen, C., Royal, D. C., Mukherjee, G., Royal, M. A., Xue, J., Schafer, W. R., Driscoll, M. (2004). The neurotoxic MEC-4 (d) DEG/ENaC sodium channel conducts calcium: implications for necrosis initiation. *Nature neuroscience*, 7(12), 1337.

- Blackshaw, S. (2022). Why has the ability to regenerate following CNS injury been repeatedly lost over the course of evolution?. *Frontiers in Neuroscience*, p.58.

- Boldrini, M., Fulmore, C.A., Tartt, A.N., Simeon, L.R., Pavlova, I., Poposka, V., Rosoklija, G.B., Stankov, A., Arango, V., Dwork, A.J., Hen, R., Mann, J. J. (2018). Human hippocampal neurogenesis persists throughout aging. *Cell stem cell*, 22(4), pp.589-599.
- Bomze, H.M., Bulsara, K.R., Iskandar, B.J., Caroni, P., Pate Skene, J.H. (2001). Spinal axon regeneration evoked by replacing two growth cone proteins in adult neurons. *Nature neuroscience*, 4(1), pp.38-43.
- Bradbury, E.J., Burnside, E.R. (2019). Moving beyond the glial scar for spinal cord repair. *Nature Communications*, 10(1), pp.1-15.
- Britten, R. J. Davidson, E. H. (1969). Gene regulation for higher cells: A theory. *Science*, 165(July), pp. 349–357.
- Brown, A.L., Fernandez-Illescas, S.M., Liao, Z., Goodman, M.B. (2007). Gain-of-function mutations in the MEC-4 DEG/ENaC sensory mechanotransduction channel alter gating and drug blockade. *The Journal of general physiology*, 129(2), pp.161-173.
- Brown, A. L., Liao, Z., Goodman, M. B. (2008). MEC-2 and MEC-6 in the *Caenorhabditis elegans* sensory mechanotransduction complex: auxiliary subunits that enable channel activity. *The Journal of general physiology*, 131(6), pp. 605–16. doi: 10.1085/jgp.200709910.
- Brown, A.L., Fernandez-Illescas, S.M., Liao, Z., Goodman, M.B. (2007). Gain-of-function mutations in the MEC-4 DEG/ENaC sensory mechanotransduction channel alter gating and drug blockade. *The Journal of general physiology*, 129(2), pp.161-173.
- Byrne, J.J., Soh, M.S., Chandhok, G., Vijayaraghavan, T., Teoh, J.S., Crawford, S., Cobham, A.E., Yapa, N.M., Mirth, C.K., Neumann, B. (2019). Disruption of mitochondrial dynamics affects behaviour and lifespan in *Caenorhabditis elegans. Cellular and Molecular Life Sciences*, 76(10), pp.1967-1985.
- Cajal, S. R. (1914). Estudios sobre la degeneración y regeneración del Sistema nervioso. Chapter II: Degeneración y regeneración de los ganglios nerviosos sensitivos (19-31); Chapter VII: *Continuación del estudio de los procesos regenerativos del cerebro* (373-401), Madrid.
- Calaza, K.C., Kam, J.H., Hogg, C., Jeffery, G. (2015). Mitochondrial decline precedes phenotype development in the complement factor H mouse model of retinal degeneration but can be corrected by near infrared light. *Neurobiology of aging*, 36(10), pp.2869-2876.
- Calixto, A., Chelur, D., Topalidou, I., Chen, X., Chalfie, M. (2010). Enhanced neuronal RNAi in *C. elegans* using SID-1. *Nature methods*, 7(7), pp.554-559.
- Calixto, A., Jara, J.S., Court, F.A. (2012). Diapause formation and downregulation of insulin-like signaling via DAF-16/FOXO delays axonal degeneration and neuronal loss. *PLoS Genet*, 8(12), e1003141.
- Callaway, E., (2022). 'The entire protein universe': AI predicts shape of nearly every known protein. *Nature*, DOI: 10.1038/d41586-022-02083-2
- Calvo-Rodriguez, M., Hou, S.S., Snyder, A.C., Kharitonova, E.K., Russ, A.N., Das, S., Fan, Z., Muzikansky, A., Garcia-Alloza, M., Serrano-Pozo, A., Hudry, E. (2020). Increased mitochondrial calcium levels associated with neuronal death in a mouse model of Alzheimer's disease. *Nature communications*, 11(1), pp.1-17

- Calvo-Rodriguez, M., Bacskai, B.J. (2021). Mitochondria and calcium in Alzheimer's disease: From cell signaling to neuronal cell death. *Trends in neurosciences*, 44(2), pp.136-151.
- Cámara-Lemarroy, C.R., Guzmán-de la Garza, F.J., Fernández-Garza, N.E. (2010). Molecular inflammatory mediators in peripheral nerve degeneration and regeneration. *Neuroimmunomodulation*, 17(5), pp.314-324.
- Campagnola, P.J., Millard, A.C., Terasaki, M., Hoppe, P.E., Malone, C.J. and Mohler, W.A., 2002. Three-dimensional high-resolution second-harmonic generation imaging of endogenous structural proteins in biological tissues. *Biophysical journal*, 82(1), pp.493-508.
- Campbell, J. C., Chin-Sang, I. D., Bendena, W. G. (2015). Mechanosensation circuitry in *Caenorhabditis elegans*: A focus on gentle touch. *Peptides*. Elsevier Inc., 68, pp. 164–174. doi: 10.1016/j.peptides.2014.12.004.
- Caneo, M., Julian, V., Byrne, A.B., Alkema, M.J., Calixto, A. (2019). Diapause induces functional axonal regeneration after necrotic insult in *C. elegans*. *PLoS Genetics*, 15(1), p.e1007863.
- Cao, J., Packer, J.S., Ramani, V., Cusanovich, D.A., Huynh, C., Daza, R., Qiu, X., Lee, C., Furlan, S.N., Steemers, F.J., Adey, A. (2017). Comprehensive single-cell transcriptional profiling of a multicellular organism. *Science*, 357(6352), pp.661-667.
- Carroll, S. B. (2008) Evo-Devo and an Expanding Evolutionary Synthesis: A Genetic Theory of Morphological Evolution. *Cell*, 134(1), pp. 25–36. doi: 10.1016/j.cell.2008.06.030.
- Chalfie, M., Sulston, J.E., White, J.G., Southgate, E., Thomson, J.N., Brenner, S. (1985). The neural circuit for touch sensitivity in *Caenorhabditis elegans. Journal of Neuroscience*, 5(4), pp.956-964.
- Chalfie, M. (1990). The differentiation of touch receptor neurons in *Caenorhabditis elegans*: a case study of genetic and molecular analysis. *Amer. Zool.*, 30(3), pp. 531–543.
- Chalfie, M., Sulston, J. (1981). Developmental genetics of the mechanosensory neurons of *Caenorhabditis elegans*. *Developmental Biology*, 82(2), pp. 358–370. doi: 10.1016/0012-1606(81)90459-0.
- Chalfie, M., Wolinsky, E. (1990). The identification and suppression of inherited neurodegeneration in *Caenorhabditis elegans. Nature*, 345(6274), 410.
- Chalfie, M., Driscoll, M. A., Huang, M. X. (1993). Degenerin similarities. *Nature*, 361, 504-1993.
- Chamberlain, K.A., Sheng, Z.H. (2019). Mechanisms for the maintenance and regulation of axonal energy supply. *Journal of neuroscience research*, 97(8), pp.897-913.
- Chang, C.Y., Liang, M.Z. Chen, L. (2019). Current progress of mitochondrial transplantation that promotes neuronal regeneration. *Translational neurodegeneration*, 8(1), pp.1-12.
- Chen, H., McCaffery, J.M., Chan, D.C. (2007). Mitochondrial fusion protects against neurodegeneration in the cerebellum. *Cell*, 130(3), pp.548-562.
- Chen, H., Chan, D.C. (2010). Physiological functions of mitochondrial fusion. *Annals of the New York Academy of Sciences*, 1201(1), pp.21-25.

- Chen, L., Chisholm, A. D. (2011). Axon regeneration mechanisms: insights from *C. elegans. Trends in cell biology*, 21(10), 577-584.
- Chen, L., Wang, Z., Ghosh-Roy, A., Hubert, T., Yan, D., O'Rourke, S., Bowerman, B., Wu, Z., Jin, Y., Chisholm, A.D. (2011). Axon regeneration pathways identified by systematic genetic screening in *C. elegans. Neuron*, 71(6), pp.1043-1057.
- Chen, X., Chalfie, M. (2014). Modulation of *C. elegans* touch sensitivity is integrated at multiple levels. *Journal of Neuroscience*, 34(19), pp.6522-6536.
- Chen, X., Barclay, J.W., Burgoyne, R.D., Morgan, A. (2015a). Using *C. elegans* to discover therapeutic compounds for ageing-associated neurodegenerative diseases. *Chemistry Central Journal*, 9(1), pp.1-20.
- Chen, Y., Bharill, S., Isacoff, E.Y., Chalfie, M. (2015b). Subunit composition of a DEG/ENaC mechanosensory channel of *Caenorhabditis elegans*. *Proceedings of the National Academy of Sciences*, 112(37), pp.11690-11695.
- Chen, Y., Bharill, S., Altun, Z., O'Hagan, R., Coblitz, B., Isacoff, E.Y., Chalfie, M., (2016a). *Caenorhabditis elegans* paraoxonase-like proteins control the functional expression of DEG/ENaC mechanosensory proteins. *Molecular biology of the cell*, 27(8), pp.1272-1285.
- Chen, Y., Bharill, S., O'Hagan, R., Isacoff, E.Y., Chalfie, M. (2016b). MEC-10 and MEC-19 reduce the neurotoxicity of the MEC-4 (d) DEG/ENaC channel in *Caenorhabditis elegans*. *G3: Genes, Genomes, Genetics*, 6(4), pp.1121-1130.
- Chien, L., Liang, M.Z., Chang, C.Y., Wang, C., Chen, L. (2018). Mitochondrial therapy promotes regeneration of injured hippocampal neurons. *Biochimica et Biophysica Acta (BBA)-Molecular Basis of Disease*, 1864(9), pp.3001-3012.
- Chierzi, S., Ratto, G.M., Verma, P., Fawcett, J.W. (2005). The ability of axons to regenerate their growth cones depends on axonal type and age, and is regulated by calcium, cAMP and ERK. *European Journal of Neuroscience*, 21(8), pp.2051-2062.
- Chinopoulos, C., Adam-Vizi, V. (2010). Mitochondria as ATP consumers in cellular pathology. *Biochimica et Biophysica Acta (BBA)-Molecular Basis of Disease*, 1802(1), pp.221-227.
- Cho, J.H., Bandyopadhyay, J., Lee, J., Park, C.S., Ahnn, J. (2000). Two isoforms of sarco/endoplasmic reticulum calcium ATPase (SERCA) are essential in *Caenorhabditis elegans. Gene*, 261(2), pp.211-219.
- Cho, Y., Porto, D.A., Hwang, H., Grundy, L.J., Schafer, W.R., Lu, H. (2017). Automated and controlled mechanical stimulation and functional imaging *in vivo* in *C. elegans. Lab on a Chip*, 17(15), pp.2609-2618.
- Chung, S. H., Sun, L., Gabel, C. V. (2013). *In vivo* neuronal calcium imaging in *C. elegans. Journal of visualized experiments: JoVE*, (74).
- Cohen, N., Sanders, T. (2014). Nematode locomotion: Dissecting the neuronal-environmental loop. *Current Opinion in Neurobiology. Elsevier* Ltd, 25, pp. 99–106. doi: 10.1016/j.conb.2013.12.003.
- Coleman, M.P., Freeman, M.R. (2010). Wallerian degeneration, wlds, and nmnat. *Annual review of neuroscience*, 33, pp.245-267.

- Colucci-D'Amato, L., Bonavita, V., Porzio, U. (2006). The end of the central dogma of neurobiology: Stem cells and neurogenesis in adult CNS. *Neurological Sciences*, 27(4), pp. 266–270. doi: 10.1007/s10072-006-0682-z.
- Conforti, L., Gilley, J., Coleman, M. P. (2014). Wallerian degeneration: An emerging axon death pathway linking injury and disease. *Nature Reviews Neuroscience*, 15(6), pp. 394–409. doi: 10.1038/nrn3680.
- Copeland, D.E., Dalton, A. (1959). An association between mitochondria and the endoplasmic reticulum in cells of the pseudobranch gland of a teleost. *The Journal of Cell Biology*, 5(3), pp.393-396.
- Corbin, K., Pinkard, H., Peck, S., Beemiller, P., Krummel, M. F. (2014). Assessing and benchmarking multiphoton microscopes for biologists. In Methods in cell biology (Vol. 123, pp. 135-151). Academic Press.
- Cregg, J.M., DePaul, M.A., Filous, A.R., Lang, B.T., Tran, A., Silver, J. (2014). Functional regeneration beyond the glial scar. *Experimental neurology*, 253, pp.197-207.
- Csordás, G., Weaver, D., Hajnóczky, G. (2018). Endoplasmic reticulum–mitochondrial contactology: structure and signaling functions. *Trends in cell biology*, 28(7), pp.523-540.
- Daegelen, P., Studier, F.W., Lenski, R.E., Cure, S., Kim, J.F. (2009). Tracing ancestors and relatives of *Escherichia coli* B, and the derivation of B strains REL606 and BL21 (DE3). *Journal of molecular biology*, 394(4), pp.634-643.
- Dalley, B. K., Golomb, M. (1992). Gene expression in the *Caenorhabditis elegans* dauer larva: developmental regulation of Hsp90 and other genes. *Developmental biology*, 151(1), 80-90.
- Darwin, C. (1859) On the origin of species by means of natural selection. Chapter XIV Recapitulation and Conclusion. Accessed 2022-08-01 at darwin-online.org.uk/converted/pdf/1861_OriginNY_F382.pdf
- Dawson, R.J., Benz, J., Stohler, P., Tetaz, T., Joseph, C., Huber, S., Schmid, G., Hügin, D., Pflimlin, P., Trube, G., Rudolph, M.G. (2012). Structure of the acid-sensing ion channel 1 in complex with the gating modifier Psalmotoxin 1. *Nature communications*, 3(1), pp.1-8.
- De Robertis, E. M. (2008) Evo-Devo: Variations on Ancestral Themes. *Cell*, 132(2), pp. 185–195.
- Decuypere, J.P., Monaco, G., Bultynck, G., Missiaen, L., De Smedt, H., Parys, J.B. (2011). The IP3 receptor–mitochondria connection in apoptosis and autophagy. *Biochimica et Biophysica Acta (BBA)-Molecular Cell Research*, 1813(5), pp.1003-1013.
- Díaz-Vegas, A.R., Cordova, A., Valladares, D., Llanos, P., Hidalgo, C., Gherardi, G., De Stefani, D., Mammucari, C., Rizzuto, R., Contreras-Ferrat, A. and Jaimovich, E. (2018). Mitochondrial calcium increase induced by RyR1 and IP3R channel activation after membrane depolarization regulates skeletal muscle metabolism. *Frontiers in physiology*, 9, p.791.
- Driscoll, M., Chalfie, M. (1991). The *mec-4* gene is a member of a family of *Caenorhabditis elegans* genes that can mutate to induce neuronal degeneration. *Nature*, 349(6310), pp.588-593.
- Dobzhansky, T. (1973). Nothing in biology makes sense except in the light of evolution. *The American Biology Teacher* 35 (3): 125–129.

- Edwards-Faret, G., González-Pinto, K., Cebrián-Silla, A., Peñailillo, J., García-Verdugo, J.M., Larraín, J. (2021). Cellular response to spinal cord injury in regenerative and non-regenerative stages in *Xenopus laevis. Neural development*, 16(1), pp.1-25.

- Erkut, C., Penkov, S., Khesbak, H., Vorkel, D., Verbavatz, J.M., Fahmy, K., Kurzchalia, T.V. (2011). Trehalose renders the dauer larva of *Caenorhabditis elegans* resistant to extreme desiccation. *Current Biology*, 21(15), pp.1331-1336.

- Erkut, C., Penkov, S., Fahmy, K., Kurzchalia, T.V. (2012). How worms survive desiccation: Trehalose pro water. In *Worm* (Vol. 1, No. 1, pp. 61-65). *Taylor & Francis*.

- Erkut, C., Vasilj, A., Boland, S., Habermann, B., Shevchenko, A., Kurzchalia, T.V. (2013). Molecular strategies of the *Caenorhabditis elegans* dauer larva to survive extreme desiccation. *PloS one*, 8(12), p.e82473.

- Eswar, N., Webb, B., Marti-Renom, M.A., Madhusudhan, M.S., Eramian, D., Shen, M.Y., Pieper, U., Sali, A. (2006). Comparative protein structure modeling using Modeller. *Current protocols in bioinformatics*, 15(1), pp.5-6.

- Ewald, C.Y., Castillo-Quan, J.I., Blackwell, T.K. (2018). Untangling longevity, dauer, and healthspan in *Caenorhabditis elegans* insulin/IGF-1-signalling. *Gerontology*, 64(1), pp.96-104.

- Fan, C., Fan, M., Orlando, B.J., Fastman, N.M., Zhang, J., Xu, Y., Chambers, M.G., Xu, X., Perry, K., Liao, M., Feng, L. (2018). X-ray and cryo-EM structures of the mitochondrial calcium uniporter. *Nature*, 559(7715), pp.575-579.

- Fariss, M.W., Chan, C.B., Patel, M., Van Houten, B., Orrenius, S. (2005). Role of mitochondria in toxic oxidative stress. *Molecular interventions*, 5(2), p.94.

- Fatouros, C., Pir, G.J., Biernat, J., Koushika, S.P., Mandelkow, E., Mandelkow, E.M., Schmidt, E., Baumeister, R. (2012). Inhibition of tau aggregation in a novel *Caenorhabditis elegans* model of tauopathy mitigates proteotoxicity. *Human molecular genetics*, 21(16), pp.3587-3603.

- Faumont, S., Lindsay, T. H., Lockery, S. R. (2012). Neuronal microcircuits for decision making in *C. elegans. Current Opinion in Neurobiology*, 22(4), pp. 580–591. doi: 10.1016/j.conb.2012.05.005.

- Fawcett, J. W., Asher, R. A. (1999). The glial scar and central nervous system repair. *Brain Research Bulletin*, 49(6), pp. 377–391

- Fitch, M.T., Silver, J. (2008). CNS injury, glial scars, and inflammation: Inhibitory extracellular matrices and regeneration failure. *Experimental neurology*, 209(2), pp.294-301.

- Flor-Garcia, M., Terreros-Roncal, J., Moreno-Jimenez, E.P., Avila, J., Rabano, A., Llorens-Martin, M. (2020). Unraveling human adult hippocampal neurogenesis. *Nature protocols*, 15(2), pp.668-693.

- Fraser, A.G., Kamath, R.S., Zipperlen, P., Martinez-Campos, M., Sohrmann, M., Ahringer, J. (2000). Functional genomic analysis of *C. elegans* chromosome I by systematic RNA interference. *Nature*, 408(6810), pp.325-330.

- Fukazawa, T., Naora, Y., Kunieda, T., Kubo, T. (2009). Suppression of the immune response potentiates tadpole tail regeneration during the refractory period. *Development*, 136 (14): pp.2323–2327.

- García-Casas, P., Arias-del-Val, J., Alvarez-Illera, P., Fonteriz, R.I., Montero, M., Alvarez, J. (2018). Inhibition of Sarco-Endoplasmic Reticulum Ca2+ ATPase extends the lifespan in *C. elegans* worms. *Frontiers in pharmacology*, 9, p.669.
- Gearhart, J., Oster-Granite, M.L., Guth, L. (1979). Histological changes after transection of the spinal cord of fetal and neonatal mice. *Experimental neurology*, 66(1), pp.1-15.
- Gee, K.R., Brown, K.A., Chen, W.U., Bishop-Stewart, J., Gray, D., Johnson, I. (2000). Chemical and physiological characterization of fluo-4 Ca^{2+}-indicator dyes. *Cell calcium*, 27(2), pp.97-106.
- Ghosh-Roy, A., Wu, Z., Goncharov, A., Jin, Y., Chisholm, A.D. (2010). Calcium and cyclic AMP promote axonal regeneration in *Caenorhabditis elegans* and require DLK-1 kinase. *Journal of Neuroscience*, 30(9), pp.3175-3183.
- Gitler, D., Spira, M.E. (1998). Real time imaging of calcium-induced localized proteolytic activity after axotomy and its relation to growth cone formation. *Neuron*, 20(6), pp.1123-1135.
- Glancy, B., Willis, W.T., Chess, D.J. and Balaban, R.S. (2013). Effect of calcium on the oxidative phosphorylation cascade in skeletal muscle mitochondria. *Biochemistry*, 52(16), pp.2793-2809.
- Goodman, M.B. (2006) Mechanosensation. WormBook, ed. The *C. elegans* Research Community, WormBook, doi/10.1895/wormbook.1.62.1, http://www.wormbook.org.
- Goldberg, J. L., Barres, B. A. (2000). Nogo in nerve regeneration. *Nature*, 403(6768), pp. 369–370.
- GrandPré, T., Nakamura, F., Vartanian, T., Strittmatter, S.M. (2000). Identification of the Nogo inhibitor of axon regeneration as a Reticulon protein. *Nature*, 403(6768), pp.439-444.
- Grishok, A., Tabara, H., Mello, C.C. (2000). Genetic requirements for inheritance of RNAi in C. elegans. science, 287(5462), pp.2494-2497.
- Grishok, A. (2005). RNAi mechanisms in *Caenorhabditis elegans. FEBS letters*, 579(26), pp.5932-5939.
- Gritti, A., Bonfanti, L., Doetsch, F., Caille, I., Alvarez-Buylla, A., Lim, D.A., Galli, R., Verdugo, J.M.G., Herrera, D.G., Vescovi, A.L. (2002). Multipotent neural stem cells reside into the rostral extension and olfactory bulb of adult rodents. *Journal of Neuroscience*, 22(2), pp.437-445.
- Grynkiewicz, G., Poenie, M., Tsien, R. Y. (1985). A new generation of Ca^{2+} indicators with greatly improved fluorescence properties', *Journal of Biological Chemistry*, 260(6), pp. 3440–3450. doi: 3838314.
- Guo, S. X., Bourgeois, F., Chokshi, T., Durr, N. J., Hilliard, M. A., Chronis, N., Ben-Yakar, A. (2008). Femtosecond laser nanoaxotomy lab-on-a-chip for *in vivo* nerve regeneration studies. *Nature methods*, 5(6), 531.
- Hammarlund, M., Jorgensen, E. M., Bastiani, M. J. (2007). Axons break in animals lacking β-spectrin. *J Cell Biol*, 176(3), 269-275.
- Han, S.M., Baig, H.S., Hammarlund, M. (2016). Mitochondria localize to injured axons to support regeneration. *Neuron*, 92(6), pp.1308-1323.

- Han, Q., Xie, Y., Ordaz, J.D., Huh, A.J., Huang, N., Wu, W., Liu, N., Chamberlain, K.A., Sheng, Z.H., Xu, X.M. (2020). Restoring cellular energetics promotes axonal regeneration and functional recovery after spinal cord injury. *Cell metabolism*, 31(3), pp.623-641.
- Han, Q., Xu, X.M. (2021). Mitochondrial integrity in neuronal injury and repair. *Neural regeneration research*, 16(4), p.674.
- Hall, B. K. (2003) Evo-Devo: evolutionary developmental mechanisms. *Int J Dev Biol*, 47(7–8), pp. 491–495. doi: 10.1387/ijdb.14756324.
- Harman, A.W., Maxwell, M.J. (1995). An evaluation of the role of calcium in cell injury. *Annual review of pharmacology and toxicology*, 35(1), pp.129-144.
- Hill, J.T., Demarest, B., Gorsi, B., Smith, M., Yost, H.J. (2017). Heart morphogenesis gene regulatory networks revealed by temporal expression analysis. *Development*, 144(19), pp.3487-3498.
- Hilliard, M.A. (2009). Axonal degeneration and regeneration: a mechanistic tug-of-war. *Journal of neurochemistry*, 108(1), pp.23-32.
- Hu, P.J. (2007). Dauer. WormBook, ed. The *C. elegans* Research Community, WormBook, doi/10.1895/wormbook.1.144.1, http://www.wormbook.org.
- Huang, M., Chalfie, M. (1994). Gene interactions affecting mechanosensory transduction in *Caenorhabditis elegans*. *Nature*, 367(6462), 467.
- Huebner, E., Strittmatter, S. M. (2009). Axon Regeneration in the Peripheral and Central Nervous Systems. *Cell biology of the axon*, pp.305-360. *Results and Problems in Cell Differentiation*.
- Hutter, H., Ng, M.P., Chen, N. (2009). GExplore: a web server for integrated queries of protein domains, gene expression and mutant phenotypes. *BMC genomics*, 10(1), pp.1-8.
- Hutter, H., Suh, J. (2016), October. GExplore 1.4: An expanded web interface for queries on *Caenorhabditis elegans* protein and gene function. In *Worm* (Vol. 5, No. 4, p. e1234659). Taylor & Francis.
- Janikiewicz, J., Szymański, J., Malinska, D., Patalas-Krawczyk, P., Michalska, B., Duszyński, J., Giorgi, C., Bonora, M., Dobrzyn, A., Wieckowski, M.R. (2018). Mitochondria-associated membranes in aging and senescence: structure, function, and dynamics. *Cell death & disease*, 9(3), pp.1-12.
- Jankowski, M.P., McIlwrath, S.L., Jing, X., Cornuet, P.K., Salerno, K.M., Koerber, H.R., Albers, K.M. (2009). Sox11 transcription factor modulates peripheral nerve regeneration in adult mice. *Brain research*, 1256, pp.43-54.
- Jasti, J., Furukawa, H., Gonzales, E.B., Gouaux, E. (2007). Structure of acid-sensing ion channel 1 at 1.9 Å resolution and low pH. *Nature*, 449(7160), pp.316-323.
- Jeong, H., Clark, S., Goehring, A., Dehghani-Ghahnaviyeh, S., Rasouli, A., Tajkhorshid, E., Gouaux, E. (2022). Structures of the TMC-1 complex illuminate mechanosensory transduction. *Nature*, pp.1-8.
- Jose, A.M., Hunter, C.P. (2007). Transport of sequence-specific RNA interference information between cells. *Annual review of genetics*, 41, p.305.

- Jumper, J., Evans, R., Pritzel, A., Green, T., Figurnov, M., Ronneberger, O., Tunyasuvunakool, K., Bates, R., Žídek, A., Potapenko, A., Bridgland, A. (2021). Highly accurate protein structure prediction with AlphaFold. *Nature*, 596(7873), pp.583-589.
- Kachaturian, Z.S. (1989) The role of calcium regulation in brain aging: reexamination of a hypothesis. *Aging* 1, 17-34
- Kaletsky, R., Lakhina, V., Arey, R., Williams, A., Landis, J., Ashraf, J., Murphy, C. T. (2016). The *C. elegans* adult neuronal IIS/FOXO transcriptome reveals adult phenotype regulators. *Nature*, 529(7584), 92.
- Kaletta, T., Hengartner, M. O. (2006). Finding function in novel targets: *C. elegans* as a model organism. *Nature Reviews Drug Discovery*, 5(5), pp. 387–399. doi: 10.1038/nrd2031.
- Kamath, R.S., Fraser, A.G., Dong, Y., Poulin, G., Durbin, R., Gotta, M., Kanapin, A., Le Bot, N., Moreno, S., Sohrmann, M., Welchman, D.P., Zipperlen, P., Ahringer, J. (2003). Systematic functional analysis of the *Caenorhabditis elegans* genome using RNAi. *Nature*, 421(6920), pp.231-237.
- Kanazawa, T., Zappaterra, M.D., Hasegawa, A., Wright, A.P., Newman-Smith, E.D., Buttle, K.F., McDonald, K., Mannella, C.A., van der Bliek, A.M. (2008). The *C. elegans* Opa1 homologue EAT-3 is essential for resistance to free radicals. *PLoS genetics*, 4(2), p.e1000022.
- Karp, X., Ambros, V. (2012). Dauer larva quiescence alters the circuitry of microRNA pathways regulating cell fate progression in *C. elegans. Development*, 139(12), pp.2177-2186.
- Kellenberger, S., Schild, L. (2002). Epithelial sodium channel/degenerin family of ion channels: a variety of functions for a shared structure. *Physiological reviews*, 82(3), 735-767.
- Kerr, R.A. (2006). Imaging the activity of neurons and muscles, WormBook, ed. The *C. elegans* Research Community, WormBook, doi/10.1895/wormbook.1.113.1, http://www.wormbook.org.
- Kerr, R. A., Schafer, W. R. (2006). Intracellular Ca^{2+} imaging in *C. elegans*. *In C. elegans Methods and Applications* (pp. 253-264). *Humana Press*.
- Khan, P.A., Crawford, M.J. (2021). Regeneration and development. An amphibian call to arms. *Developmental Dynamics*, 250(6), pp.896-901.
- Khor, B.Y., Tye, G.J., Lim, T.S., Choong, Y.S. (2015). General overview on structure prediction of twilight-zone proteins. *Theoretical Biology and Medical Modelling*, 12(1), pp.1-11.
- Kiefer, J. C. (2010) Primer and interviews: molecular mechanisms of morphological evolution. *Developmental dynamics*, 239(12), pp. 3497–3505.
- Kiryu-Seo, S., Kiyama, H. (2019). Mitochondrial behavior during axon regeneration/degeneration in vivo. *Neuroscience research*, 139, pp.42-47.
- Knott, A.B., Perkins, G., Schwarzenbacher, R., Bossy-Wetzel, E. (2008). Mitochondrial fragmentation in neurodegeneration. *Nature Reviews Neuroscience*, 9(7), pp.505-518.
- König, K. (2000). Multiphoton microscopy in life sciences. *Journal of microscopy*, 200(2), 83-104.

- Kottis, V., Thibault, P., Mikol, D., Xiao, Z.C., Zhang, R., Dergham, P., Braun, P.E. (2002). Oligodendrocyte-myelin glycoprotein (OMgp) is an inhibitor of neurite outgrowth. *Journal of neurochemistry*, 82(6), pp.1566-1569.
- Kragl, M., Knapp, D., Nacu, E., Khattak, S., Maden, M., Epperlein, H.H., Tanaka, E.M. (2009). Cells keep a memory of their tissue origin during axolotl limb regeneration. *Nature*, 460(7251), pp.60-65.
- Krieg, M., Dunn, A. R., Goodman, M. B. (2014). Mechanical control of the sense of touch by β-spectrin. *Nature cell biology*, 16(3), 224.
- Kunkel-Bagden, E., Dai, H.N., Bregman, B.S. (1992). Recovery of function after spinal cord hemisection in newborn and adult rats: differential effects on reflex and locomotor function. *Experimental neurology*, 116(1), pp.40-51.
- Kuruma, A., Hartzell, H.C. (1999). Dynamics of calcium regulation of chloride currents in *Xenopus oocytes*. *American Journal of Physiology-Cell Physiology*, 276(1), pp.C161-C175.
- Kury, P., Stoll, G., Muller, H. W. (2001). Molecular mechanisms of cellular interactions in peripheral nerve regeneration. *Curr Opin Neurol*, 14(5), pp. 635–639.
- Labbadia, J., Brielmann, R.M., Neto, M.F., Lin, Y.F., Haynes, C.M., Morimoto, R.I. (2017). Mitochondrial stress restores the heat shock response and prevents proteostasis collapse during aging. *Cell reports*, 21(6), pp.1481-1494.
- Levin, M. (2014) Endogenous bioelectrical networks store non-genetic patterning information during development and regeneration. *Journal of Physiology*, 592(11), pp. 2295–2305.
- Li, W., Kang, L., Piggott, B.J., Feng, Z., Xu, X.Z. (2011a). The neural circuits and sensory channels mediating harsh touch sensation in *Caenorhabditis elegans. Nature communications*, 2(1), pp.1-9.
- Li, X.D., Chiu, Y.H., Ismail, A.S., Behrendt, C.L., Wight-Carter, M., Hooper, L.V., Chen, Z.J. (2011b). Mitochondrial antiviral signaling protein (MAVS) monitors commensal bacteria and induces an immune response that prevents experimental colitis. *Proceedings of the National Academy of Sciences*, 108(42), pp.17390-17395.
- Li, C., Hisamoto, N., Matsumoto, K. (2015). Axon Regeneration Is Regulated by Ets–C/EBP Transcription Complexes Generated by Activation of the cAMP/Ca2+ Signaling Pathways. *PLoS genetics*, 11(10), p.e1005603.
- Lie, D.C., Song, H., Colamarino, S.A., Ming, G.L., Gage, F.H. (2004). Neurogenesis in the Adult Brain: New Strategies for Central Nervous System Diseases. *Annu. Rev. Pharmacol. Toxicol*, 44, pp.399-421.
- Lim, S.F., Riehn, R., Ryu, W.S., Khanarian, N., Tung, C.K., Tank, D., Austin, R.H. (2006). *In vivo* and scanning electron microscopy imaging of upconverting nanophosphors in *Caenorhabditis elegans. Nano letters*, 6(2), pp.169-174.
- Liu, Y., Jin, M., Wang, Y., Zhu, J., Tan, R., Zhao, J., Ji, X., Jin, C., Jia, Y., Ren, T., Xing, J. (2020). MCU-induced mitochondrial calcium uptake promotes mitochondrial biogenesis and colorectal cancer growth. *Signal transduction and targeted therapy*, 5(1), pp.1-13.

- Lourenço, A.B., Muñoz-Jiménez, C., Venegas-Calerón, M., Artal-Sanz, M. (2015). Analysis of the effect of the mitochondrial prohibitin complex, a context-dependent modulator of longevity, on the *C. elegans* metabolome. *Biochimica et Biophysica Acta (BBA)-Bioenergetics*, 1847(11), pp.1457-1468.
- Lourenço, A.B., Artal-Sanz, M. (2021). The Mitochondrial Prohibitin (PHB) Complex in *C. elegans* Metabolism and Ageing Regulation. *Metabolites*, 11(9), p.636.
- Lu, Y., Rolland, S.G., Conradt, B. (2011). A molecular switch that governs mitochondrial fusion and fission mediated by the BCL2-like protein CED-9 of *Caenorhabditis elegans. Proceedings of the National Academy of Sciences*, 108(41), pp.E813-E822
- Lu, Y., Shan, Q., Ling, M., Ni, X.A., Mao, S.S., Yu, B. Cao, Q.Q. (2022). Identification of key genes involved in axon regeneration and Wallerian degeneration by weighted gene co-expression network analysis. *Neural regeneration research*, 17(4), p.911.
- Lunney, G.H., 1970. Using analysis of variance with a dichotomous dependent variable: an empirical study. *Journal of educational measurement*, 7(4), pp.263-269.
- Luongo, T.S., Lambert, J.P., Gross, P., Nwokedi, M., Lombardi, A.A., Shanmughapriya, S., Carpenter, A.C., Kolmetzky, D., Gao, E., Van Berlo, J.H., Tsai, E.J. (2017). The mitochondrial Na+/Ca2+ exchanger is essential for Ca2+ homeostasis and viability. *Nature*, 545(7652), pp.93-97.
- Lust, K., Wittbrodt, J. (2018). Activating the regenerative potential of Müller glia cells in a regeneration-deficient retina. *Elife* 7:e32319.
- Maguire, S. M., Clark, C. M., Nunnari, J., Pirri, J. K., Alkema, M. J. (2011). The *C. elegans* touch response facilitates escape from predacious fungi. *Current Biology* 21(15), 1326-1330.
- Mapunda, J.A., Tibar, H., Regragui, W., Engelhardt, B. (2022). How Does the Immune System Enter the Brain?. *Frontiers in immunology*, 13.
- Marambaud, P., Dreses-Werringloer, U., Vingtdeux, V. (2009). Calcium signaling in neurodegeneration. *Molecular neurodegeneration*, 4(1), pp.1-15.
- Marchant, J.S. (2018). Heterologous protein expression in the Xenopus oocyte. *Cold Spring Harbor Protocols*, 2018(4), pp.pdb-prot096990.
- Marongiu, F., Marongiu, M., Contini, A., Serra, M., Cadoni, E., Murgia, R., Laconi, E. (2017). Hyperplasia vs hypertrophy in tissue regeneration after extensive liver resection. *World Journal of Gastroenterology*, 23(10), p.1764.
- Martini, R., Fischer, S., López-Vales, R., David, S. (2008). Interactions between Schwann cells and macrophages in injury and inherited demyelinating disease. *Glia*, 56(14), pp.1566-1577.
- McPhail, L.T., Fernandes, K.J., Chan, C.C., Vanderluit, J.L., Tetzlaff, W. (2004). Axonal reinjury reveals the survival and re-expression of regeneration-associated genes in chronically axotomized adult mouse motoneurons. *Experimental neurology*, 188(2), pp.331-340.
- Michalopoulos GK, DeFrances MC. (1997). Liver regeneration. *Science*; 276: 60– 66.
- Michalopoulos, G. K. (2007). Liver regeneration. *Journal of Cellular Physiology*, 213(2), pp. 286–300. doi: 10.1002/jcp.21172.

- Miller, D. J., Ball, E. E. (2009) The gene complement of the ancestral bilaterian - Was Urbilateria a monster?. *Journal of Biology*, 8(10), pp. 10–13.
- Miyawaki, A., Griesbeck, O., Heim, R., Tsien, R.Y. (1999). Dynamic and quantitative Ca^{2+} measurements using improved cameleons. *Proceedings of the National Academy of Sciences*, 96(5), pp.2135-2140.
- Mladinic, M., Wintzer, M. (2002). Changes in mRNA content of developing opossum spinal cord at stages when regeneration can and cannot occur after injury. *Brain research reviews*, 40(1-3), pp.317-324.
- Moeendarbary, E., Weber, I.P., Sheridan, G.K., Koser, D.E., Soleman, S., Haenzi, B., Bradbury, E.J., Fawcett, J., Franze, K. (2017). The soft mechanical signature of glial scars in the central nervous system. *Nature communications*, 8(1), pp.1-11.
- Mondal, P. P. (2014). Temporal resolution in fluorescence imaging. *Frontiers in molecular biosciences*, 1, 11.
- Moreau-Fauvarque, C., Kumanogoh, A., Camand, E., Jaillard, C., Barbin, G., Boquet, I., Love, C., Jones, E.Y., Kikutani, H., Lubetzki, C., Dusart, I. (2003). The transmembrane semaphorin Sema4D/CD100, an inhibitor of axonal growth, is expressed on oligodendrocytes and upregulated after CNS lesion. *Journal of Neuroscience*, 23(27), pp.9229-9239.
- Moreno-Jiménez, E.P., Flor-García, M., Terreros-Roncal, J., Rábano, A., Cafini, F., Pallas-Bazarra, N., Ávila, J., Llorens-Martín, M. (2019). Adult hippocampal neurogenesis is abundant in neurologically healthy subjects and drops sharply in patients with Alzheimer's disease. *Nature medicine*, 25(4), pp.554-560.
- Morrison, J.I., Lööf, S., He, P., Simon, A. (2006). Salamander limb regeneration involves the activation of a multipotent skeletal muscle satellite cell population. *The Journal of cell biology*, 172(3), pp.433-440.
- Muddapu, V.R., Dharshini, S.A.P., Chakravarthy, V.S., Gromiha, M.M. (2020). Neurodegenerative diseases–is metabolic deficiency the root cause?. *Frontiers in neuroscience*, 14, p.213.
- Muszyński, P., Kulczyńska-Przybik, A., Borawska, R., Litman-Zawadzka, A., Słowik, A., Klimkowicz-Mrowiec, A., Pera, J., Dziedzic, T., Mroczko, B. (2017). The relationship between markers of inflammation and degeneration in the central nervous system and the blood-brain barrier impairment in Alzheimer's disease. *Journal of Alzheimer's Disease*, 59(3), pp.903-912.
- Nadeau, S., Hein, P., Fernandes, K.J., Peterson, A.C., Miller, F.D. (2005). A transcriptional role for C/EBP β in the neuronal response to axonal injury. *Molecular and cellular neuroscience*, 29(4), pp.525-535.
- Nakai, J., Ohkura, M., Imoto, K. (2001). A high signal-to-noise ca^{2+} probe composed of a single green fluorescent protein. *Nature Biotechnology*, 19(2), pp. 137–141. doi: 10.1038/84397.
- Nakata, K., Abrams, B., Grill, B., Goncharov, A., Huang, X., Chisholm, A.D., Jin, Y. (2005). Regulation of a DLK-1 and p38 MAP kinase pathway by the ubiquitin ligase RPM-1 is required for presynaptic development. *Cell*, 120(3), pp.407-420.

- Namsolleck, P., Culman, J., Thomas Unger, T. (2015). The protective arm of the renin-angiotensin system (RAS): functional aspects and therapeutic implications, *Chapter 8 – AT2R in Nervous System. Academic Press*.
- Navarro-González, C., Moukadiri, I., Villarroya, M., López-Pascual, E., Tuck, S. Armengod, M.E. (2017). Mutations in the *Caenorhabditis elegans* orthologs of human genes required for mitochondrial tRNA modification cause similar electron transport chain defects but different nuclear responses. *PLoS genetics*, 13(7), p.e1006921.
- Neumann, B., Nguyen, K. C., Hall, D. H., Ben-Yakar, A., Hilliard, M. A. (2011). Axonal regeneration proceeds through specific axonal fusion in transected *C. elegans* neurons. *Developmental Dynamics*, 240(6), 1365-1372.
- Neumann, B., Coakley, S., Giordano-Santini, R., Linton, C., Lee, E. S., Nakagawa, A., Xue, D., Hilliard, M. A. (2015). EFF-1-mediated regenerative axonal fusion requires components of the apoptotic pathway. *Nature*, 517(7533), 219.
- Neve, I.A., Sowa, J.N., Lin, C.C.J., Sivaramakrishnan, P., Herman, C., Ye, Y., Han, L., Wang, M.C. (2020). *Escherichia coli* metabolite profiling leads to the development of an RNA interference strain for *Caenorhabditis elegans. G3: Genes, Genomes, Genetics*, 10(1), pp.189-198.
- Nogami, K.I., Maruyama, Y., Sakai-Takemura, F., Motohashi, N., Elhussieny, A., Imamura, M., Miyashita, S., Ogawa, M., Noguchi, S., Tamura, Y., Kira, J., Aoki, Y., Takeda, S., Miyagoe-Suzuki, Y. (2021). Pharmacological activation of SERCA ameliorates dystrophic phenotypes in dystrophin-deficient mdx mice. *Human molecular genetics*, 30(11), pp.1006-1019.
- O'Hagan, R., Chalfie, M., Goodman, M. B. (2005). The MEC-4 DEG/ENaC channel of *Caenorhabditis elegans* touch receptor neurons transduces mechanical signals. *Nature Neuroscience*, 8(1), pp. 43–50. doi: 10.1038/nn1362.
- O'Riordan, V. B., Burnell, A. M. (1989). Intermediary metabolism in the dauer larva of the *nematode Caenorhabditis elegans*—1. Glycolysis, gluconeogenesis, oxidative phosphorylation and the tricarboxylic acid cycle. *Comparative Biochemistry and Physiology*, 92(2), 233-238.
- O'Riordan, V. B., Burnell, A. M. (1990). Intermediary metabolism in the dauer larva of the nematode *Caenorhabditis elegans* II. The glyoxylate cycle and fatty-acid oxidation. *Comparative Biochemistry and Physiology*, 95(1), 125-130.
- Oxenoid, K., Dong, Y., Cao, C., Cui, T., Sancak, Y., Markhard, A.L., Grabarek, Z., Kong, L., Liu, Z., Ouyang, B., Cong, Y. (2016). Architecture of the mitochondrial calcium uniporter. *Nature*, 533(7602), pp.269-273.
- Pacelli, C., Giguère, N., Bourque, M.J., Lévesque, M., Slack, R.S., Trudeau, L.É. (2015). Elevated mitochondrial bioenergetics and axonal arborization size are key contributors to the vulnerability of dopamine neurons. *Current Biology*, 25(18), pp.2349-2360.
- Palominos, M.F., Calfún, C., Nardocci, G., Candia, D., Torres-Paz, J., Whitlock, K.E. (2022). The Olfactory Organ Is a Unique Site for Neutrophils in the Brain. *Frontiers in Immunology*, p.2110.
- Park, S., Hwang, H., Nam, S.W., Martinez, F., Austin, R.H., Ryu, W.S. (2008). Enhanced *Caenorhabditis elegans* locomotion in a structured microfluidic environment. *PloS one*, 3(6), p.e2550.

- Pathak, D., Berthet, A., Nakamura, K. (2013). Energy failure: does it contribute to neurodegeneration?. *Annals of neurology*, 74(4), pp.506-516.
- Pearl, J. (2009). Causal inference in statistics: An overview. *Statistics surveys*, 3, 96-146.
- Pekny, M., Nilsson, M. (2005). Astrocyte activation and reactive gliosis. *Glia*, 50(4), pp.427-434.
- Periasamy, M., Kalyanasundaram, A. (2007). SERCA pump isoforms: their role in calcium transport and disease. *Muscle & Nerve: Official Journal of the American Association of Electrodiagnostic Medicine*, 35(4), pp.430-442.
- Petzold, B.C., Park, S.J., Mazzochette, E.A., Goodman, M.B., Pruitt, B.L. (2013). MEMS-based force-clamp analysis of the role of body stiffness in *C. elegans* touch sensation. *Integrative Biology*, 5(6), pp.853-864.
- Picard, M., Shirihai, O.S. (2022). Mitochondrial signal transduction. *Cell Metabolism*, 34(11), pp.1620-1653.
- Piggott, B.J., Liu, J., Feng, Z., Wescott, S.A., Xu, X.S. (2011). The neural circuits and synaptic mechanisms underlying motor initiation in *C. elegans. Cell*, 147(4), pp.922-933.
- Pirri, J. K., Alkema, M. J. (2012). The neuroethology of C. elegans escape. *Current Opinion in Neurobiology*. pp. 187–193. doi: 10.1016/j.conb.2011.12.007.
- Plancke, C., Vigeolas, H., Höhner, R., Roberty, S., Emonds-Alt, B., Larosa, V., Willamme, R., Duby, F., Onga Dhali, D., Thonart, P., Hiligsmann, S. (2014). Lack of isocitrate lyase in Chlamydomonas leads to changes in carbon metabolism and in the response to oxidative stress under mixotrophic growth. *The Plant Journal*, 77(3), pp.404-417.
- Pottorf, W.J., De Leon, D.D., Hessinger, D.A., Buchholz, J.N. (2001). Function of SERCA mediated calcium uptake and expression of SERCA3 in cerebral cortex from young and old rats. *Brain research*, 914(1-2), pp.57-65.
- Qu, W., Ren, C., Li, Y., Shi, J., Zhang, J., Wang, X., Hang, X., Lu, Y., Zhao, D., Zhang, C. (2011). Reliability analysis of the Ahringer *Caenorhabditis elegans* RNAi feeding library: a guide for genome-wide screens. *BMC genomics*, 12(1), pp.1-8.
- Rabinowitch, I., Treinin, M., Bai, J. (2016). Artificial Optogenetic TRN Stimulation of *C. elegans. Bio-protocol*, 6(20).
- Raivich, G., Bohatschek, M., Da Costa, C., Iwata, O., Galiano, M., Hristova, M., Nateri, A.S., Makwana, M., Riera-Sans, L., Wolfer, D.P., Lipp, H.P. (2004). The AP-1 transcription factor c-Jun is required for efficient axonal regeneration. *Neuron*, 43(1), pp.57-67.
- Ramachandran, R., Fausett, B. V., Goldman, D. (2010). Ascl1a regulates Müller glia dedifferentiation and retinal regeneration through a Lin-28-dependent, *let-7* microRNA signaling pathway. *Nature Cell Biology*, 12(11), pp. 1101–1107. doi: 10.1038/ncb2115.
- Reuben, A. (2004). Prometheus and Pandora—together again. *Hepatology*, 39(5), pp.1460-1463.
- Rock, K. L. Kono, H. (2008). The Inflammatory Response to Cell Death. *Annual Review of Pathology-mechanisms of Disease*, 3, pp. 67–97. doi: 10.1146/annurev.path.

- Rodriguez-Arribas, M., Yakhine-Diop, S.M.S., Pedro, J.M., Gomez-Suaga, P., Gomez-Sanchez, R., Martinez-Chacon, G., Fuentes, J.M., Gonzalez-Polo, R.A., Niso-Santano, M. (2017). Mitochondria-associated membranes (MAMs): overview and its role in Parkinson's disease. *Molecular neurobiology*, 54(8), pp.6287-6303.
- Royal, D.C., Bianchi, L., Royal, M.A., Lizzio, M., Mukherjee, G., Nunez, Y.O., Driscoll, M. (2005). Temperature-sensitive mutant of the *Caenorhabditis elegans* neurotoxic MEC-4 (d) DEG/ENaC channel identifies a site required for trafficking or surface maintenance. *Journal of Biological Chemistry*, 280(51), pp.41976-41986.
- Schafer, W.R. (2015). Mechanosensory molecules and circuits in *C. elegans. Pflügers Archiv-European Journal of Physiology*, 467(1), pp.39-48.
- Saftig, P. (2015). Proteases at work: cues for understanding neural development and degeneration. *Frontiers in Molecular Neuroscience*, pp. 1–7. doi: 10.3389/fnmol.2015.00013.
- Sakamoto, K., Soh, Z., Suzuki, M., Iino, Y., Tsuji, T. (2021). Forward and backward locomotion patterns in *C. elegans* generated by a connectome-based model simulation. *Scientific Reports*, 11(1), pp.1-13.
- Sarasija, S., Laboy, J.T., Ashkavand, Z., Bonner, J., Tang, Y., Norman, K.R. (2018). Presenilin mutations deregulate mitochondrial Ca2+ homeostasis and metabolic activity causing neurodegeneration in *Caenorhabditis elegans. Elife*, 7, p.e33052.
- Schmitt, A.B., Breuer, S., Liman, J., Buss, A., Schlangen, C., Pech, K., Hol, E.M., Brook, G.A., Noth, J., Schwaiger, F.W. (2003). Identification of regeneration-associated genes after central and peripheral nerve injury in the adult rat. *BMC neuroscience*, 4(1), pp.1-13.
- Schneidman-Duhovny, D., Inbar, Y., Nussinov, R., Wolfson, H.J. (2005). PatchDock and SymmDock: servers for rigid and symmetric docking. *Nucleic acids research*, 33, pp.W363-W367.
- Sheng, Z.H. (2017). The interplay of axonal energy homeostasis and mitochondrial trafficking and anchoring. *Trends in cell biology*, 27(6), pp.403-416.
- Shi, S., Mutchler, S.M., Blobner, B.M., Kashlan, O.B., Kleyman, T.R. (2018). Pore-lining residues of MEC-4 and MEC-10 channel subunits tune the *Caenorhabditis elegans* degenerin channel's response to shear stress. *Journal of Biological Chemistry*, 293(27), pp.10757-10766.
- Shimizu, Y., Kawasaki, T. (2021). Differential regenerative capacity of the optic tectum of adult medaka and zebrafish. *Frontiers in cell and developmental biology*, 9, p.686755.
- Shipley, F.B., Clark, C.M., Alkema, M.J., Leifer, A.M. (2014). Simultaneous optogenetic manipulation and calcium imaging in freely moving *C. elegans. Frontiers in neural circuits*, 8, p.28.
- Siekevitz, P. (1957). Powerhouse of the cell. *Scientific American*, 197(1), pp.131-144.
- Silver, J., Miller, J. H. (2004). Regeneration beyond the glial scar. *Nature Reviews Neuroscience*, 5(2), pp. 146–156. doi: 10.1038/nrn1326.
- Sims, N.R., Muyderman, H. (2010). Mitochondria, oxidative metabolism and cell death in stroke. *Biochimica et Biophysica Acta (BBA)-Molecular Basis of Disease*, 1802(1), pp.80-91.

- Singh, R., Bartok, A., Paillard, M., Tyburski, A., Elliott, M., Hajnóczky, G. (2022). Uncontrolled mitochondrial calcium uptake underlies the pathogenesis of neurodegeneration in MICU1-deficient mice and patients. *Science advances*, 8(11), p.eabj4716.
- Syntichaki, P., Xu, K., Driscoll, M., Tavernarakis, N. (2002). Specific aspartyl and calpain proteases are required for neurodegeneration in *C. elegans. Nature*, 419(6910), pp.939-944.
- Skuhersky, M., Wu, T., Yemini, E., Nejatbakhsh, A., Boyden, E., Tegmark, M., 2022. Toward a more accurate 3D atlas of *C. elegans* neurons. *BMC bioinformatics*, 23(1), pp.1-18.
- Skulachev, V.P. (2001). Mitochondrial filaments and clusters as intracellular power-transmitting cables. *Trends in biochemical sciences*, 26(1), pp.23-29.
- Snyder, P.M., Bucher, D.B., Olson, D.R. (2000). Gating induces a conformational change in the outer vestibule of ENaC. *The Journal of general physiology*, 116(6), pp.781-790.
- Sorrells, S.F., Paredes, M.F., Cebrian-Silla, A., Sandoval, K., Qi, D., Kelley, K.W., James, D., Mayer, S., Chang, J., Auguste, K.I., Chang, E.F., Alvarez-Buylla, A. (2018). Human hippocampal neurogenesis drops sharply in children to undetectable levels in adults. *Nature*, 555(7696), pp.377-381.
- Stiernagle, T. (2006) Maintenance of *C. elegans*. WormBook, ed. The *C. elegans* Research Community, WormBook, doi/10.1895/wormbook.1.101.1, http://www.wormbook.org.
- Stoll, G., Jander, S., Myers, R. R. (2002). Degeneration and regeneration of the peripheral nervous system: From Augustus Waller's observations to neuroinflammation. *Journal of the Peripheral Nervous System*, 7(1), pp. 13–27. doi: 10.1046/j.1529-8027.2002.02002.x.
- Sulston, J.E., Horvitz, H.R. (1977). Post-embryonic cell lineages of the nematode, *Caenorhabditis elegans. Developmental biology*, 56(1), pp.110-156.
- Sulston, J.E., Schierenberg, E., White, J.G., Thomson, J.N. (1983). The embryonic cell lineage of the nematode *Caenorhabditis elegans. Developmental biology*, 100(1), pp.64-119.
- Sun, L., Shay, J., McLoed, M., Roodhouse, K., Chung, S.H., Clark, C.M., Pirri, J.K., Alkema, M.J., Gabel, C.V. (2014). Neuronal regeneration in *C. elegans* requires subcellular calcium release by ryanodine receptor channels and can be enhanced by optogenetic stimulation. *Journal of Neuroscience*, 34(48), pp.15947-15956.
- Svoboda, K., Yasuda, R. (2006). Principles of two-photon excitation microscopy and its applications to neuroscience. *Neuron*, 50(6), 823-839.
- Tanaka, E. M., Ferretti, P. (2009). Considering the evolution of regeneration in the central nervous system. *Nature Reviews Neuroscience*, 10(10), pp. 713–723. doi: 10.1038/nrn2707.
- Terreros-Roncal, J., Moreno-Jiménez, E.P., Flor-García, M., Rodríguez-Moreno, C.B., Trinchero, M.F., Cafini, F., Rábano, A., Llorens-Martín, M. (2021). Impact of neurodegenerative diseases on human adult hippocampal neurogenesis. *Science*, 374(6571), pp.1106-1113.
- Temple, S., Alvarez-Buylla, A (1999). Stem cells in the adult mammalian central nervous system. *Current opinion in neurobiology*, 9, pp. 135–141. doi: S0959-4388(99)80017-8 [pii].

- Theodoulou, F.L., Miller, A.J. (1995). Xenopus oocytes as a heterologous expression system. *Plant Gene Transfer and Expression Protocols*, pp.317-340.
- Timmons, L., Fire, A. (1998). Specific interference by ingested dsRNA. *Nature*, 395(6705), pp.854-854.
- Timmons, L., Court, D.L., Fire, A. (2001). Ingestion of bacterially expressed dsRNAs can produce specific and potent genetic interference in *Caenorhabditis elegans. Gene*, 263(1-2), pp.103-112.
- Tran, A.P., Warren, P.M., Silver, J. (2021). New insights into glial scar formation after spinal cord injury. *Cell and Tissue Research*, pp.1-18.
- Trizzino, M., Park, Y., Holsbach-Beltrame, M., Aracena, K., Mika, K., Caliskan, M., Perry, G.H., Lynch, V.J., Brown, C.D. (2017). Transposable elements are the primary source of novelty in primate gene regulation. *Genome research*, 27(10), pp.1623-1633.
- Trusolino, L., Bertotti, A., Comoglio, P. M. (2010) MET signalling: Principles and functions in development, organ regeneration and cancer. *Nature Reviews Molecular Cell Biology*, 11(12), pp. 834–848.
- Ureta, T. (2011) "La creciente molecularización de las explicaciones evolutivas. Lo que Darwin no podía saber", Chapter 5th of Veloso A., and Spotorno, A.E, "Darwin y la evolución. Avances en la Universidad de Chile" *Editorial Universitaria*, 165-188
- van der Vlist, M., Raoof, R., Willemen, H.L., Prado, J., Versteeg, S., Gil, C.M., Vos, M., Lokhorst, R.E., Pasterkamp, R.J., Kojima, T. and Karasuyama, H. (2022). Macrophages transfer mitochondria to sensory neurons to resolve inflammatory pain. *Neuron*, 110(4), pp.613-626.
- Vance J.E. (2014) MAM (mitochondria-associated membranes) in mammalian cells: lipids and beyond. *Biochim. Biophys. Acta* 1841, 595-609.
- Varadarajan, S.G., Hunyara, J.L., Hamilton, N.R., Kolodkin, A.L., Huberman, A.D. (2022). Central nervous system regeneration. *Cell*, 185(1), pp.77-94.
- Waharte, F., Spriet, C., Héliot, L. (2006). Setup and characterization of a multiphoton FLIM instrument for protein-protein interaction measurements in living cells. *Cytometry Part A*, 69(4), 299-306.
- Waller, A. (1850). XX. Experiments on the section of the glossopharyngeal and hypoglossal nerves of the frog, and observations of the alterations produced thereby in the structure of their primitive fibres. *Philosophical transactions of the Royal society of London*, (140), pp.423-429.
- Waller A. D. (1891) An Introduction to physiology, Chapter X Peripheral Nervous System. Nerve Lon: Longmans, *Green and Co.*, 344-378
- Waller, A. D. (1895). Two fundamental "laws" of nerve action in relation to the modern nerve cell. *Science Progress* (1894-1898), 3(15), 186-192.
- Wang, J. T., Medress, Z. A., Barres, B. A. (2012). Axon degeneration: Molecular mechanisms of a self-destruction pathway. *Journal of Cell Biology*, 196(1), pp. 7–18. doi: 10.1083/jcb.201108111.
- Wang, Q., Cai, H., Hu, Z., Wu, Y., Guo, X., Li, J., Wang, H., Liu, Y., Liu, Y., Xie, L., Xu, K. (2019). Loureirin B promotes axon regeneration by inhibiting endoplasmic reticulum stress: induced mitochondrial

dysfunction and regulating the Akt/GSK-3β pathway after spinal cord injury. *Journal of Neurotrauma*, 36(12), pp.1949-1964.

- Wang, B., Huang, M., Shang, D., Yan, X., Zhao, B., Zhang, X. (2021). Mitochondrial behavior in axon degeneration and regeneration. *Frontiers in Aging Neuroscience*, 13, p.650038.
- Webb, B., Sali, A. (2016). Comparative protein structure modeling using MODELLER. *Current protocols in bioinformatics*, 54(1), pp.5-6.
- White, J.G., Southgate, E., Thomson, J.N., Brenner, S. (1986). The structure of the nervous system of the nematode *Caenorhabditis elegans. Philos Trans R Soc Lond B Biol Sci*, 314(1165), pp.1-340.
- WormBase ID WBbt:0003832: AVM, accessed on July 8thof 2022 from https://wormbase.org/species/all/anatomy_term/WBbt:0003832
- Wray, S. (2010). Calcium Signaling in Smooth Muscle. *Handbook of Cell Signaling*, 1009–1025.
- Wright, D.C. (2007). Mechanisms of calcium-induced mitochondrial biogenesis and GLUT4 synthesis. *Applied Physiology, Nutrition, and Metabolism*, 32(5), pp.840-845.
- Wu, H., Wade, M., Krall, L., Grisham, J., Xiong, Y., Van Dyke, T. (1996). Targeted in vivo expression of the cyclin-dependent kinase inhibitor p21 halts hepatocyte cell-cycle progression, postnatal liver development and regeneration. *Genes & development*, 10(3), pp.245-260.
- Wu, H., Kanatous, S.B., Thurmond, F.A., Gallardo, T., Isotani, E., Bassel-Duby, R., Williams, R.S. (2002). Regulation of mitochondrial biogenesis in skeletal muscle by CaMK. *Science*, 296(5566), pp.349-352.
- Xu, H., Van Remmen, H. (2021). The SarcoEndoplasmic Reticulum Calcium ATPase (SERCA) pump: a potential target for intervention in aging and skeletal muscle pathologies. *Skeletal Muscle*, 11(1), pp.1-9.
- Xu, K., Tavernarakis, N., Driscoll, M. (2001). Necrotic cell death in *C. elegans* requires the function of calreticulin and regulators of Ca^{2+} release from the endoplasmic reticulum. *Neuron*, 31(6), pp.957-971.
- Xu, S., Chisholm, A.D. (2014). *C. elegans* epidermal wounding induces a mitochondrial ROS burst that promotes wound repair. *Developmental cell*, 31(1), pp.48-60.
- Xu, Y., Ren, X.C., Quinn, C.C., Wadsworth, W.G. (2011). Axon response to guidance cues is stimulated by acetylcholine in *Caenorhabditis elegans. Genetics*, 189(3), pp.899-906.
- Yan, D., Wu, Z., Chisholm, A.D., Jin, Y. (2009). The DLK-1 kinase promotes mRNA stability and local translation in *C. elegans* synapses and axon regeneration. *Cell*, 138(5), pp.1005-1018.
- Yang, M., Li, C., Yang, S., Xiao, Y., Xiong, X., Chen, W., Zhao, H., Zhang, Q., Han, Y., Sun, L. (2020). Mitochondria-associated ER membranes–the origin site of autophagy. *Frontiers in Cell and Developmental Biology*, 8, p.595.
- Yang, T., Dai, Y., Chen, G., Cui, S. (2020). Dissecting the dual role of the glial scar and scar-forming astrocytes in spinal cord injury. *Frontiers in cellular neuroscience*, 14, p.78.

- Yang, Y., Liu, N., He, Y., Liu, Y., Ge, L., Zou, L., Song, S., Xiong, W., Liu, X. (2018). Improved calcium sensor GCaMP-X overcomes the calcium channel perturbations induced by the calmodulin in GCaMP. *Nature communications*, 9(1), pp.1-18.
- Yanik, M. F., Cinar, H., Cinar, H. N., Chisholm, A. D., Jin, Y., Ben-Yakar, A. (2004). Neurosurgery: functional regeneration after laser axotomy. *Nature*, 432(7019), 822.
- Yoo, J., Wu, M., Yin, Y., Herzik Jr, M.A., Lander, G.C., Lee, S.Y. (2018). Cryo-EM structure of a mitochondrial calcium uniporter. *Science*, 361(6401), pp.506-511.
- Zampese, E., Wokosin, D.L., Gonzalez-Rodriguez, P., Guzman, J.N., Tkatch, T., Kondapalli, J., Surmeier, W.C., D'Alessandro, K.B., De Stefani, D., Rizzuto, R. and Iino, M., Molkentin, J. D., Chandel, N.S., Schumacker, P. T., Surmeier, D. J. (2022). Ca2+ channels couple spiking to mitochondrial metabolism in substantia nigra dopaminergic neurons. *Science Advances*, 8(39), p.eabp8701.
- Zečić, A., Braeckman, B.P. (2020). DAF-16/FoxO in *Caenorhabditis elegans* and its role in metabolic remodeling. *Cells*, 9(1), p.109.
- Zhang, L., Theise, N., Chua, M., Reid, L.M. (2008). The stem cell niche of human livers: symmetry between development and regeneration. *Hepatology*, 48(5), pp.1598-1607.
- Zhang, M., Jiang, N., Chu, Y., Postnikova, O., Varghese, R., Horvath, A., Cheema, A.K., Golestaneh, N. (2020). Dysregulated metabolic pathways in age-related macular degeneration. *Scientific reports*, 10(1), pp.1-14.
- Zhou, B., Yu, P., Lin, M.Y., Sun, T., Chen, Y., Sheng, Z.H. (2016). Facilitation of axon regeneration by enhancing mitochondrial transport and rescuing energy deficits. *Journal of Cell Biology*, 214(1), pp.103-119.
- Zipfel, W. R., Williams, R. M., Webb, W. W. (2003). Nonlinear magic: multiphoton microscopy in the biosciences. *Nature biotechnology*, 21(11), 1369.
- Zwaal, R.R., Van Baelen, K., Groenen, J.T., Van Geel, A., Rottiers, V., Kaletta, T., Dode, L., Raeymaekers, L., Wuytack, F., Bogaert, T. (2001). The sarco-endoplasmic reticulum Ca2+ ATPase is required for development and muscle function in *Caenorhabditis elegans. Journal of Biological Chemistry*, 276(47), pp.43557-43563.